Deformation mechanisms, Rheology and Tectonics 2017

Inverness: 30 April - 7 May

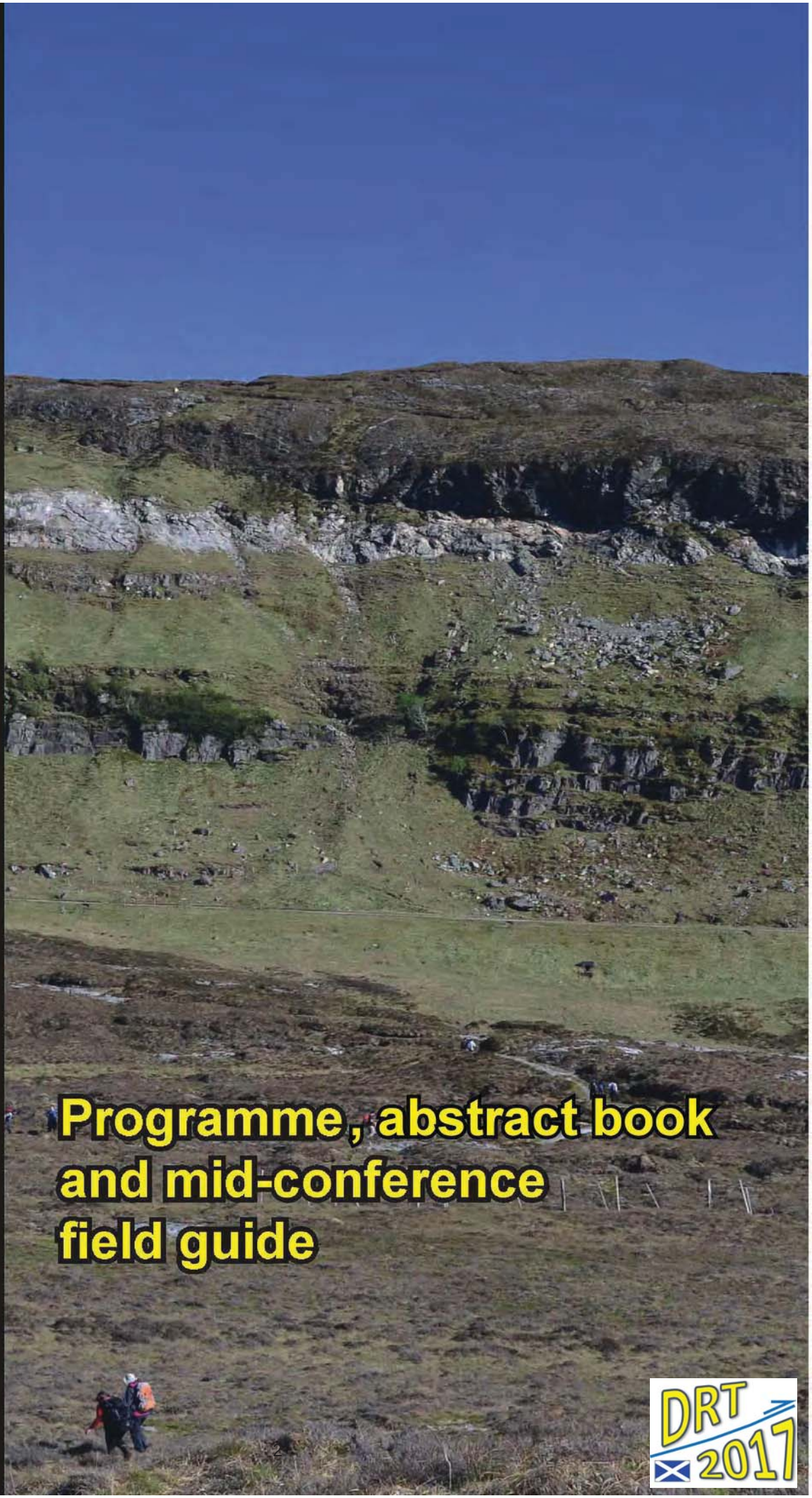

Programme, abstract book and mid-conference field guide

DRT 2017

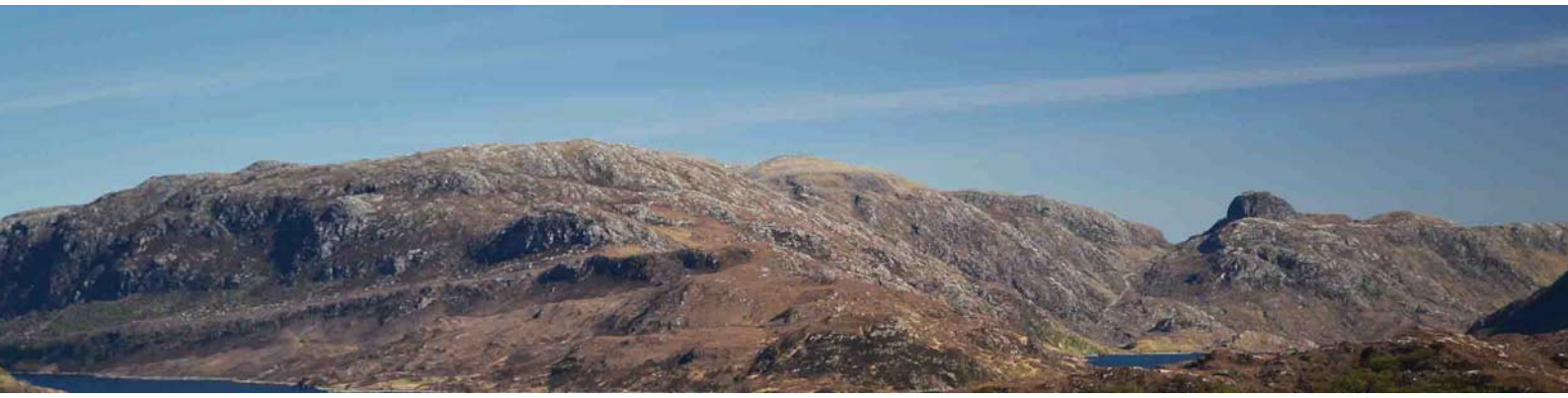

Welcome to Inverness and DRT 2017, the 21st instalment of "Deformation mechanisms, Rheology and Tectonics".

Inverness is the capital of the Scottish Highlands and lies astride the Great Glen Fault. An hour's drive to the west lies the Moine Thrust Belt - the front of the Caledonian orogenic belt on mainland Scotland (and the outcrop edge of the Laurentian shield). We'll all visit this geology - within the NW Highlands Geopark - during the mid-conference field excursion. Either side of this there is a packed science programme of talks and posters.
This booklet contains the scientific programme, the delegate list and the guide for the mid conference field excursion.
We thank the science committee for helping us put this all together, the keynote speakers and session chairs and our sponsors: TecTask, TSG and the University of Aberdeen.
And we hope you enjoy the unique geological and cultural delights of the Scottish Highlands.

Welcome!

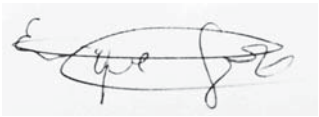

Enrique Gomez-Rivas (on behalf of the Aberdeen team)

Organising Committee (University of Aberdeen)

Enrique Gomez-Rivas
Rob Butler
Dave Healy
Clare Bond
Ian Alsop
David Iacopini
Hannah Watkins
Dave Cornwell
Randell Stephenson

Sciencific advisory board

Rick Law (Virginia Tech)
John Wheeler (University of Liverpool)
Albert Griera (Autonomous University of Barcelona)
Stephen Laubach (University of Texas at Austin)
Susanne Buiter (Geological Survey Norway)
Janos Urai (RWTH University Aachen)
Lucie Tajcmanova (ETH Zürich)
Giorgio Pennacchioni (University of Padova)
Christie Rowe (McGill University)

Summary timetable

Sunday 30th April

08.00	Pre-conference excursions depart Eden Court
16:00	Registration desk opens.
17:00-19:00	Icebreaker reception and group 1 posters.

Monday 1st May

09:00	Welcome and introduction, by Enrique Gomez-Rivas
09.05	Oral presentations begin (posters in breaks)

including briefing for mid-conference field excursion, by Rob Butler, Rick Law and John Wheeler (at 12:30)

17:15 – 18:45	Poster group 1 and evening reception
19:00-20:30	Optional discussion session "The Strabo data system: From mapping to microstructure", led by Julie Newman (Texas A&M University) and Randy Williams (University of Wisconsin–Madison)

Tuesday 2nd May

08:00	Mid-conference field excursion to NW Highlands Geopark. Depart from Eden Court
18:00	Return to Inverness

Wednesday 3rd May

09.00	Oral presentations begin (posters in breaks)
17:15 – 18:45	Group 2 posters and evening reception

Thursday 4th May

09.00	Oral presentations begin (posters in breaks)
17:30 – 18:00	DRT Business meeting (Chair: Enrique Gomez-Rivas)
19:00 for 19:30	Conference Dinner at the Mercure Hotel, Church St, Inverness IV1 1DX

Friday 5th May – Sunday 7th May

Post-conference field excursion – departs 08:00 from Eden Court.
Ends Inverness c 18:00 on 7th May.

Logistics

Group 1 posters
Hang from 16:00 on Sunday. Remove 18:45-19:00 on Monday

Group 2 posters
Hang 08:30-09:00 on Wednesday. Remove between 15:15 and 15:45 (final tea interval).

Oral presentations.
Please upload your powerpoint presentations by the start of the break before your session.
All presentations will be deleted at the end of the conference.

DRT Business meeting.

All agenda items to Enrique Gomez-Rivas by 18:00 on Wednesday 3rd May.

Poster group 1

1 Christian Stenvall, Å. Fagereng, J. Diener and C. Harris
Rheological effects of retrograde hydrous mineral assemblages; insights from the Kuckaus Mylonite Zone, Namibia

2 Tohru Watanabe, K. Kawasaki and K. Michibayashi
Anisotropy in seismic velocity and magnetic susceptibility in antigorite-bearing serpentinite mylonites

3 Livia Nardini, L. Morales, E. Rybacki and G. Dresen
Influence of boundary conditions on the nucleation of shear zones around material heterogeneities

4 James Gilgannon, F. Fussies, L. Menegon, K. Regenauer-Lieb and J. Buckman
Hierarchical creep cavity formation in mono-mineralic quartz domains of an ultramylonite from the Redbank Shear Zone

5 Joe Aslin, E. Mariani, J. Wheeler, D. Faulkner and K. Dawson
Mica deformation mechanisms in mylonitic shear zones: implications for strain localisation and rheology in the mid-crust

6 Richard Law, S. Mazza, R. Thigpen, C. Mako, K. Ashley and M. Krabbendam
Shear senses and deformation temperatures indicated by quartz c-axis fabrics and microstructures in a NW-SE transect across the Moine and Sgurr Beag thrust sheets of northern Scotland

7 M. Finch, Paul Bons, E. Gomez-Rivas, A. Griera, G.-M., Llorens, H. Ran and F. Steinbach
The ephemeral development of shear bands in mylonites

8 David Greenawald and R. Law
Early quartz fabrics from the Caledonides of northern Scotland: a new look at old data

9 Renee Heilbronner, R. Kilian and J. Tullis
Re-measuring recrystallized grain sizes in quartz shearing experiments

10 Prokop Zavada, J. Bruthans, S. Adine and M. Zare
Glaciers of salt or deformed gypsum rich caprock? A new perspective on the episodic halokinesis in the eastern Fars province, Iran

11 Alan Hollinsworth, D. Koehn and T.J. Dempster
Permeability evolution in crystalline basement fault zones

12 Bella Nke Bertille Edith, T. Njanko, M.A. Mamtani, P. Rochette and E. Njonfang
Kinematic evolution of Pan-African granitoids of Western Cameroon-Domain: an anisotropy of magnetic susceptibility (AMS) and electron backscattered diffraction (EBSD) approach

13 E. Fazio, Rosalda Punturo, R. Cirrincione, H. Kern, A. Pezzino, H-R. Wenk, S. Goswami and M.A. Mamtani
Quartz CPO analysis of mylonitic leuco-granodiorites from a ductile crustal scale shear zone (Calabria, southern Italy)

14 Nathan Daczko, S. Piazolo, D. Da Silva, U. Meek, C.A. Stuart and H. Ghatak
Recognition of melt flux through shear zones

15 Taija Torvela, A. L. Lee and S. Coyle
Style and distribution of deformation in partially molten continental crust

16 L. Spruzeniece, Sandra Piazolo and H.E. Maynard-Casely
Deformation-resembling microstructure created by fluid-mediated dissolution-precipitation reactions

17 Zita Bukovska, T. Larikova and J. Klomínský
Metamorphic interaction and deformation in the contact of olivine melilitite dyke with granite, the Krkonoše-Jizera Composite Massif, Czech Republic

18 C. Kellner and Stephen Kirby
Emplacement mechanisms of block-and-matrix serpentinite in the California Coast Ranges from 35 to 39° N: largely cold intrusions facilitated by weak rheology governed by dissolution and growth processes under hydrothermal conditions

Sunday 30th April and Monday 1st May

19 Jamie Levine and J.M. Rahl
An association between subgrain boundaries, Dauphiné twinning, and partial melting in migmatites

20 Rob Butler and T. Torvela
The pegmatite paradox: competing rates of deformation and crystallization

21 Uvana Meek, N. Daczko and S. Piazolo
Microstructural indicators of channelled melt flow through the lower crust

22 David Burianek, L. Megerssa and K. Verner
Fabric pattern and emplacement of post-collisional Tekeze Pluton (Arabian-Nubian Shield; Northern Ethiopia)

23 Robyn Gardner, S. Piazolo and N. Daczko
Flow behaviour of the middle and lower crust: Insights from field observations and numerical modelling

24 F. Hentschel, C. Hsu and Claudia Trepmann
Deformation behaviour of feldspar in greenschist facies pegmatitic mylonites from the Austroalpine basement to the south of the western Tauern window, Eastern Alps

25 L. Seybold and Claudia Trepmann
The deformation record of the HP-LT metamorphic lowermost tectonic units of the Cretan nappe pile in the Talea Ori

26 Christoph Schrank, A. Karrech, D. A. Boutelier and K. Regenauer-Lieb
Modelling viscoelastic shear zones at large strains and rotations

27 Dave Healy, R. Rizzo, D. Cornwell, N. Farrell, H. Watkins, N. Timms and E. Gomez-Rivas
FracPaQ: a MATLAB™ toolbox for the quantification of fracture patterns

28 J. Browning, P. Meredith, Dave Healy, S. Harland, C. Stuart and T. Mitchell
Crack damage evolution in rocks deformed under true triaxial loading

29 Alodie Bubeck, R.J. Walker, D. Healy, T. Davies, M. Dobbs and D.A. Holwell
Pore geometry as a control on rock strength

30 Aina Margalef and J.M. Casas
Restored cross sections in complex deformation zones: usefulness and limitations

31 Hannah Watkins, R. Butler and C. E. Bond
Forelimb damage styles in carbonate fold-thrust structures; French Sub-Alpine Chains

32 Pritam Ghosh and K. Bhattacharyya
Structural and kinematic evolution of deformation profiles of dominant thrusts: Insights from Main Central thrust and Pelling thrust faults, Sikkim Himalayan FTB

33 Sergio Llana-Fúnez, J.L. Alonso, N. Caldera and M.A. Lopez-Sanchez
Fault rocks at the base of the Somiedo Nappe (Variscan Orogen, NW Spain)

34 Alexey Ostapchuk, E.M. Gorbunova and V.V. Efremov
Microstructure and Rheology of Samples of Primorsky Fault Core

35 David Iacopini and R. Butler
Seismic expression of fault deformation Zones using multi-attributes: limits and challenges

Monday

09:00 Welcome and introduction, by Enrique Gomez-Rivas

Session 1. Chairs: Rob Butler and Sandra Piazolo

09:05 **KEYNOTE** – **Nick Timms**, D. Healy and M. Pearce
Anisotropy of elasticity and its role in plastic deformation of minerals

09:35 **Tamara de Riese**, P.D. Bons, M. Finch, E. Gomez-Rivas, A. Griera, M.-G. Llorens, H. Ran and F. Steinbach
Shear localisation in homogeneous, anisotropic materials

09:50 **Katrina Sauer**, F. Renard, V.G. Toy and the DFDP-2 Science Team
Phase mixing and the spatial distribution of grain-boundary pores in a crustal fault zone: Insights from New Zealand's Alpine Fault

10:05 **Joe Gardner**, J. Wheeler and E. Mariani
Evolution of an inherited texture during pressure solution

10:20 DISCUSSION

10:35 -11:15 Coffee and Posters (group 1)

Session 2. Chairs: Phil Skemer and Claudia Trepmann

11:15 **Kevin Mahan**, V. Schulte-Pelkum, C. Condit, T. Leydier, P. Goncalves, A. Raju, S.J. Brownlee and O.F. Orlandini
Detecting localized shear zones versus distributed tectonic fabrics with crustal seismic anisotropy using examples from western North America and the European Alps

11:30 **Yuval Boneh**, D. Wallis, L. Hansen, M. Krawczynski and P. Skemer
Anisotropic grain growth and modification of 'frozen texture' in the lithospheric mantle

11:45 **Rosalda Punturo**, M.A. Mamtani, E. Fazio and R. Cirrincione
The nature of petrophysical anisotropy in the continental crust: a case study from the Serre Massif (Calabria, Italy)

12:00 J. Idárraga-García and Carlos Vargas
On the relationship between mantle dynamics and the configuration of subduction-related continental margins

12:15 DISCUSSION

12:30 Field excursion introduction, by Rob Butler, Rick Law and John Wheeler

12:45 – 13:45 Lunch and posters (session 1)

1st May

Session 3. **Chairs: Susanne Buiter and Rick Law**

13:45 **Nathan Daczko**, S. Piazolo, C.A. Stuart and U. Meek
Melt flux through the root of a magmatic arc under static versus dynamic conditions

14:00 **Matej Pec**, B.K. Holtzman, M.E. Zimmerman and D.L. Kohlstedt
Reactive Melt Migration in the Upper Mantle

14:15 **Zita Bukovska**, K. Verner, P. Dobeš, I. Soejono, D. Buriánek, R. Nahodilová, O. Švagera, F. Tomek, L. Vondrovic & Z. Pécskay
Initial research on geological conditions in the Underground Research Facility Bukov, Bohemian Massif, Czech Republic

14.30 **Prokop Zavada**, M. Racek, P. Hasalová, P. Jeřábek, K. Schulmann, A. Roberts, R.F. Weinberg and P. Štípská
Porous melt flow in high pressure felsic crust driving weakening and exhumation dynamics of subducted continents

14.45 DISCUSSION

15:00-15:45 **Tea and posters (group 1)**

Session 4. **Chairs: Dave Healy and Ake Fagereng**

15:45 **KEYNOTE – Mike Heap**, J. Farquharson, M. Violay, P. Baud, F. Wadsworth, J. Vasseur, Y. Lavallée and T. Reuschlé
The mechanical behaviour and failure modes of volcanic rocks

16:15 **Bernhard Schuck**, A. M. Schleicher, C. Janssen, V. G. Toy and G. Dresen
Fault core microstructures and resulting implications for faulting mechanisms of the Alpine Fault, New Zealand

16:30 **Yukitsugu Totake**, R.W.H. Butler, C.E. Bond, D. Iacopini and A. Aziz
Sandstones along thrusts: their origins and implications

16:45 **Silvia Sosio de Rosa**, Z. Shipton, R. Lunn, Y. Kremer and T. Murray
Fault zone architecture and deformation mechanisms of a normal fault in poorly lithified sediments, Miri (Malaysia)

17:00 DISCUSSION

17:15 – 18:45 Posters (group 1) and evening reception

19:00-20:30 Optional discussion session
"The Strabo data system: From mapping to microstructure", organised by Julie Newman (Texas A&M University) and Randy Williams (University of Wisconsin–Madison)

Poster group 2

1 Karel Martinek, K. Verner and M. Svojtka
Krkonoše Piedmont Basin inversion: Mesozoic – Cenozoic cooling, exhumation and deformation history based on detrital apatite fission track analysis and field structural data

2 Pablo Rodríguez-Salgado, C. Childs, P.M. Shannon and JJ. Walsh
Structural style and kinematic analysis of Cenozoic inversion structures in the Celtic Sea basins, offshore Ireland

3 Susanne Buiter and G. Shephard
Investigating the interplay of rift velocity variations and initial crustal rheology for the North Atlantic rifted margins

4 Artem Moiseev, S. Sokolov, M. Tuchkova, V. Verzhbitskii and N. Malyshev
Pre Late Mesozoic deformations' phases of Wrangel Island's northen part

5 Jeffrey Rahl and A.J. McGrew
Kinematic analysis of quartzite mylonite from the Ruby-East Humboldt extensional shear zone, Elko County, Nevada

6 Ginaldo Campanha and F. Faleiros
The transcurrent shear zone system of the Ribeira Belt, SE Brazil

7 Rüdiger Kilian
Dispersion axes of deformed quartz grains - mapping, interpretation and applications

8 Ruth Keppler, M. Stipp and N. Froitzheim
Microstructures and crystallographic preferred orientations from the exhumation of the high-pressure Adula Nappe (Switzerland)

9 Taija Torvela, D. Grujic, J. Moreau and G. Hetényi
Re-interpretation of the INDEPTH deep seismic profiles (Himalaya)

10 Farzan Ahmed, J. Gogoi and K. Bhattacharyya
Kinematic evolution of the far-eastern Arunachal Himalayan fold thrust belt: insights from Siang Window, India

11 Lars Kaislaniemi and D. Whipp
What controls deformation in a bent three-dimensional orogen? An example from the Bolivian Andes

12 Randy Williams, L. Goodwin, W. Sharp and P. Mozley
A 400,000-year record of earthquake recurrence for an intraplate normal fault: Inferences on the role of fluids in determining earthquake periodicity

13 M. Scarsi, L. Crispini, P. S. Garofalo and Giovanni Capponi
Evidence for paleo-seismic cycles in carbonated peridotite: microstructural analysis of carbonated-coated grains in fault damage zones (Voltri Massif, Ligurian Alps)

14 Matthew Tarling, J.S. Rooney, S.A.F. Smith, J.M. Scott and K.C. Gordon
Sub-micron Raman Spectroscopy analysis of pressure-solution microstructures in scaly serpentinite: the Livingstone Fault, New Zealand

15 G. Piris, Albert Griera, E. Gomez-Rivas, I. Herms and X. Goula
Simulation of induced seismicity associated with fluid injection in single fractures: influence on the fracture slip regime

16 Sandra Piazolo, P. Trimby, N.R. Daczko and C. Kong
Earthquakes at depth: Insights from high resolution orientation and chemical analysis

17 Bettina Richter, H. Stünitz and R. Heilbronner
Microstructure and mechanical behaviour of experimentally sheared quartz gouge at the brittle-to-viscous transition

18 Kathryn Hayward, P.W.F. Forsyth, B.J.J. Slagmolen, D.A. Shaddock and S.F. Cox
Capturing the first milliseconds of earthquake slip

Wednesday 3rd May - Thursday 4th May

19 Hamid Roohafza, R. Ramesani and A. Taheri
The influence of tectonics on Shirband cave formation: Damqan, Northern Iran

20 James Gilgannon, M. Herwegh and A. Berger
A microstructural characterisation of transitioning rheological behaviour at greenschist-facies conditions

21 Jennifer Ziesch, D. Tanner, S. Hanstein, H. Buness, C.M. Krawczyk and R. Thomas
3-D seismic interpretation and structural analysis in the exploration of geothermal energy in Munich, Germany

22 Daeyeong Kim, D. Prior, Y. Han, C. Qi, L. Craw, C-K. Lee, K. Lilly, J.I. Lee and S.D. Hur
Microstructures of natural ice from Northern Victoria Land, Antarctica

23 Albert Griera, M.-G. Llorens and E. Gomez-Rivas
The influence of the deformation history on the microstructural evolution of polycrystalline olivine and how it affects the interpretation of mantle seismic anisotropy

24 Enrique Gomez-Rivas, A. Griera, M.-G. Llorens, P.D. Bons and R.A. Lebensohn
Full-field numerical simulations of subgrain rotation recrystallisation during shearing of dry halite polycrystals

25 E. Humphrey, Enrique Gomez-Rivas, D. Koehn, P. Bons, J.D. Martín-Martín and J. Schoenherr
Stylolite-controlled diagenesis of a mudstone carbonate reservoir: examples from the Ca2 Stassfurt carbonate (Central European Basin, NW Germany)

25 Abhisek Basa, F. Ahmed, K. Bhattacharyya and P. Sanyal
Structural evolution of Arunachal Lesser Himalayan Fold Thrust Belt: preliminary results from fracture and stable isotope analysis of carbonates

26 Daniel Koehn, N. Beaudoin and Z. Robinson
Stress and veins at stylolite tips, the anti-crack problem

27 J. Aleksans, Daniel Koehn and R. Toussaint
Simulating hydraulic fracture, seismicity and failure mode in hard versus soft rock

28 Hannah Watkins, C. E. Bond, A. J. Cawood, M. Cooper and M. Warren
Controls on fracture intensity and orientation on a plunging carbonate anticline; Sawtooth Range, Montana

29 Tamara de Riese, P. D. Bons and T. Sachau
Dynamics of bimodal, diffusional and ballistic transport systems in the Earth’s crust

30 E. Fazio, Rosalda Punturo, G. Barreca, S. Gambino, R. Maniscalco and R. Butler
Deformation bands in Numidian sandstones of Sicily: a petrographic-structural study

31 Flora Menezes and C. Lempp
The Rotliegend fracture patterns: a transition between continuous and discontinuous geomechanical behaviour

32 Flora Menezes, C. Lempp, A. Neumann, K. Svensson and H. Pöllmann
Geomechanical behaviour changes of a Bunter Sandstone due to scCO2 injection effects

33 Clare Bond
Fluid flow in deforming media: interpreting stable isotope signatures of marbles

34 Vladimir Kusbach, Z. Roxerová, M. Machek, M. Racek and P.F. Silva
Shear zone in calcite: AMS and microstructure

Wednesday

Session 5. **Chairs: Djordje Grujic and Giovanni Capponi**

09:00 **KEYNOTE - Antonio Teixell**
Mountain belts formed after rift basins

09:30 **Alodie Bubeck**, R.J. Walker, J. Imber, R.E. Holdsworth, R.W. England and D.A. Holwell
Vertical axis rotations during normal fault propagation and linkage: application to the evolution of the NE Atlantic

09:45 **Karel Martinek**, K. Verner, D. Buriánek, L. Alemayehu Megerssa and T. Hroch
Neotectonic history and landslides in the Main Ethiopian Rift (MER) and Afar triple junction revealed by analysis of remote sensing data and field mapping

10:00 **Carolina Giorgetti**, M.M. Scuderi, T. Tesei and C. Collettini
The role of pre-existing anisotropies in fault mechanics: experimental insights from triaxial saw-cut experiments

10:15 **Adam Cawood** and C.E. Bond
Deformation of a stacked fluvio-deltaic succession – linking strain partitioning and fracture 'damage'

10:30 DISCUSSION

10:45 – 11:15 **Coffee and posters (session 2)**

Session 6. **Chairs: Paul Bons and Virginia Toy**

11:15 **Phil Skemer**, A. Cross and Y. Boneh
The long path to steady state: Transient microstructures in the crust and upper mantle

11:30 **Stephen Kirby**, M. Uno, M. Lewis and C. Kellner
Orogenic block-and-matrix serpentinites in the Franciscan mélange of California: petrographic and field evidence of multi-stage serpentinization and dissolution-and-growth rheology during cold intrusion through the crust from the Coast-Range mantle

11:45 **Robyn Gardner**, S. Piazolo and N. Daczko
Patterns of strain localization in heterogeneous, polycrystalline rocks – a numerical perspective

12:00 **Nicholas Hunter**, R. F. Weinberg, C.J.L. Wilson, V. Luzin and S. Misra
The anatomy of 'hot-on-cold' shear zones: insights from quartzites of the Main Central Thrust in the Alaknanda region (Garhwal Himalaya)

12:15 L. Calhoun, **Joe White** and C.W. Jefferson
Paradoxical mid-crustal displacements, transposition and stratigraphic continuity: an integrated geological and geophysical study of tectonic evolution of the Paleoproterozoic Amer Group, Nunavut, Canada

12:30 DISCUSSION

12:45 – 13:45 **Lunch and posters (session 2)**

3rd May

Session 7. **Chairs: Albert Griera and Chris Wilson**

13:45 **KEYNOTE - Dave Prior**, L. Craw, W.B. Durham, J. Eccles, D. Goldsby, C. Hulbe, D. Kim, C. Qi, D. Peyroux, M. Seidemann and M. Vaughan
Microstructure, CPO and rheology of ice: scaling from the laboratory to ice sheets and ice shelves

14:15 **Maria-Gema Llorens**, A. Griera, F. Steinbach, P.D. Bons, E. Gomez-Rivas, D. Jansen, J. Roessiger, R.A. Lebensohn and I. Weikusat
Effect of vorticity on polycrystalline ice deformation

14:30 **Lisa Craw**, D. Prior, C. Hulbe, M. Vaughan and K. Lilly
Microstructure and mechanics of ice under constriction: data from the field and laboratory

14:45 **Paul Bons**, D. Jansen, M.-G. Llorens, T. de Riese, T. Sachau, F. Steinbach and I. Weikusat
Folds and shear zones in the Greenland Ice Sheet

15:00 DISCUSSION

15:15-15:45 **Tea and posters (group 2)**

Session 8. **Chairs: Clare Bond and Daniel Koehn**

15:45 **Ake Fagereng**
Deformation mechanisms, rheology, and the geophysically observed phenomena of slow slip and tremor

16:00 **Kathryn Hayward**, S. F. Cox
Stress-driven versus fluid-driven slip: using experiments to explore differences in modes of earthquake rupture

16:15 **Sivaji Lahiri**, V. Rana and M.A. Mamtani
Quantifying variation in effective normal stress responsible for gold mineralization: comparing vein orientation data from mineralized and non-mineralized zones of Dharwar Craton (Southern India)

16:30 **Giacomo Pozzi**, N. De Paola, S.B. Nielsen and R.E. Holdsworth
Viscous Flow Controls Slip Zone Thickness and Weakening during Coseismic slip in Calcite Gouges.

16:45 **Lucy Campbell**, G. Lloyd, R. Phillips, R. Walcott and R.E. Holdsworth
Seismic behaviour and strength evolution of heterogeneous upper crustal fault zones: environmental constraints on pseudotachylytes in the Outer Hebrides Fault Zone, UK

17:00 DISCUSSION

17:15 – 18:45 **Posters (group 2) and evening reception**

Thursday

Session 9. **Chairs: John Wheeler and Nathan Daczko**

09:00 **KEYNOTE - Jessica Warren** and C. Teyssier
The role of fluids in the brittle-ductile transition at oceanic transform faults

09:30 **Daniele Maestrelli**, M. Bonini, D. Delle Donne, L. Piccardi and F. Sani
Mud Volcanoes eruptions in response to the August-October 2016 Central Italy seismic sequence

09:45 **Manuel de Paz Alvarez**, B. Uunk, F. Brouwer and J. Wijbrans
Implications of structural analysis, P-T pseudosection modelling and white mica 40Ar/39Ar age distributions for the interpretation of the tectonometamorphic history of Syros (Cyclades, Greece)

10:00 **Matthew Tarling**, S.A.F. Smith and J.M. Scott
Metasomatism, brecciation and slip dynamics in ultramafic-quartzofeldspathic shear zones: The Livingstone Fault, New Zealand

10:15 **Stephen Laubach**, J.E. Olson, R.H. Lander and J.N. Hooker
Chemical-mechanical feedback and fracture size and spacing patterns

10:30 DISCUSSION

10:45 – 11:15 **Coffee and posters (group 2)**

Session 10. **Chairs: Renée Heilbronner and Elisabetta Mariani**

11:15 **John Wheeler**
Grain shapes and geometric weakening during diffusion creep

11:30 **Claudia Trepmann**, C. Hsu and F. Hentschel
Recrystallization of quartz after low-temperature plasticity – the record of stress relaxation in different tectonic regimes

11:45 **Martina Kirilova**, V. Toy, J. Rooney, K. Gordon, C. Giorgetti and C. Collettini
Structural Disorder of Graphite and Implications for Graphite Thermometry

12:00 **Krystof Verner**, O. Pour, F. Tomek, L. Megerssa, D. Buriánek and J. Žák
New insights to late-Variscan geodynamic evolution of the south-western Moldanubian Zone (Bohemian Massif)

12:15 **Chris Wilson**, M. Peternell and D.M. Hammes
Insights into strain rate cycling and localisation of strain on a grain-scale during high temperature creep

12:30 DISCUSSION

12:45 – 13:45 **Lunch and posters (session 2)**

4th May

Session 11. **Chairs: Stephen Laubach and Sergio Llana-Fúnez**

13:45 **Elisabetta Mariani**, S.J. Covey-Crump, J. Wheeler, D. Wallis and D.J. Prior
The role of twinning in microstructure evolution during the static recrystallization of cold-worked Carrara marble

14:00 **Daniel Koehn**, N. Beaudoin, M.P. Rood, P.D. Bons and E. Gomez-Rivas
Stylolite classification to estimate compaction and permeability variations

14:15 **Sina Marti**, R. Heilbronner, H. Stünitz, O. Plümper and M. Drury
An experimental study on the brittle-viscous transition in mafic rocks and the importance of strain dependent rheology

14:30 **Andrew Cross** and P. Skemer
Ultramylonite generation via phase mixing in high strain experiments

14:45 **Hao Ran**, P.D. Bons, G. Wang, M. Finch, F. Steinbach, A. Griera, S. Ran and X. Liang
Deformation of conglomerates with layered pebbles under simple shear: a numerical approach

15:00 DISCUSSION

15:15-15:45 **Tea**

Session 12. **Chairs: Georg Dresen and Kevin Mahan**

15:45 **Christoph Schrank**, M. Veveakis, T. Poulet and K. Regenauer-Lieb
Transient cnoidal waves: a new model for fault-damage zones

16:00 **Virginia Toy**, A. Niemeijer, F. Renard, L. Morales and R. Wirth
Striation and slickenline development on quartz fault surfaces at crustal conditions: origin and effect on friction

16:15 **Sandra Piazolo**, A. La Fontaine, P. Trimby, S. Harley, L. Yang, R. Armstrong, C. Corcoran and J.M. Cairney
Atoms on the move: Deformation-induced trace element redistribution in zircon revealed using atom probe tomography

16:30 **Charles Gumiaux**, B. Cochelin, D. Chardon, Y. Denele and B. Le Bayon
Geostatistics applied to strain field analysis: application to the Variscan orogen, Pyrenees

16:45 **Sergio Llana-Funez**, L. Rodríguez-Rodríguez, D. Ballesteros, P. Valenzuela, L.M. Díaz, P. Cadenas, G. Fernández-Viejo, M.J. Domínguez-Cuesta, M. Jiménez-Sánchez, M. Meléndez-Asensio and C. López-Fernández
The effect of gradient in crustal thickness in relief development in the Cantabrian Mountains (N Iberia)

17:00 **Djordje Grujic**, K. T. Ashley, M. A. Coble, I. Coutand, D. A. Kellett and N. Whynot
Inverted temperature fields: role of progressive deformation

17:15 DISCUSSION

17:30 – 18:00 **DRT Business meeting** (Chair: Enrique Gomez-Rivas)

DRT 2017 Delegate list

Farzan Ahmed (IISER Kolkata)
Ian Alsop (University of Aberdeen)
Joe Aslin (University of Liverpool)
Abhisek Basa (IISER Kolkata)
Bella Nke Bertille Edith (University of Maroua)
Clare Bond (University of Aberdeen)
Yuval Boneh (Washington University in St. Louis)
Marco Bonini (Università degli Studi di Firenze)
Paul D. Bons (University of Tübingen)
Alodie Bubeck (University of Leicester)
Susanne Buiter (Geological Survey of Norway)
Zita Bukovska (Czech Geological Survey)
David Buriánek (Czech Geological Survey)
Rob Butler (University of Aberdeen)
Ginaldo Campanha (Universidade de São Paulo)
Lucy Campbell (University of Plymouth)
Giovanni Capponi (University of Genova)
Adam Cawood (University of Aberdeen)
Giovanni Mario Cella (ENI Corporate University SPA)
Rebecca Coats (University of Liverpool)
Dave Cornwell (University of Aberdeen)
Lisa Craw (University of Otago)
Andrew Cross (Washington University in St. Louis)
Nathan Daczko (Macquarie University)
Manuel de Paz Álvarez (Vrije Universiteit Amsterdam)
Tamara de Riese (University of Tübingen)
Natalie Debenham (Australian School of Petroleum)
Georg Dresen (Universität Potsdam)
Benjamin Duncan (University of Aberdeen)
Lynn Evans (Monash University)
Ake Fagereng (Cardiff University)
Eugenio Fazio (Università degli Studi di Catania)
Salvatore Gambino (Università degli Studi di Catania)
Robyn Gardner (Macquarie University)
Joe Gardner (University of Liverpool)
Pritam Ghosh (IISER Kolkata)
James Gilgannon (Universität Bern)
Carolina Giorgetti (Università di Roma)
Enrique Gomez-Rivas (University of Aberdeen)
David Greenawald (The University of North Carolina at Chapel Hill)
Albert Griera (Universitat Autònoma de Barcelona)
Djordje Grujic (Dalhousie University)
Charles Gumiaux (Université d'Orléans)
Kathryn Hayward (Australian National University)
David Healy (University of Aberdeen)
Michael Heap (University of Strasbourg)
Renée Heilbronner (University of Basel)
Allan Hollinsworth (University of Glasgow)
Nicholas Hunter (Monash University)
David Iacopini (University of Aberdeen)
Lars Kaislaniemi (University of Helsinki)
Ruth Keppler (Rheinische Friedrich-Wilhelms-Universität Bonn)
Rüdiger Kilian (University of Basel)
Daeyeong Kim (Korea Polar Research Institute)
Stephen Kirby (U.S. Geological Survey)
Martina Kirilova (University of Otago)
Daniel Koehn (University of Glasgow)
Vladimir Kusbach (Institute of Geophysics of the CAS)
Sivaji Lahiri (IIT kharagpur)
Anthony Lamur (University of Liverpool)
Larry Lane (Geological Survey of Canada)
Stephen Laubach (University of Texas)
Richard Law (Virginia Polytechnic Institute and State University)
Jamie Levine (Appalachian State University)
Sergio Llana-Fúnez (University of Oviedo)
Maria-Gema Llorens (University of Tübingen)
Amy MacLellan (University of Aberdeen)
Daniele Maestrelli (Università di Pisa)
Kevin Mahan (University of Colorado Boulder)
Aina Margalef (Institut d'Estudis Andorrans)
Elisabetta Mariani (University of Liverpool)
Sina Marti (Universität Basel)
Karel Martinek (Czech Geological Survey)
Uvana Meek (Macquarie University)
Flora Menezes (Martin-Luther-Universität Halle-Wittenberg)
Artem Moiseev (Russian Academy of Sciences)
Zuzanna Mycon (University of Aberdeen)
Livia Nardini (GFZ Potsdam)
Julie Newman (Texas A&M University)
Alexey Ostapchuk (Russian Academy of Sciences)
Matej Pec (Massachusetts Institute of Technology)
Sandra Piazolo (Macquarie University)
Giacomo Pozzi (University of Durham)
David Prior (University of Otago)
Rosalda Punturo (Universita degli studi di Catania)
Jeffrey Rahl (Washington and Lee University)
Hao Ran (University of Tübingen)
Bettina Richter (University of Basel)
Pablo Rodríguez-Salgado (Irish Centre for Research in Applied Geosciences)
Hamid Roohafza (Shahrood University)
Katrina Sauer (University of Otago)
Christoph Schrank (Queensland University of Technology)
Bernhard Schuck (GFZ Potsdam)
Philip Skemer (University of Washington in Saint Louis)
Silvia Sosio de Rosa (University of Strathclyde)
Christian Stenvall (University of Cardiff)
Randell Stephenson (University of Aberdeen)
Matthew Tarling (University of Otago)
Antonio Teixell (Universitat Autonoma de Barcelona)
Nicholas Timms (Curtin University)
Taija Torvela (University of Leeds)
Yukitsugu Totake (University of Aberdeen)
Virginia Toy (University of Otago)
Claudia Trepmann (Ludwig-Maximilians-Universität München)
Carlos Alberto Vargas (Universidad Nacional de Colombia)
Krystof Verner (Czech Geological Survey)
Jessica Warren (University of Delaware)
Tohru Watanabe (University of Toyama)
Hannah Watkins (University of Aberdeen)
John Wheeler (University of Liverpool)
Joseph White (University of New Brunswick)
Randy Williams (University of Wisconsin–Madison)
Chris Wilson (Monash University)
Prokop Zavada (Institute of Geophysics of the CAS)
Jennifer Ziesch (Leibniz Institute for Applied Geophysics

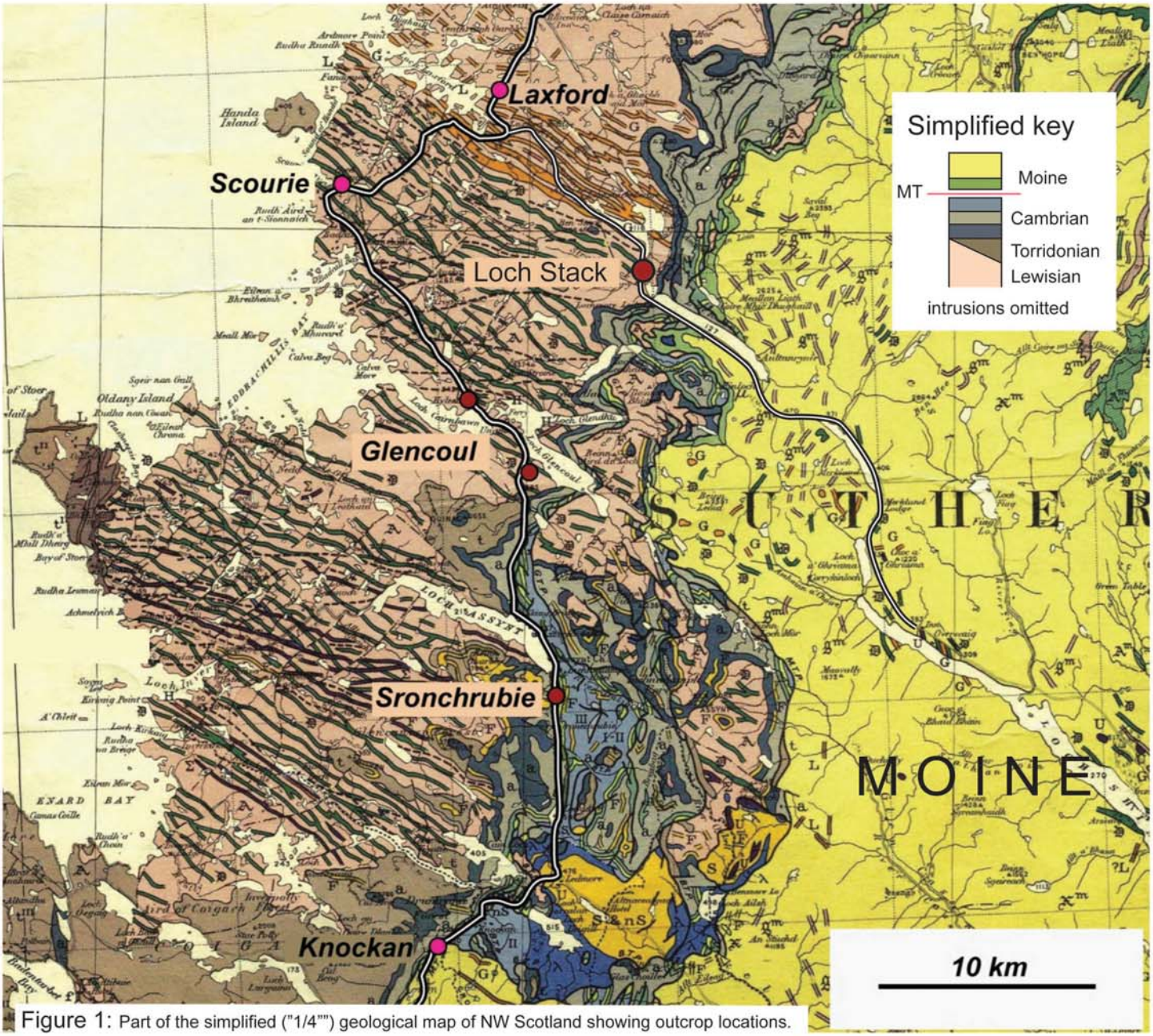

Figure 1: Part of the simplified ("1/4"") geological map of NW Scotland showing outcrop locations.

Mid-conference field excursion

This one-day field excursion aims to introduce aspects of the structural geology and tectonics of NW Scotland. Locations are shown on the simplified geological map (Fig. 1).

Geological notes

It is convenient to summarise the geology of NW Scotland referencing the Caledonian orogenic front - the Moine Thrust. This carries Proterozoic meta-sediments of the Moine Supergroup (with their "Lewisianoid" basement) onto a foreland of Cambro-Ordovician sediments that were deposited above a planar unconformity. This steps across the Proterozoic Torridon Group sediments and the Archaean-Palaeoproterozoic Lewisian basement. The Moine Thrust formed at end Silurian (c 430Ma), was WNW-directed and involves slices of foreland units below: the Moine Thrust Belt.

The Lewisian basement records a long tectono-metamorphic history with protoliths dating from c 3.1 Ga to the youngest ductile reworking (the "Laxfordian") at c 1.7 Ga. Chiefly comprising TTG gneisses, mafic intrusions ("Scourie dykes"; c 2.4 - 1.9 Ga) are important markers for separating tectonic epiosodes. Lewisian rocks in Fig 1 are chiefly of the "Central Block" (dykes are undeformed, TTG gneisses preserve UHT metamorphism - so-called "Badcallian" tectono-metamorphism: c 2750 Ma). These dyke, in the northern Lewisian are sheared, at amphibolite grade and cross-cut by granites/pegmatites within the "Laxford shear zone". Torridon Group clastics (1200-1000 Ma) are unconformable upon the Lewisian. The Moine Thrust Belt shows complex lateral structural variations formed by basement slices and imbricated Cambrian strata (stratigraphy shown on Fig. 2), with multiple detachments.The Moine thrust formed a roof to these. Total displacements probably exceeded 100km and the system shows fauts rocks transitioning from cataclasites passing up into greenschist mylonites. The Moine sheet includes complex structures and variable high-grade Caledonian and older metamorphism.

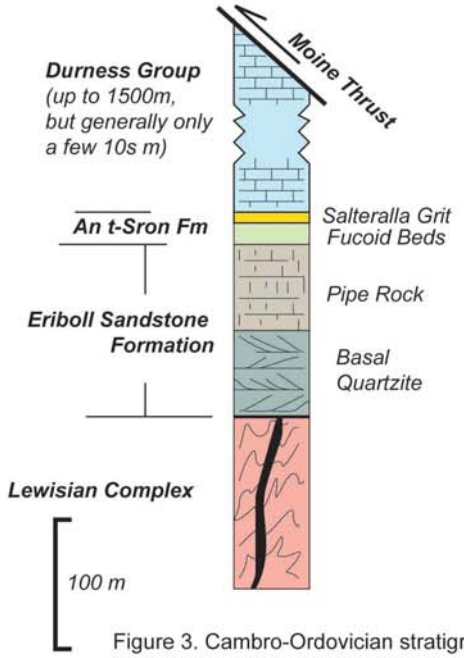

Figure 3. Cambro-Ordovician stratigraphy and thicknesses which are near constant both along and across strike in the foreland and thrust belt.

Conservation notes

All field-trip stops (except the Loch Stack viewpoint) are locations within the Geological Conservation Review and thus are especially sensitive. It is illegal to damage (hammer etc) or remove material (even loose rock) from Sites of Special Scientific Interest. Please contact Scottish Natural Heritage if you wish to gain sampling permision.

STOP A - Loch Stack viewpoint (GR NC296408). Looking North - the hill of Arkle (787m) comprises Cambrian quartzites above SE-dipping unconformity with Lewisian basement. Note dip increasing to E on cliff-section picking out imbricates in the Moine Thrust Belt. MT lies in back hills. See Fig. 4.

STOP B. Laxford (Loch na Fiacall roadcuts)
TAKE GREAT CARE WITH TRAFFIC . These photogenic cuts (Fig. 5) are through "Laxfordianized" Lewisian with amphibolitized "Scourie dykes" and various syn-kinematic granitic intrusions. Note flanking folds. Mineral lineations plunge gently SE.

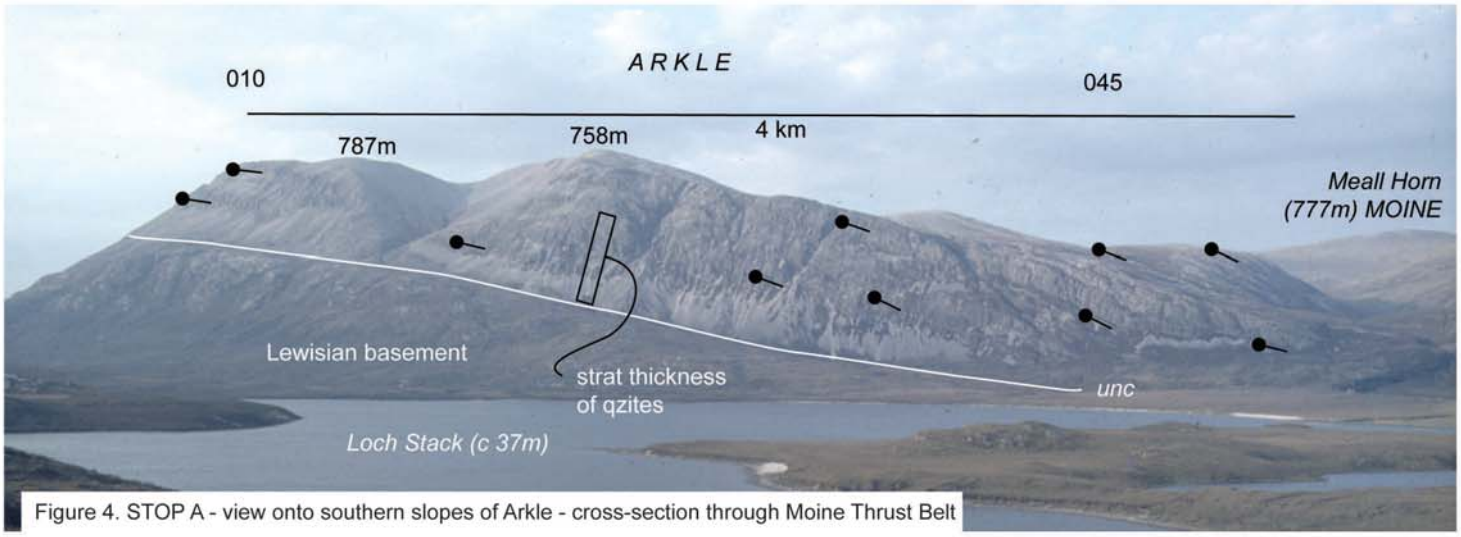

Figure 4. STOP A - view onto southern slopes of Arkle - cross-section through Moine Thrust Belt

Figure 5. STOP B - The Loch na Fiacall road cuts (GR 230482 - 241498) aka the "multicoloured rock stop". Laxfordianized Lewisian.

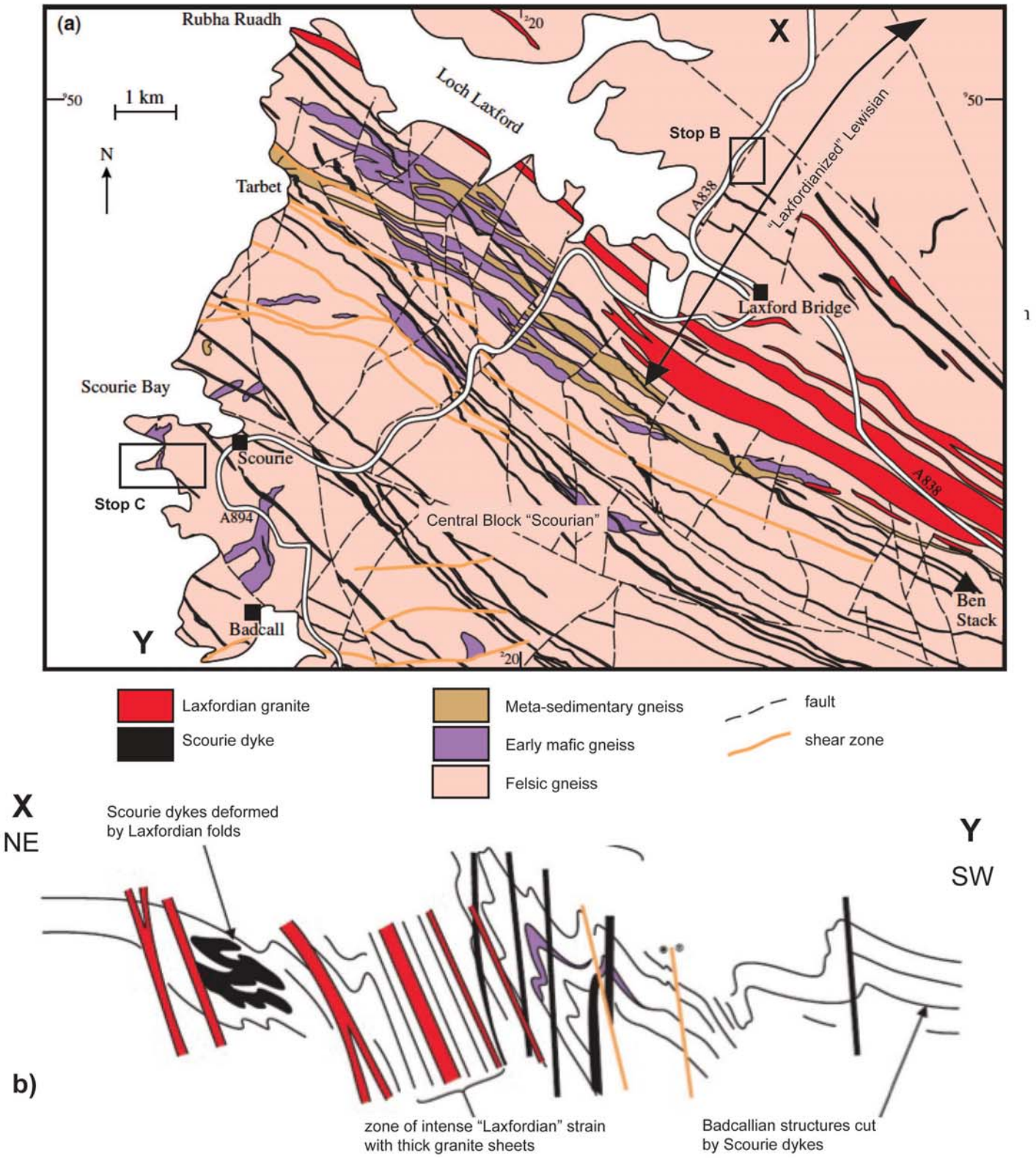

Figure 5. Simplified map (a) and section (b) showing relationship between Laxford Shear Zone (Stop B) and Central Block Scourian (Stop C). Modified after Goodenough et al. 2010; GSL Spec Publ 335).

STOP C. Scourie More (GR NC141442)

These outcrops are accessed via a 1 km walk from the road and display relationships between various key geological elements of the Central Block. These include tonalitic grey "Scourian" gneisses; stunning plag, 2 px., gt. granulites and a very coarse k-rich pegmatite (dated at c 2.54 Ga) with local retrogression of adjacent granulites. The assemblage is cross-cut by NW-SE trending undeformed basic sheets of the Scourie dyke suite.

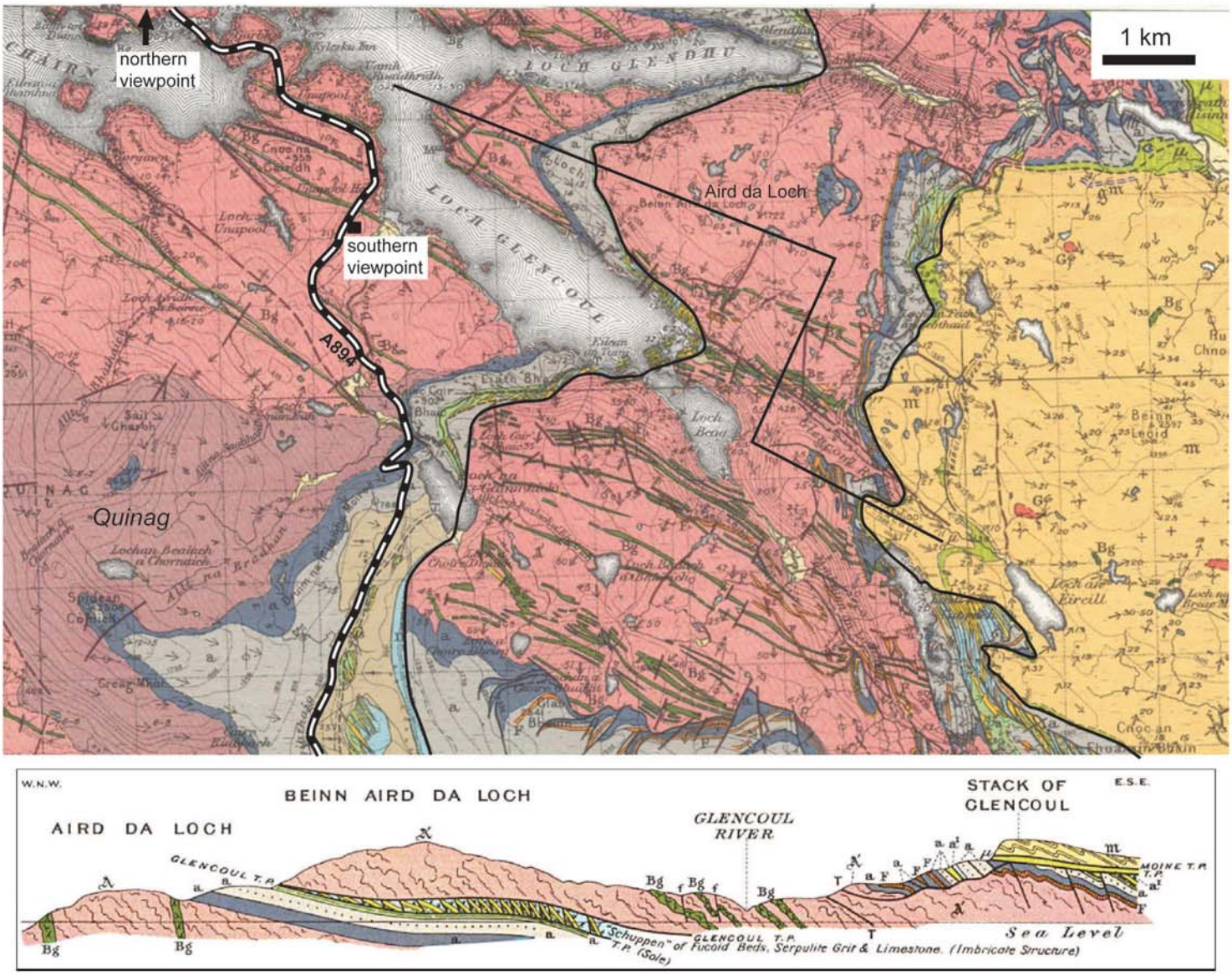

Figure 6. Original map (a) and section (b) derived from 1880s mapping by the Geological Survey of the Glencoul area of the Moine Thrust Belt.

STOP D. Glencoul (GRs NC212350 and 236320). Two sites provide excellent views (Fig. 7) into the classic Glencoul sector of the Moine thrust Belt. The Glencoul Thrust was first described by Callaway in 1883 and this area mapped by Clough in the mid 1880s - simplified in Fig. 6. The Glencoul Thrust moved 25-33 km and carries a c 600m slice of Lewisian basement and its Cambrian cover - with virtually no internal strain. In contrast the quartzites beneath the Moine Thrust at the Stack of Glencoul are strongly mylonitized and thinned.

.

Figure 7. Glencoul panoramas (a) from northern stop, (b) from southern.

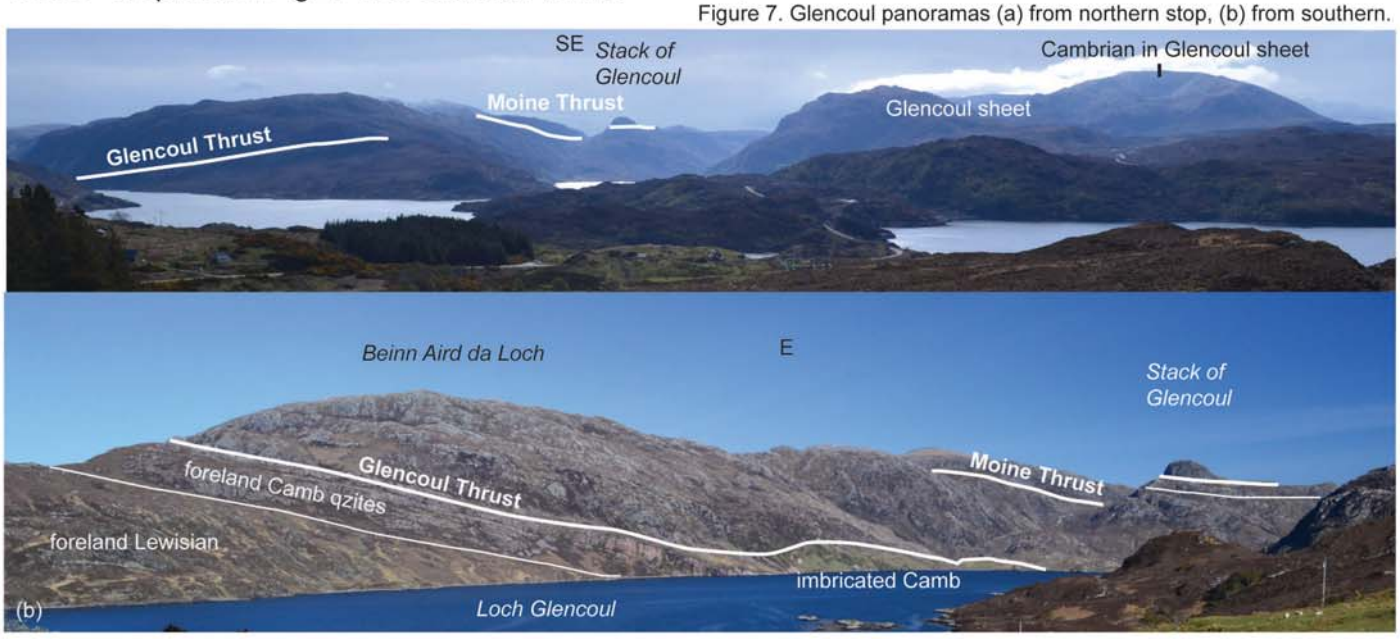

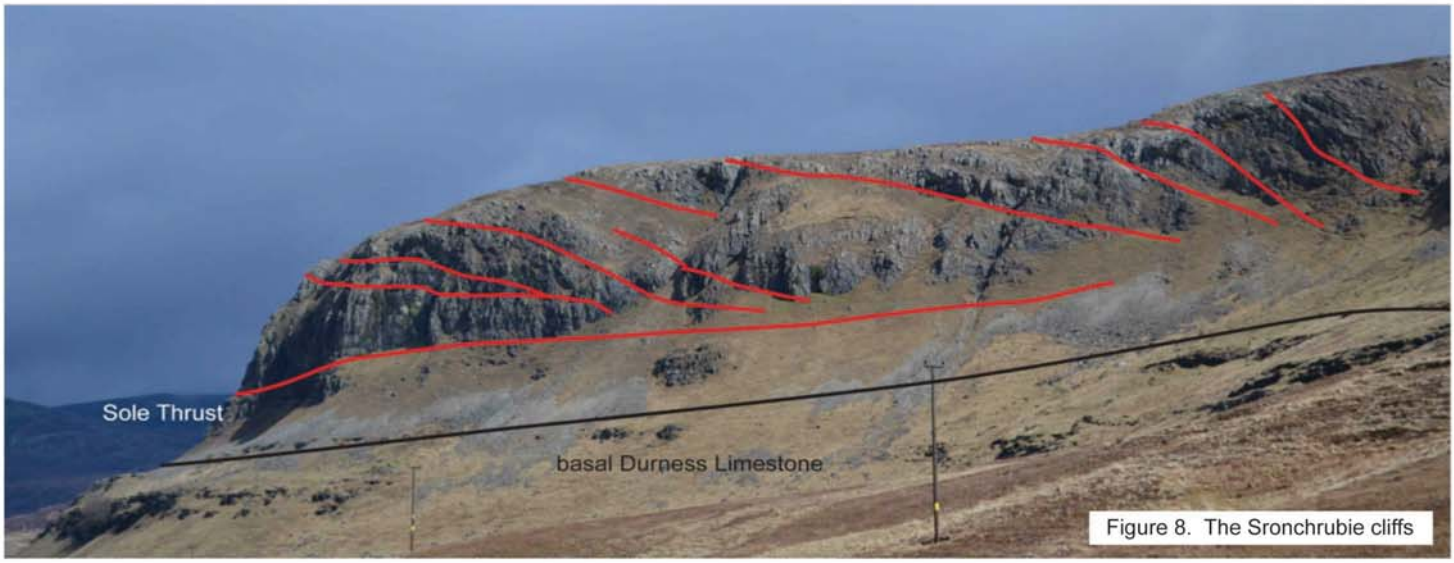

Figure 8. The Sronchrubie cliffs

STOP E. Sronchrubie (GR NC248204). Viewpoint onto the frontal imbricates in Durness Group carbonates (Fig. 8). Note sills in the lower section. The site also gives a cross-sectional view of northern Assynt (Fig. 9) and the dip-slope of Cambrian quartzites (minor intrusions) of the foreland to the west.

STOP F. Knockan Crag (GR NC188091). The Moine Thrust and Geopark visitor centre - accessed via a trail. The thrust here has no imbricates below as the thrusts of Assynt both converge southwards and aremcut (over-stepped) by the Moine Thrust (Fig. 10). Its hangingwall contains mylonites of Moine rocks, the lower 1m of which are now cataclased (and locally re-foliated again within a few cm of the thrust plane).

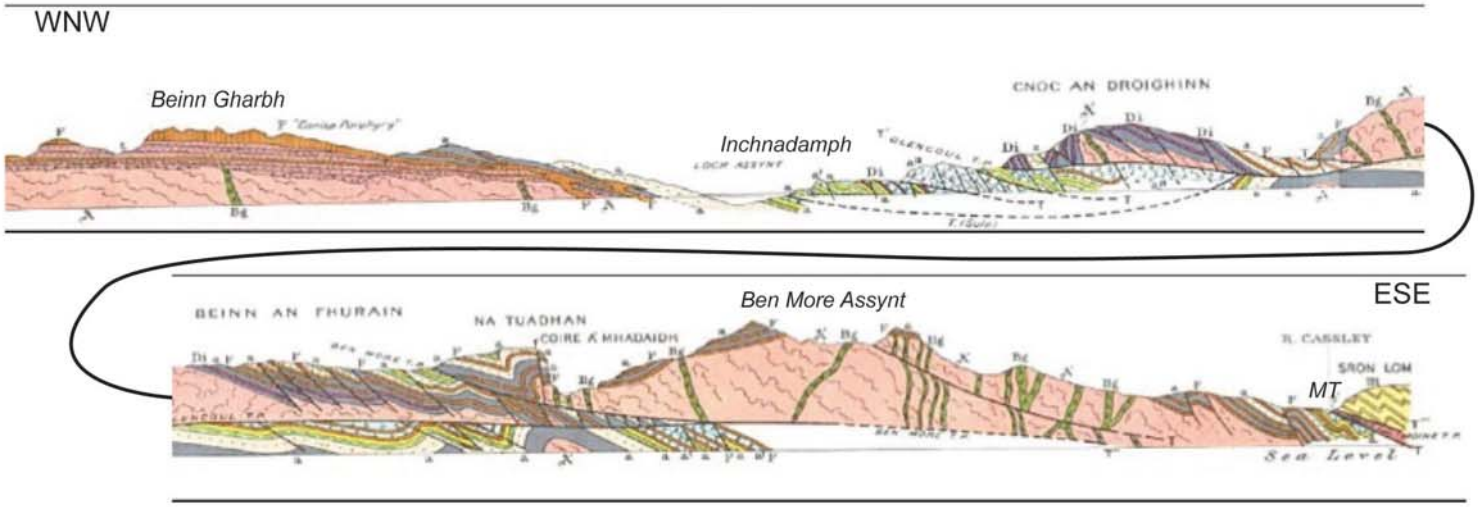

Figure 9. Peach and Horne's cross-section from 1880s fieldwork through northern Assynt showing the various scales of imbrication chiefly in the Cambrian sediments but also the slices of Lewisian basement in the Glencoul and Ben More thrust sheets. The Moine thrust (MT) is in the eastern part of the section. The geology on the eastern halfof this section is not visible from Sronchrubie lay-by.

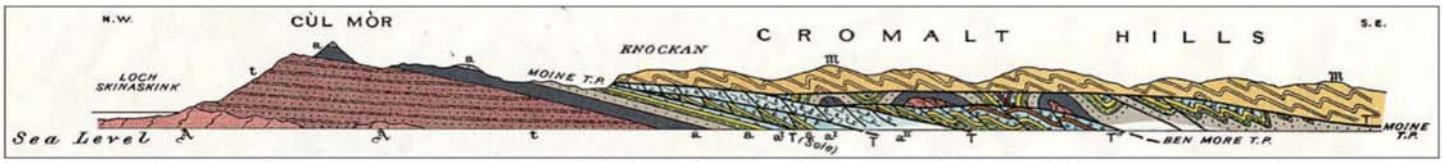

Figure 10. Peach and Horne's cross-section from 1880s fieldwork through southern Assynt showing the Moine thrust over-stepping imbricates and folds in its footwall so that it carries Moine rocks (yellow) directly onto Cambrian strata of the foreland at Knockan Crag.

References and further information are available as downloads from the DRT 2017 website

DRT 2017 Inverness

21st International Conference on
Deformation Mechanisms, Rheology and Tectonics
30th April - 4th May 2017
Inverness, Scotland

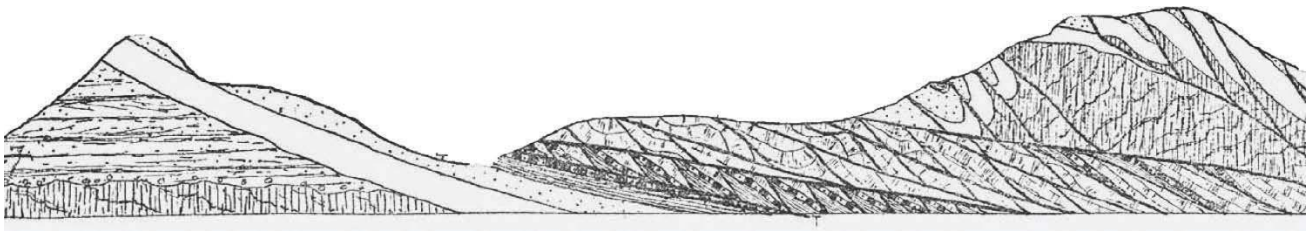

ABSTRACT BOOK

Please note that the underlined author is the presenting author

Kinematic evolution of the far-eastern Arunachal Himalayan fold thrust belt: Insights from Siang Window, India

F. Ahmed[1], J. Gogoi[1] & K. Bhattacharyya[1]
[1]*Indian Institute of Science Education and Research Kolkata, India (fa13ip036@iiserkol.ac.in)*

Total minimum shortening estimates from published balanced cross-sections along the Himalayan arc reveal a significant lateral variation. These studies indicate that the footwall structures of the Main Central thrust (MCT), i.e., the Lesser Himalayan structures accommodate ~50-70% of the total minimum shortening, and record the maximum lateral variation. Therefore, deciphering the structural geometry of the Lesser Himalayan sequence (LHS) is critical to evaluate the kinematic evolution of the Himalayan fold thrust belt (FTB). We focus this study on the Siang window in far-eastern Arunachal Lesser Himalayan fold thrust belt (FTB) that exposes the MCT footwall rocks. We mapped ~2800 km^2 area in and around the Siang window along N-S, E-W and SW-NE transects. We marked the structural contacts based on presence of fault rocks and stratigraphy. The Pelling thrust (PT) is the northernmost thrust of our study area that brings hangingwall Paro schist over the footwall Daling phyllites of the LHS. The Ramgarh thrust (RT) lies in the footwall of the PT, and forms the roof thrust of Lesser Himalayan Duplex (LHD). The Bomdo thrust (BT) is the next footwall thrust, named after nearest habitation, carrying the Buxa carbonate in the hanging wall over the Abor volcanics in the footwall. The BT is folded in a transport-perpendicular doubly plunging fold along 26^0,279^0 and 12^0,120^0. The Abor volcanics lie in structural contact with the structurally underlying, younger, Yingkiong Formation along the Geku thrust (GT). The GT sheet also forms a doubly plunging fold along 29^0,280^0 and 17^0,040^0. The doubly plunging folds are restricted to the middle of the transect, and dies out in the southern imbricates, with the footwall Yingkiong sheet folded in an antiform along 4^0, 311^0. Such structures indicate structural culmination, possibly associated with a structurally underlying duplex.

We have initiated constructing a transport-parallel, regional balanced cross-section to arrive at the kinematic evolution and to quantify the minimum shortening. Based on orientation of hinge lines of mesoscopic and macroscopic folds in the foreland, and stretching lineation, the transport direction is estimated at 342^0-162^0. We calculated thicknesses of the various thrust sheets by incorporating the outcrop widths, average foliation data, altitude correction. The thickness of the undeformed footwall template is estimated at ~16km. The regional dip of the detachment is estimated at ~2.5^0 N, and it ramps from a depth of ~14km through the Buxa Group. The footwall of the PT has a duplex system comprising atleast 9 lower LHS horses and 4 upper LHS horses. The RT is the roof thrust of the upper LHS horses. The southern-most ramp of the MFT is determined by restoring the Siwalik Group. With progressive footwall imbrication, the detachment climbs up the section in the foreland at ~7 km below the Siwalik Group. In the MBT sheet, the forelimb of the fault-bend antiform is constrained by the southerly dipping beds of the Siwalik Group. Based on preliminary results, we estimate a minimum shortening of ~405 km without incorporating slip on the MCT.

To examine grain-scale strain partitioning among the various thrust sheets, we quantified 2D penetrative strain using modified Fry Method. The penetrative strain progressively decreased in the thrust sheets from hinterland to foreland suggesting a forelandward progression of deformation. Vorticity analysis using rigid grain method indicates overall general deformation of the studied thrust sheets in Arunachal Himalayan FTB.

Simulating hydraulic fracture, seismicity and failure mode in hard versus soft rock

J. Aleksans[1], D. Koehn[1] & R. Toussaint[2]
[1]*School of Geographical and Earth Sciences, University of Glasgow, Glasgow, UK (Daniel.koehn@glasgow.ac.uk)*
[2]*CNRS, IPGS-EOST, Strasbourg, France*

In this contribution we discuss the dynamic development of hydraulic fractures, their evolution and the resulting seismicity during fluid injection in a coupled numerical model. The model describes coupling between a solid that can fracture dynamically and a compressible fluid that can push back at the rock and open fractures. We simulate fluid injection at a point source in a vertical two-dimensional slice of rock at depths of 1 to 3km with an initial compaction of the solid due to gravity. The model allows the monitoring of single fracturing events as well as movement of fracture walls and thus the related seismicity. In our simulations, hydrofracturing is caused by local fluid overpressure that exceeds the sum of the least compressive stress and the tensile strength of the rock and evolves in 4 distinct steps during injection: a stress build up, the main fracturing, a phase of residual fracturing and finally seeping of fluid through the build-up fracture network. With a series of numerical simulations we show how the fracture pattern and seismicity change depending on changes in depth, injection rate, Young's Modulus and breaking strength. Our simulations indicate that the Young's Modulus has the largest influence on the fracture dynamics and also the related seismicity. Simulations of rocks with a Young's modulus smaller than 10 GPa show dominant mode I failure and a growth of fracture aperture with a decrease in Young's modulus. Simulations of rocks with a higher Young's modulus than 10 GPa show fractures with a constant aperture and fracture growth that is mainly governed by a growth in crack length and an increasing amount of mode II failure. We propose that two distinct failure regimes are observed in the simulations, above 10 GPa rocks break with a constant critical stress intensity factor whereas below 10 GPa they break reaching a critical cohesion, i.e a critical tensile strength. These results are very important for the prediction of fracture dynamics and seismicity during fluid injection, especially since we see a transition from one failure regime to another at around 10 GPa, a Young's modulus that lies in the middle of possible values for natural shale rocks.

Mica deformation mechanisms in mylonitic shear zones: implications for strain localisation and rheology in the mid-crust

J. Aslin[1], E. Mariani[1], J. Wheeler[1], D. Faulkner[1] & K. Dawson[2]

[1]School of Environmental Sciences, University of Liverpool, Liverpool, UK (joeaslin@liverpool.ac.uk)
[2]Nanoinvestigation Centre at Liverpool, University of Liverpool, Liverpool, UK

Phyllosilicates such as micas are ubiquitous in the Earth's crust and are often observed to play a key role in the localisation of strain in crustal shear zones. Despite this, relatively little is known of the deformation behaviour of micas in the mid crust relative to other common phases such as quartz and feldspar. It is recognised that low stresses are required to activate dislocation glide on the basal plane of micas, but is this sustainable to high strains? The pile-up of dislocations and kinking processes lead to strain hardening and other mechanisms must be active that can accommodate deformation to high strain. This work aims to determine the mechanisms responsible for deformation within micas under mid crustal conditions through the study of a phyllosilicate-rich mylonitic shear zone at a variety of scales. Detailed field mapping and systematic sample collection was conducted along several transects of the amphibolite facies Cossato-Mergozzo-Brissago (CMB) line in Northern Italy. This was followed by microstructural observations using optical, scanning electron (SEM) and transmission electron microscopy (TEM) techniques. The mylonites studied had granitic (typical assemblage: quartz + albite + K feldspar + biotite + muscovite) and pelitic (typical assemblage: quartz + albite + biotite + muscovite + garnet +/- silimanite +/- kyanite) protoliths and were rich in phyllosilicates. Basal slip appears to be the dominant mechanism within micas during the initial stages of deformation and at lower strain. However, under higher strain conditions biotite undergoes extensive grain size reduction by means of a currently undetermined recrystallisation mechanism. This results in the development of an interconnected network of very fine grained (≈1μm) biotite and quartz. Muscovite by contrast is apparently unaffected by this recrystallisation stage, retaining a coarser grain size even in the highest strain ultramylonites. Nanostructural observations via TEM imaging reveal a variety of microstructures which could provide insights into the deformation mechanisms active within this fine grained matrix. Strain partitioning into a weak mica phase may have a significant impact on the strength of mica-rich mid-crustal shear zones as well as our understanding of crustal rheology.

Structural evolution of Arunachal Lesser Himalayan Fold Thrust Belt: Preliminary results from fracture and stable isotope analysis of carbonates

A. Basa[1], F. Ahmed[1], K. Bhattacharyya[1] & P. Sanyal[1]
[1]*Indian Institute of Science Education and Research Kolkata, India*
(ab14ip046@iiserkol.ac.in)

Fractures of different orientations form as deformation progresses in an evolving orogenic wedge. Orientation of fracture sets and their population vary as a function of structural position of the host rock in a fold thrust belt (FTB). These fractures exert a strong influence in fluid migration. In Siang Valley of Arunachal Himalayan FTB, the Buxa Group of rocks of the Main Boundary thrust (MBT) sheet is repeated at least twice at different structural positions, and is folded by the underlying footwall structures. We integrate fracture population study and stable isotope analysis of the Buxa carbonate rocks from the Siang Valley to examine the forelandward progressive evolutionary path of the deformation front.

Microscopic analysis from five samples each from the hinterland and the foreland MBT sheets suggests that the hinterlandmost thrust sheet records ~37% of fractures which increases to ~63% in the foreland. This increase is due to forelandward dominance of frictional deformation mechanisms as overburden decreases towards the foreland, coupled with shallower depth of fault rocks due to fault cutting up-section. Additionally, there is a spatial variation in the orientation of fractures in the carbonate samples. Buxa carbonates from the hinterland thrust sheet record almost similar percentages of high angle (~35%), oblique (~33%) and sub-parallel (~32%) fractures, all measured with respect to the bedding. In contrast, the forelandmost thrust sheet records a dominance of late, high angle fractures (~48%), while abundance of oblique and sub-parallel fractures are ~26%. Based on offset of fractures, studied at both outcrop and microscopic scales, the earliest fractures are the low-angle fractures, while the high-angle fractures are the youngest. Most of these fractures are filled in by fluids forming veins composed of calcite, dolomite and quartz. There is no systematic variation in the composition of veins across the thrust sheets. Cross-cutting relationships suggest that fluid activity played a major role in almost every stage of deformation. In the hinterland, ~70% of the fractures are converted to veins, while ~91% of the fractures are fluid filled in the foreland. This indicates an increase in fluid activity as deformation progresses forelandward. The deformation temperature of the veins estimated from recrystallized quartz grain sizes decreases from hinterland (440$\pm$30°C) to foreland (375$\pm$30°C). Interestingly, the preliminary results indicate that the low-angle to oblique veins record a lower deformation temperature than the high angle veins in both the thrust sheets.

Preliminary results from stable isotope analysis of the calcite veins suggest different sources for the veins. For example, the bedding sub-parallel and oblique veins have less difference in their $\partial^{18}O$ values (~0.5-2 ‰ in VPDB), with respect to the host rock, indicating intraformational fluid source. In contrast, some of the late high-angle veins in both hinterland and foreland thrust sheets show prominent difference in $\partial^{18}O$ values, relative to the host rocks (~5-7‰ in VPDB). This possibly suggests a signature of channelized flow and meteoric influence.

Kinematic evolution of Pan-African granitoids of Western Cameroon-Domain: an anisotropy of magnetic susceptibility (AMS) and electron backscattered diffraction (EBSD) approach

B.E. Bella Nke[1,2,3], T. Njanko[1,4], M.A. Mamtani[3], P. Rochette[5] & E. Njonfang[6]
[1]Laboratory of Environmental Geology, Department of Earth Sciences, University of Dschang, P.O. Box 67, Dschang - Cameroon; bellankeedith@gmail.com;
[2]Department of Earth Sciences, Faculty of Sciences, University of Maroua; P.O. Box 46, Maroua - Cameroon;
[3]Department of Geology & Geophysics, Indian Institute of Technology, Kharagpur, 721302, India;
[4]Ministry of Scientific Research and Innovation, DPSP/CCAR, P.O. Box 1457, Yaoundé - Cameroon;
[5]CEREGE UMR7330 Aix-Marseille Université CNRS, 13545 Aix-en-provence, France;
[6]Laboratory of Geology, High Teacher Training School, University of Yaoundé I, P.O. Box 47, Yaoundé - Cameroon.

The emplacement and tectonic evolution of granitoids is often controlled by deformation and tectonics that affects adjacent shear zones. Therefore, fabric that develops in granitoids is known to be a manifestation of regional tectonics, particularly the last stage of the deformation. However, since granites do not always develop visible foliations/lineations, their fabric is commonly detected by carrying out anisotropy of magnetic susceptibility (AMS) measurements. Moreover, detailed microstructural studies, particularly quartz textures are sensitive to temperature, and hence are useful in deciphering the temperature at which magnetic fabric evolved. In this study, we integrate AMS, microstructural and crystallographic preferred orientation (CPO) data from the Mbakop granitic pluton (MGP) of Central Cameroon Shear Zone (CCSZ) in order to decipher its kinematic evolution. The N-S oriented MGP is located at the NW edge of the N30°E branch of the CCSZ in the western part of the Pan-African belt in Cameroon. The pluton comprises biotite (± amphibole) granites that have emplaced in mylonitized gneissic basement. AMS studies on samples from 44 sites within the pluton and 15 sites from the basement gneiss were carried out. The trend of the magnetic foliation varies from NNW to NNE, while the magnetic lineation plunges gently towards the north or south. The rocks have high mean magnetic susceptibility and magneto-mineralogical investigations reveal the presence of multi-domain magnetite. Microstructural studies indicate solid-state deformation marked by the recrystallization of quartz grains and feldspar porphyroclasts wrapped by biotite and quartz ribbons. Kinematic markers such as porphyroclasts and mineral fish indicate that the sense of shear is dominantly top-to-the-north. Electron backscatter diffraction (EBSD) analysis was done to study the CPO of quartz *c*-axis. Three slip systems viz. rhomb <a>, prism <a> and prism <c> were recorded. These slip systems are consistent with microstructure of medium- to high-temperature related to the upper greenschist/lower amphibolite facies conditions. The distribution of quartz *c*-axis is asymmetrical, which implies the role of non-coaxial deformation in controlling the tectonic evolution of fabric in the MGP. The orientation of the CCSZ in the vicinity of MGP is N30°E, which is oblique to the mean orientation of the magnetic foliation (N12°E). Assuming that the latter traces the orientation of maximum instantaneous stretching axis of the strain ellipse, its angular relationship with the former implies that the emplacement and fabric development of the MGP took place under a combination of pure and simple shear. This indicates transpression was important during MGP emplacement.

Acknowledgments: B.E. Bella Nke thanks the Organization for Women in Science for the Developing World (OWSD) to carry out part of this study at IIT Kharagpur (India).

Fluid flow in deforming media: interpreting stable isotope signatures of marbles

C. E. Bond[1]
[1]*School of Geosciences, University of Aberdeen, Aberdeen, UK (clare.bond@abdn.ac.uk)*

Fluid flow in the crust is controlled by permeable networks. These networks can be created and destroyed dynamically during rock deformation. Rock deformation is therefore critical in controlling fluid pathways in the crust and hence the location of mineral and other resources. Here, evidence for deformation-enhanced fluid infiltration shows that a range of deformation mechanisms control fluid flow and chemical and isotopic equilibration. The results attest to localised fluid infiltration within a single metamorphic terrain (12km) over a range of metamorphic grades; ecologite- blueschist to greenschist. For fluid infiltrating marbles during ductile deformation, chemical and isotopic signatures are now homogenous; whilst fluid infiltration associated with brittle deformation results in chemical and isotopic heterogeneity at a microscale. The findings demonstrate how ductile deformation enhances equilibration of $\delta^{18}O$ at a grain scale whilst brittle deformation does not.

The control of deformation mechanisms in equilibrating isotopic and chemical heterogeneities have implications for the understanding of fluid-rock interaction in the crust. Interpretation of bulk stable isotope data, particularly in the use of isotope profiles to determine fluid fluxes into relatively impermeable units that have been deformed need to be used with care when trying to determine fluid fluxes and infiltration mechanisms.

Anisotropic grain growth and modification of 'frozen texture' in the lithospheric mantle

Y. Boneh[1], D. Wallis[2], L. Hansen[2], M. Krawczynski[1] & P. Skemer[1]
[1]Washington University in St. Louis, Department of Earth and Planetary Sciences, One Brooking Drive, MO 63130 (boneh@levee.wustl.edu).
[2]Oxford University, Department of Earth Sciences, Oxford, United Kingdom

Seismic anisotropy is widely observed in both the lithospheric and asthenospheric upper mantle, and is mainly caused by flow-induced alignment of anisotropic olivine crystals. Crystallographic preferred orientation (CPO) in the asthenosphere is thought to reflect the dynamics of current mantle flow. In contrast, the lithosphere is relatively viscous, and, it is assumed that texture in the lithosphere retains a memory of past flow (e.g., lithospheric mantle in an oceanic basin preserves texture that originated from corner flow at the mid-oceanic-ridge). Although the viscosity of the lithosphere is high in comparison to the asthenosphere, temperatures are high enough that non-deformational, microstructural processes may still be significant for texture evolution. Here we use an experimental approach to simulate a textured mantle annealed under high temperature, high pressure, and hydrostatic conditions, in order to investigate whether microstructural evolution due to static annealing could modify texture in the lithospheric mantle.

Starting material for the experiments was a synthetic Fo50 olivine aggregate that was previously deformed in torsion (Hansen et al., 2016) to shear strains up to ~10. The sample has a mean grain-size of ~15 microns and a narrow, unimodal grain-size distribution, high dislocation-densities (up to ~10^{15} m^{-2}), and exhibits a strong A-type CPO. Sub-samples of the deformed specimen were annealed under hydrostatic conditions using a piston cylinder apparatus at T = 1250º C, P = 1 GPa for up to one week. After annealing, the samples were cut into thin sections and the crystal orientations were measured by electron backscatter diffraction (EBSD). The samples show clear evidence for abnormal grain growth due to annealing (with maximum grain sizes of ~1 mm). The abnormally large grains grew at the expense of the smaller matrix grains, and grain-size distributions became distinctly bimodal. The small grains not consumed by abnormal grain growth have similar CPO strength, symmetry, and orientation compared with the starting material's CPO. The orientation of the abnormally large grains is typically 10–30 degrees away from the original CPO on the X-Z plane. This observation is consistent with predictions that abnormal grain growth favors grains with low initial Schmid factors. Seismic anisotropy of both deformed and annealed mantle layers were calculated and compared. We conclude that reorientation and weakening of olivine CPO is expected during periods of tectonic quiescence, which will modify the anisotropic signature imposed during the primary deformation event.

References:

Hansen, L.N., Warren, J.M., Zimmerman, M.E., Kohlstedt, D.L., 2016. Viscous anisotropy of textured olivine aggregates, Part 1: Measurement of the magnitude and evolution of anisotropy. Earth and Planetary Science Letters 445, 92-103.

Folds and shear zones in the Greenland Ice Sheet

P.D. Bons[1], D. Jansen[2], M.-G. Llorens[1,2], T. de Riese[1], T. Sachau[1], F. Steinbach[1,2] & I. Weikusat[1,2]

[1]Dept. of Geosciences, Eberhard Karls University Tübingen, Germany (paul.bons@uni-tuebingen.de)
[2]Glaciology Department, Alfred Wegener Institute, Helmholtz Centre for Polar and Marine Research, Bremerhaven, Germany

The flow of ice towards the margins of ice sheets is far from homogeneous. Ice streams show much higher flow velocities than their surroundings and may extend, as does the North East Greenland Ice Stream (NEGIS), towards the centre of the sheet. The elevated flow velocity inside an ice stream causes marginal shearing and convergent flow, which in turn leads to folding of ice layers. Such folding was documented in the Petermann Glacier in northern Greenland by Bons et al. (2016).

3-dimensional structural modelling using radargrams shows that folding is more intense adjacent to NEGIS than inside it, despite the strong flow perturbation at NEGIS. Analysis of fold amplitude as a function of stratigraphic level indicates that folding adjacent to NEGIS ceased in the early Holocene, while it is currently active inside NEGIS.

The presence of folds adjacent of NEGIS, but also at other sites far in the interior of the Greenland Ice Sheet with no direct connection to the present-day surface velocity field, indicates that ice flow is not only heterogeneous in space (as the present-day flow velocity field shows), but also in time. The observations suggest that ice streams are dynamic, ephemeral structures that emerge and die out, and may possibly shift during their existence, but leave traces within the stratigraphic layering of the ice.

The dynamic nature of ice streams such as NEGIS speaks against deterministic models for their accelerated flow rates, such as bedrock topography or thermal perturbations at their base. Instead, we suggest that ice streams can also result from strain localisation induced inside the ice sheet by the complex coupling of rheology, anisotropy, grain-size changes and possibly shear heating.

Bons, P.D., Jansen, D., Mundel, F., Bauer, C.C., Binder, T., Eisen, O., Jessell, M.W., Llorens, M.-G, Steinbach, F., Steinhage, D. & Weikusat, I. 2016. Converging flow and anisotropy cause large-scale folding in Greenland's ice sheet. Nature Communications 7:11427, DOI: 10.1038/ncomms11427.

Crack damage evolution in rocks deformed under true triaxial loading

J. Browning[1], P. Meredith[1], D. Healy[2], S. Harland[2], C. Stuart[1] & T. Mitchell[1]

[1]Department of Earth Sciences, University College London, Gower Street WC1E 6BT (j.browning@ucl.ac.uk)
[2]School of Geosciences, University of Aberdeen, Aberdeen AB24 3UE.

Microcrack damage in rocks evolves in response to differential loading. However, the vast majority of experimental studies investigate damage evolution using conventional triaxial stress states ($\sigma_1 > \sigma_2 = \sigma_3$), whereas in nature the stress state is in general truly triaxial ($\sigma_1 > \sigma_2 > \sigma_3$). We present a comparative study of conventional triaxial vs. true triaxial stress conditions using results from measurements made on cubic samples of sandstone deformed in three orthogonal directions with independently controlled stress paths. We have measured, simultaneously with stress and strain, the changes in ultrasonic compressional and shear wave velocities in the three principal directions, together with the bulk acoustic emission (AE) output. Changes in acoustic wave velocities are associated with both elastic closure and opening of pre-existing cracks, and the formation of new, highly oriented, cracks by inelastic processes. By contrast, AE is associated only with the inelastic growth of new cracks. Crack growth is shown to be a function of differential stress regardless of the mean stress. New cracks can form due to a decrease in the minimum principal stress, which reduces mean stress but increases the differential stress. We measure the AE, in both conventional triaxial and true triaxial tests and find an approximately fivefold decrease in the number of events in the true triaxial case. In essence, we create two end-member crack distributions; one displaying cylindrical transverse isotropy (conventional triaxial) and the other planar transverse isotropy (true triaxial). By measuring the acoustic wave velocities throughout each test we were able to model comparative crack densities and orientations. When taken together the AE data, the velocities and the crack density data indicate that the intermediate principal stress plays a key role in suppressing the total amount of crack growth and concentrates it in a single plane, but the size of individual cracks remains constant. Hence, the differential stress at which rocks fail (strength) will be significantly increased under true triaxial stress conditions than under the much more commonly applied condition of conventional triaxial stress. Through a series of cyclic loading tests, we show that while individual stress states are important, the stress path by which this stress state is reached is equally important. Whether or not that stress state has been 'visited' before is also vitally important in determining and understanding damage states. Finally, we show that damage evolution can be anisotropic and must be considered as a three-dimensional problem. Such results are important for understanding three-dimensional crack damage evolution which is likely a key control on fluid migration in volcanoes and fault zones.

Pore geometry as a control on rock strength

A. Bubeck[1], R.J. Walker[1], D. Healy[2], T. Davies[2], M. Dobbs[3] & D.A. Holwell[1]
[1]*Department of Geology, University of Leicester, Leicester, UK (ab711@le.ac.uk)*
[2]*School of Geosciences, University of Aberdeen, Aberdeen, UK*
[3]*Rock Mechanics and Physics Laboratory, British Geological Survey, Keyworth, UK*

The strength of porous rocks in the subsurface is critically important across the geosciences, with implications for fluid flow, mineralization, seismicity, and the deep biosphere. Most studies of porous rock strength consider the scalar quantity of porosity, in which strength shows a broadly inverse relationship with total porosity, but pore shape is not explicitly defined. It is typical to assume either isotropic porosity, or anisotropic porosity related to foliations (bedding, fractures, banding). Porosity in these cases is dominated by pores and cracks with a low aspect ratio (i.e. much longer than they are wide).

Here we focus on the mechanical response of intermediate aspect ratio pores to an applied load. We present uniaxial compressive strength (UCS) measurements of a combination of isotropic and anisotropic porous lava samples, and numerical models to consider the influence of porosity *and* pore shape on rock strength. Samples were collected from a pristine 750-year-old lava from the south flank of Kilauea Volcano, Hawai'i, which is representative of near-surface pahoehoe lavas in the area. Detailed physical characterisation reveals an internal architecture that can be separated into three components, based on changes in the distribution of vesicles: (1) a top zone with 20-30% porosity; (2) a core zone with 10-12% porosity; and (3) a base zone with 15-19% porosity. Micro-computed tomography (CT) of prepared samples show that pores in lavas range from sub-spherical in the top and core zones, to elongate and flat quasi-ellipsoidal in the base zones, and these are aligned sub-horizontally (parallel to bedding); in the lava core and top zones, the minor fraction of non-spherical vesicles appear to be randomly oriented.

Compressive strength shows a general inverse relationship with porosity, but basal zone samples that contain aligned flat pores exhibit a large strength anisotropy, dependent on the compression direction relative to pore short axes. When compression is applied parallel to the pore short axes (i.e. across the minimum curvature), samples are weak; compression applied parallel to the long axes (i.e. across the maximum curvature) are stronger by nearly an order of magnitude. The porosity for these samples was relatively constant at ~15-19%, hence porosity itself is not responsible for the variation in measured rock strength. 2D numerical models for isolated elliptical pores show that compression applied across the minimum curvature results in a relatively broad tensile stress perturbation, compared to compression applied across the maximum curvature, implying that this configuration is relatively stable under compression, supporting UCS results. We also present findings from 3D numerical models, which demonstrate that stress distributions around pores are not only controlled by their geometry, but also their orientation and proximity to neighbouring pores.

At a larger scale, certain pore shapes may be relatively stable and remain open in the upper crust under a given remote stress field, facilitating persistent cavities. These high permeability zones could provide sustained conduits or stores for economic resources, or even sites for sub-seafloor microbial reservoirs. Quantifying the shape, orientation, and statistical distributions of pores is a critical step in strength testing of rocks. Without adequate characterisation, mechanical test results are not directly comparable and porosity-based models are not robust.

Vertical axis rotations during normal fault propagation and linkage: application to the evolution of the NE Atlantic

A. Bubeck[1], R.J. Walker[1], J. Imber[2], R.E. Holdsworth[2], R.W. England[1] & D.A. Holwell[1]
[1]*Department of Geology, University of Leicester, Leicester, UK (ab711@le.ac.uk)*
[2]*Department of Earth Sciences, Durham University, Durham, UK*

Mechanical interaction between propagating normal fault segments can have an important influence on the geometry of the evolving fault system, including the linkage geometry of first order faults, and the development of second order faults and fractures within developing inter-fault (relay) zones. Displacement on normal faults is typically considered with emphasis on the vertical motion (fault throw), which can be measured using offset bedding, either in the field, or using high-resolution seismic imaging. In horizontally layered materials, displacement (throw) gradients on en echelon normal faults are commonly accommodated by relay structures, requiring horizontal axis bending of the host layering. The relay ramp also requires a component of vertical axis rotation to maintain the connection between the hanging wall and footwall, and accommodate bounding fault heave gradients. Few studies, however, account for either the vertical axis rotation, or the heave gradient profile between faults. Heave gradients are particularly important in horizontally layered materials, because the material is required to bend or stretch within the layer plane, which may lead to complex fault and fracture patterns.

Here we present field examples of growth faults from two active volcanic rift zone segments - the Koa'e (Big Island, Hawaii) and Krafla (northern Iceland) fault systems - to illustrate the importance of vertical axis rotations. Regional extension in these fault systems is accommodated by a series of segmented normal faults that are parallel to the main rift system. Detailed field mapping reveals that second order faults and fractures within the relay zones can be separated into two sets: (1) *rift-normal* extension mode fractures that strike at a high angle (i.e. >45°) to the main rift faults; and (2) *rift-oblique* extensional shear faults that strike at a low angle (i.e. <45°). We propose that rift-oblique faults facilitate a vertical axis rotation between the main rift faults, following a bookshelf-like faulting mechanism, which would typically involve a rift-normal material thickening, and a rift-parallel material thinning. Rift-normal fractures provide a negligible contribution to the regional extension vector, but facilitate a rift parallel extension that counteracts rift-parallel thinning, resulting in an overall volume increase within the rift zone. At the surface, this increase is accommodated by the development of open fissures, but importantly, may be accommodated in the subsurface by dyke emplacement oblique to, and normal to the rift axis.

Block rotations have been shown previously to operate across all scales, including between rift segments. Here we apply a block rotation model to deformation associated with the propagation and linkage of segmented rift basins on the NE Atlantic margins. New and published data for fault and intrusion sets in the Kangerlussuaq region (East Greenland margin), and the Faroe Islands (European margin) show that continental rifting and basin development was contemporaneous with rift-oblique extensional shear faults and dykes, and rift-normal dykes and normal faults. Traditionally these ancillary structural sets have been interpreted as transfer zones. Here we interpret them to represent ancillary fault and intrusion sets as a consequence of rotational strains driven by a progressive vertical axis block rotation during the propagation of a dual rift system: in this instance, involving a NE-propagating Reykjanes ridge, and a SW-propagating Aegir ridge.

Investigating the interplay of rift velocity variations and initial crustal rheology for the North Atlantic rifted margins

S. Buiter[1,2] & G. Shephard[2]
[1]*Geological Survey of Norway, Trondheim, Norway (susanne.buiter@ngu.no)*
[2]*Centre for Earth Evolution and Dynamics, University of Oslo, Norway*

The continental margins of Norway and Greenland formed during intermittent rifting over several hundreds of millions of years, starting in the Carboniferous and finally leading to seafloor spreading in the early Eocene. Several alternative regional plate reconstructions predict different timings and rates of relative motion between Norway and Greenland. Notably, the models predict varying episodes of compression or quiescence, not only orthogonal or oblique rifting. The velocity of rifting affects plate margin architecture because of the velocity dependence of ductile crustal rheology and because of thermal cooling (and associated ductile strengthening) during periods of tectonic quiescence.

The interdependency of velocity and rheology also implies that the choice of initial crustal rheology is of prime importance in dynamic models of rifted margin formation. However, we have little constraint on crustal thickness and rheology at the onset of each successive rifting phase for the North Atlantic margins. Caledonian mountain building caused by the Silurian continent-continent collision between Baltica and Laurentia was followed by extensional collapse and the formation of Devonian sedimentary basins. The crust at the onset of initial rifting must thus have been characterized by profound structural inheritance, but neither it's extent nor the crustal thickness are known.

Here we use numerical models of rifting to test how alternative rift velocity histories, as predicted by different regional plate reconstructions, interplay with crustal rheology and initial crustal thickness. We use the 2D version of SULEC, a thermo-mechanical finite-element code that solves the incompressible momentum equation coupled with the energy equation. We quantify the duration of rifting until break-up, surface topography and velocity variations over the margins. Our experiments confirm earlier results that intermediate to high strength crust tends to favour fast continental breakup with reduced sensitivity to the applied extension velocity. A systematic suite of experiments illustrates how structural inheritance (in the form of small domains of low brittle strength) and crustal thickness variations increase the sensitivity of margin architecture to velocity variations.

Metamorphic interaction and deformation in the contact of olivine melilitite dyke with granite, the Krkonoše-Jizera Composite Massif, Czech Republic

Z. Bukovská[1], T. Larikova[1] & J. Klomínský[1]
[1]*Czech Geological Survey, Prague, Czech Republic (zita.bukovska@geology.cz)*

This contribution represents first results of detailed investigation of mineral chemistry and deformation on the microscale of the interaction between olivine melilitite and granite studied using electron back-scattered diffraction and microprobe analysis.

A swarm of melilitite dykes (polzenites) in the Krkonoše-Jizera Composite Massif occurs along NE-SW cross faults showing interconnection with the “Devil Walls” tectonic structures in the Bohemian Cretaceous Basin (Klomínský et al. 2002). Alkaline and ultraalkaline rocks with melilititic association of upper cretaceous up to paleogene age are of mantle origin and represent products of magmatic activity of Eger rift (Ulrich et al. (1988). One of these olivine-melilititic dykes (approx. 70 cm thick) outcropped in an abandoned quarry in Liberec granite (Gränzer 1929) on the Výšina hill in Liberec. The dark grey olivinic melilitite with porphyric texture consists of olivine, augite, melilite and biotite, magnetite, perovskite and haüyn. Idiomorphic crystals of olivine (up to 2 mm) are completely serpentinized; pyroxenes are zoned . This melilite dyke is 61.9 ± 3.0 Ma old according to the K-Ar dating (Pécskay, 2008), and it encloses xenolites of Liberec granite of Variscan age (320 Ma, U/Pb zircon age, Žák et al. 2013) with tracks of ‘pyrometamorphic destruction’ (Grapes 2006). Thermal shock in the granite caused by melilitite emplacement is recorded by volume expansion, hydraulic cracking, microfracturing and local melting; this is evident from transformation of biotite to magnetite, partial melting of alkali feldspars, and occurrence of glass and mullite. This mineral association may document the temperature at the exocontact around 900 °C, and also rapid cooling of the rocks (Kaczor et al 1988).

Metasomatic zoning (~5 mm in width) with several clear zones was found at the contact of the olivine-melilitite and granite. The mineral composition of the zones varies according to the gradients in composition, temperature and chemical potentials, showing different mobility of the elements during this interaction.

References:

Gränzer, J. (1929): Tertiare vulkanische Gesteine in der Umgebung von Reichenberg in Bohmen. Mitteilungen des Vereines der Naturfreunde in Reichenberg 51. Jahrgang.
Grapes, R. (2006): Pyrometamorphism. Springer-Verlag Berlin Heidelberg. pp. 275.
Kaczor, S.M., et al (1988): Disequilibrium melting of granite at the contact with a basic plug: A geochemical and petrografic study. Journal of Geology ,1988,vol.96, p. 61-78.
Klomínský. J., Mrázová, Š., Šalanský, K. (2002): Neovolcanites in the vicinity of Liberec, its geophysical significance and regional geological importance (in Czech). Zprávy o geologických výzkumech v roce 2001, 36-39.
Pécskay, Z. (2008): K/Ar age determination on intrusive magmatic rocks of SURAO project 2008. Institute of Nuclear Research of the Hungarian Academy of Sciences (ATOMKI), Debrecen, Hungary. Research report.
Žák, J., Verner, K., Sláma, J., Kachlík, V., Chlupáčová M. (2013): Multistage magma emplacement and progressive strain accumulation in the shallow-level Krkonoše-Jizera Massif complex, Bohemian Massif. Tectonics, 32, 1493–1512.

Initial research on geological conditions in the Underground Research Facility Bukov, Bohemian Massif, Czech Republic

Z. Bukovská[1], K. Verner[1], P. Dobeš[1], I. Soejono[1], D. Buriánek[1], R. Nahodilová[1], O. Švagera[1], F. Tomek[2], L. Vondrovic[3] & Z. Pécskay[4]

[1]Czech Geological Survey, Prague, Czech Republic (zita.bukovska@geology.cz)
[2]Institute of Geology, Czech Academy of Sciences, Prague, Czech Republic
[3]Radioactive Waste Repository Authority (RAWRA), Prague, Czech Republic
[4]Institute for Nuclear Research, Hungarian Academy of Sciences, Debrecen, Hungary

In the high-grade rocks of the Moldanubian Domain (Bohemian Massif) is being built unique underground research laboratory Bukov situated on level 12 of the uranium mine Rožná. The laboratory is projected for series of research experiments focused on long term safety and technical feasibility of a future deep geological repository of radioactive waste. Newly excavated underground complex provides exclusive possibility to understand the overall geological conditions of the rock environment at the depth of c. 550 m below the surface and obtain relevant data to build representative geological model. The initial multidisciplinary research included detailed study of petrology, geochemistry, structural geology, systematic study of radiometric dating of mineralisation events, hydrogeology and hydrogeochemistry.

The underground laboratory is situated mostly in migmatites, migmatitic paragneisses and amphibolites that were affected by several ductile and brittle deformation events. Discrete fractures along shear zones are filled with quartz and carbonates, whereas the up to several meters wide altered zones are formed mostly by calcite, chlorite, micas, hematite, palygorskite, kaolinite, smectite, illite and zeolite. On the basis of structure, stable isotope and fluid inclusions, at least two generations of post-uranium veins were distinguished.
K–Ar dating of newly-formed illite/smectite mineral fractions from two major shear zones yielded ages of 287-307 Ma for E–W trending zone, and 250-256 Ma for N–S trending zone. These newly obtained K–Ar ages are in full accordance with the previous K–Ar and U–Pb data of altered zones of the Rožná uranium deposit (Kříbek et al. 2009) and unequivocally post-date the major fault activity. Quantification of magnetic fabrics and parameters, using the anisotropy of magnetic susceptibility (AMS) technique, revealed two different clusters of magnetic foliations concordant with observed macroscopic metamorphic fabrics. Less pronounced, relatively older magnetic foliations are steep and strike ~NNW–SSE with associated magnetic lineations varying from mostly subvertical to shallowly plunging to the ~SSE. Dominant, younger magnetic foliations are gently to moderately diping to the ~S–SW and are associated with lineations gently plunging to the ~SSE–SSW.

Taken together, our data show that the rocks of the underground research laboratory Bukov represent volcano-sedimentary complex intensively reworked during the Variscan orogeny at about 340 Ma. The fabric pattern probably reflects the complicated tectonometamorphic evolution of thickened orogenic root in the mid-crustal level. The older fabrics, most likely related to the initial ~ENE–WSW subhorizontal compression, were heterogeneously overprinted by subvertical shortening and ~N–S horizontal stretching during final exhumation. The region subsequently underwent polyphase faulting, shear reactivations and associated mineralization events prior to the end of Permian. Obtained data will be further investigated and presented in the form of 3D model, moreover the AMS data will be correlated with observations from electron back-scattered diffraction analysis and results from diffusion experiments.

Fabric pattern and emplacement of post-collisional Tekeze Pluton (Arabian-Nubian Shield; Northern Ethiopia)

D. Buriánek[1], L. Megerssa[2,3] & K. Verner[1,2]
[1]*Czech Geological Survey, Klárov 3, Prague, 11821, Czech Republic (david.burianek@geology.cz)*
[2]*Institute of Petrology and Structural Geology, Charles University, Albertov 6, Prague, 12843, Czech Republic*
[3]*Geological Survey of Ethiopia, CMC Road, P.O.Box 2302, Addis Ababa, Ethiopia*

The Tekeze pluton (~7 km by 5 km in extent) built by pyroxene-amphibole to amphibole-biotite monzodiorite and quartz monzonite is a typical post-collisional intrusive body emplaced into low-grade metasedimentary sequence of the Neoproterozoic Tambien Group belonging to the Tokar-Barka terrain in the southern part of the Arabian–Nubian Shield. The pluton has a discordant intrusive contacts with asymmetrically folded metamorphic foliation having steep ~NW or SE dipping axial planes and gently ~NE plunging fold axes. The thermal and structural aureole reaches about 500 meters in extent around the pluton. Well-developed magmatic to sub-magmatic foliation dips steeply from ~NW to NNW which is partly discordant to the intrusive contacts and fabrics in the thermal aureole of the pluton. We used the Anisotropy of Magnetic Susceptibility method (AMS) to evaluate mezoscopic fabric pattern. The mean bulk magnetic susceptibility (km) ranges widely from 2,02 x 10^{-4} to 3.18 x 10^{-3} [SI]. The degree of anisotropy (P parameter) is relatively low ranging from 1.069 to 1.161. The susceptibility ellipsoid shapes (T parameter) are almost evenly distributed between slightly prolate to oblate with values ranging from -0.64 and 0.86. Our AMS study revealed magnetic foliations dipping gently to moderately to ~SW with lineations shallowly plunging to the ~S to SSW and magnetic foliations having a subvertical orientation trending ~ENE–WSW bearing steeply plunging magnetic lineations. Monzodiorites to quartz monzonites contain biotites (^{IV}Al = 2.29–2.43 apfu, X_{Fe} = 0.45–0.53) partly affected by a pervasive chloritization. Amphiboles range from magnesio-hornblende, pargasite, edenite to actinolite (Si = 6.34–7.70; X_{Mg} = 0.59–0.79). Rare diopsides (X_{Fe} = 0.26–0.27) are often overgrown by amphiboles. These rocks display a high-K calc-alkaline trend (K_2O = 1.1–3.3 wt. %), have an intermediate to acidic (SiO_2 = 51.7–62.7 wt. %), subalkaline (K_2O+N_2O = 5.3–7.8 wt. %) and metaluminous composition (A/CNK = 0.79–0.98). These rocks show HREE-depleted REE patterns (La_N/Yb_N = 6.8–15.6) with either no Eu anomaly or small negative Eu anomalies (Eu/Eu* = 0.8–1.0). Zircons extracted from the quartz monzonite with clear, euhedral-shape crystals and uniform bright sector zonation in CL were used for dating. The apparent darker cores provided identical U/Pb ages to the rims, indicating they grew during a single magmatic event of magma solidification with a concordant age 618.1 ± 1.5 Ma. P–T conditions of magma emplacement were calculated using amphibole and plagioclase at 0.32–0.43 GPa and 680 to 777 °C. Similar P-T data (0.41 ± 0.09 GPa and 634 ± 78 °C) were obtained based on stable mineral assemblage of garnet-biotite-cordierite hornfels xenolite. Chemical difference between monzodiorite and quartz monzonite results from magma mingling and hybridization. The Tekeze pluton was emplaced diapirically at around 13 kilometers in depth. During magma crystallization the pluton recorded an increment of regional stress-field of ~NW–SE transpression of Pan-African Orogeny.

The pegmatite paradox: competing rates of deformation and crystallization

R. Butler[1] & T. Torvela[2]
[1]*School of Geosciences, University of Aberdeen, UK (rob.butler@abdn.ac.uk)*
[2]*School of Earth and Environment, University of Leeds, UK*

Broadly syn-tectonic granitic pegmatites are widely found within exhumed parts of ancient (and modern) orogens. Hydrous granitic melts are significantly less viscous than their anhydrous counterparts and consequently granitic pegmatites that crystallize from them are widely separated both spatially and thermally from their source regions. Just as their low-viscosity permits long-distance migration, these fluids might be expected focus strain if they intrude actively deforming crust. Yet commonly pegmatite veins are buckled, their interfaces are cuspate and they have boudinaged into pods – structures that collectively indicate that they deformed more competently than the rocks within which they reside. Pegmatite pods commonly show "stiff inclusion" rotational behaviours indicated by the geometry of the deflected foliation in surrounding rocks. Thus the structure of granitic pegmatites indicates that they were stronger, not weaker, than the rocks into which they were emplaced. We illustrate this paradox using an example from the Scottish Caledonides – the Torrisdale vein complex of northern Sutherland. We conclude that although deformation of the pegmatites happened before they were fully crystallized, the syn-kinematic crystal mush was more competent than the surrounding country rocks. Even the partially crystallized pegmatites behaved more competently than the surrounding rocks. The absence of weak inclusion behaviour requires that the pegmatite veins achieved their competent state significantly more rapidly than they were able to accumulate strain. This deduction conforms with modern results that indicate exceptionally fast ($cm.a^{-1}$) crystal growth rates for the undercooled magmas from which pegmatites are formed. Thus although very weak melts were present in the Caledonian crust (and other examples) as it deformed, they retained this rheology for tectonically insignificant time-scales.

Paradoxical mid-crustal displacements, transposition and stratigraphic continuity: an integrated geological and geophysical study of tectonic evolution of the Paleoproterozoic Amer Group, Nunavut, Canada

L. Calhoun[1], J.C. White[1] & C.W. Jefferson[2]
[1]Dept. of Earth Sciences, University of New Brunswick, Fredericton, NB Canada (clancy@unb.ca)
[2]Geological Survey of Canada, 601 Booth Street, Ottawa, ON Canada

The Paleoproterozoic Amer Group, central Nunavut, comprises four dominantly sedimentary sequences (PS1 through PS4) deposited unconformably on Archean basement of the Rae structural sub-province. Intense deformation and crustal thickening occurred as three events, where D1 produced multiple transposition (three fold generations) and displacement along discrete detachments resulting in sub-horizontal axial surfaces and tectono-stratigraphy, D2 generated the regional, generally upright synclinoria, and is separated from D1 by the Ps3-Ps4 unconformity. Late D3 folds with sub-horizontal axial surfaces are rare. The region is transected by arrays of ENE- and NW- trending faults. A major historical distraction in correlation of this belt with temporally related, higher-grade sequences has been the gross stratigraphic continuity of the sedimentary packages when compared to type sections; that is, there was an underlying inference of minimal internal disruption that produced an distinct tectonic paradox.

The difficulties of dealing with this polydeformed terrane are exacerbated by the absence of exposure in critical areas. This problem has been addressed by integrating detailed outcrop examination with high-resolution aeromagnetic data, legacy drill hole data and gravity modelling. The analysis is dependent on the strong, but distinct magnetic responses of the magnetite-bearing Three Lakes and Showing Lakes formations that, in preserved stratigraphic sequences are separated by the Oora Lake Fm. The aforesaid approach has enabled identification of a consistent, yet distinctly different geometry for the Amer Group “basins”. In contrast to the apparent straightforward structure of the regional D2 synclinoria, it is demonstrated that the D1 tectono-stratigraphy forms large, regional recumbent structures masked by the lack of outcrop, but for which evidence occurs at all scales and within separate data sets i.e. field, geophysics, drill hole. The occurrence in some areas of elongate “cigar-shaped” mineralized zones reflects concentration within D1 hinge zones coaxially overprinted by D2. The heterogeneity of deformation throughout this mid-crustal section again emphasizes the inherent importance of rheological partitioning during continental crust evolution.

The transcurrent shear zone system of the Ribeira Belt, SE Brazil

G. Campanha[1] & F. Faleiros[1]
[1]*Institute of Geosciences, University of São Paulo, São Paulo, Brazil, ginaldo@usp.br*

The Neoproterozoic Ribeira Belt in Southeastern Brazil is characterized by a braided network system of dextral strike-slip shear zones that extends for about 950 km (outcropping). It can be viewed as a macro deformation band bordered by major directional shear zones with a sigmoidal internal pattern of shear lenses observable in the most different scales.

This system has great importance in the regional tectonic compartimentation and in the strain distribution pattern, not only in the shear zones but also in the structures of the intervening blocks, as shown by the broad sigmoidal inflections of the regional structures, the increasing deformation toward the shear zone centers, and the prevalence of subhorizontal stretching lineations.

Minimum ductile displacements were estimated for some individual shear zones: 150 km (Lancinha), 70 km (Ribeira) 100 km (Taxaquara) and 150 km (Além Paraíba). The sum of the individual displacements along the strike-slip system is at least 600 km.

There are roughly two tectonic trends, an older with NNE-SSW direction, and a younger ENE-WSW. The ENE structures deflect and rotate the NNE with a dextral sense. Directions around NNE are the same of Brasilia and Araçuai belts to the north. The strike-slip system corresponds to the termination of these two orogens.

Especially important crustal limits have been assigned to the shear zones of Jundiuvira / Rio Preto to the north, and Lancinha / Cubatão to the south. These two megastructures delimit a central belt with upright foliations with respect to adjacent blocks, in which low dip-angle shear zones in a fan-like pattern predominate, both north and south.

Seismic anisotropy shows that the ENE vertical foliation with subhorizontal lineation reaches the upper mantle under the Ribeira Belt. Thus, the region was probably a transform plate limit in the period 600-500 Ma, involving both continental crust and closing oceans.

The collisional suture zone was dismembered during this continental-scale strike-slip system and the Lancinha-Cubatão Fault Zone probably does not represent exactly the locus of the suture zone, but it is mostly likely a transcurrent reactivation during the late oblique collisional period.

Seismic behaviour and strength evolution of heterogeneous upper crustal fault zones: environmental constraints on pseudotachylytes in the Outer Hebrides Fault Zone, UK

L. Campbell[1], G. Lloyd[2], R. Phillips[2], R. Walcott[3] & R. Holdsworth[4]
[1]School of Geography, Earth and Environmental Sciences, Plymouth University, UK (lucy.campbell@plymouth.ac.uk)
[2]School of Earth and Environment, University of Leeds, UK
[3]National Museums Scotland, Edinburgh, UK
[4]Department of Earth Sciences, Durham University, Durham, UK

Major crustal faults may exhibit long-lived seismic activity (and hence strength) despite the progressive evolution of processes such as fault core weakening and localisation associated with fault maturity. This is due to heterogeneity resulting from variable fluid infiltration, lithological variation and structural segmentation through the fault zone. In the Outer Hebrides Fault Zone (OHFZ), NW Scotland, evidence for repeated seismicity occurs in the form of widespread pseudotachylyte, a coseismically generated frictional melt.

The scattered nature of these small seismic faults, with estimated earthquake moment magnitudes ranging between 1.9 – 6.3 M_W, is indicative of a strong, immature fault zone. Strength was maintained across many areas of the fault zone, as indicated by the rarity of multiple slip episodes along individual fault planes. The yield shear strength of pseudotachylyte generating faults is calculated to be as high as ~300-350 MPa, consistent with dry felsic gneisses at depths of 10 km or deeper. This depth range is supported by constraints from ambient temperature estimates, including: a) later greenschist facies alteration; b) undercooling estimated from pseudotachylyte crystalline quench morphologies; and c) plagioclase – amphibole thermometry on pseudotachylyte matrix phases, as well as published temperatures for associated deformation mechanisms.

Pseudotachylytes delineate scattered fault structures across the OHFZ and indicate a variety of kinematic slip phases, including oblique reverse, strike slip, and extension. Discrete generations of pseudotachylyte generation are not distinguishable within the constraints on depth and temperature of seismicity, and apart from a frequent late extensional generation phase, cross-cutting relationships are rarely conclusive. However, these slip senses fit with the progressive kinematic evolution of the OHFZ through the Caledonian Orogeny. Many alternative fault structures used for such kinematic indicators suggest weakening of the fault zone due to weakening reactions and frictional-viscous (aseismic) deformation mechanisms, for example as observed in phyllonite bands. It is concluded that, with seismicity on small, strong, dispersed faults being characteristic of the early brittle history of the OHFZ, fault heterogeneity allowed continued seismic activity along local fault segments even as aseismic deformation developed on weaker fault segments along strike. This has important implications for the strength modelling of mature but heterogeneous major faults, and for the consideration of seismic hazard along active equivalents.

Deformation of a stacked fluvio-deltaic succession – linking strain partitioning and fracture 'damage'

A.J. Cawood[1] & C.E. Bond[1]
[1]Geology & Petroleum Geology, School of Geosciences, University of Aberdeen, Kings College, Aberdeen, AB24 3UE, UK (adam.cawood@abdn.ac.uk)

3D seismic datasets allow increasingly detailed mapping of fold-thrust belts in the subsurface but limits to resolution mean that the full complexity of sedimentary facies variation, deformation structures, and fracture distribution is often unresolvable. To characterise the influence of sedimentary architecture on structural style, strain partitioning, and associated fracture distribution, we utilize a high resolution Virtual Outcrop of Monkstone Point, Pembrokeshire, SW Wales. Detailed digital mapping, supplemented with field data and XRF analysis, reveals significant variation in sedimentary body geometry and internal structure within this Upper Carboniferous multi-layer sequence. Rapid lateral variations in strain accommodation, on a scale of tens of metres, is fundamentally controlled by this depositional architecture. Thickness variations of mechanically 'weak' and 'strong' units coupled with body geometries and internal sedimentary structures contribute to the complex interplay between depositional architecture and subsequent deformation. Given the observed structural complexity, fracture distribution within mechanical units is remarkably uniform, with fracture intensity primarily controlled by bed thickness, lithology and structural position. This contrast has implications for timing of fracture development in this multilayer sequence, but may also help to infer fracture distribution in subsurface examples of similar settings.

Microstructure and mechanics of ice under constriction: data from the field and laboratory

L. Craw[1], D. Prior[1], C. Hulbe[2], M. Vaughan[1] & K. Lilly[1]
[1]*Department of Geology, University of Otago, Dunedin, New Zealand (crali915@student.otago.ac.nz)*
[2]*School of Surveying, University of Otago, Dunedin, New Zealand*

Ice flowing in glaciers undergoes constructional deformation as it passes through narrowing topography. This contribution will explore the mechanics and microstructure of constriction through both lab experiments, and an analysis of aerial image data from the Byrd Glacier, Antarctica.

An apparatus has been custom-built at the University of Otago using concepts adapted from metallurgy, allowing cylinders of standard ice with an initially uniform crystallographic preferred orientation (CPO) to be forced through a narrowing tube, subjecting it to constrictional strain under a constant temperature of -5°C. Electron Backscatter Diffraction (EBSD) maps of these samples reveal the microstructural characteristics of ice at increasing levels of radial strain. As the secondary creep stage is reached, strain is accommodated by grain rotation and dynamic recrystallisation through grain boundary bulging, and CPOs are present in the form of clusters at ~45° to the greatest principal stresses. However, no samples deformed in this manner have reached the tertiary creep stage.

Our analysis of Byrd Glacier uses a new approach, focussing on incremental radial strain as a result of topography. Integrating pre-existing velocity datasets for the glacier, we have derived radial strain rates and ice mass flux down its length. Variations of strain rate as a function of strain suggest that ice in the glacier does not pass through the secondary creep minimum, undergoing only a smooth transition into tertiary creep.

Considering our data alongside published conventional laboratory results, we conclude that differences between our laboratory and Byrd Glacier datasets are explained by a pre-existing CPO controlling the Byrd Glacier rheology.

Ultramylonite generation via phase mixing in high strain experiments

A.J. Cross[1] & P. Skemer[1]
[1]*Department of Earth & Planetary Sciences, Washington University in St. Louis, St. Louis, USA (andrew.cross@wustl.edu)*

Dynamic recrystallization and phase mixing are considered to be important processes in ductile shear zone formation, as they collectively enable a permanent transition to the strain-weakening, grain-size-sensitive (GSS) deformation regime. While dynamic recrystallization is well-understood, the underlying physical processes and timescales required for phase mixing remain enigmatic. We present results from high-strain phase mixing experiments on calcite-anhydrite composites. A poorly-mixed starting material was synthesized from fine-grained calcite and anhydrite powders. Samples were deformed in the Large Volume Torsion (LVT) apparatus at 500°C and shear strain rates of $5x10^{-5}$ to $5x10^{-4}$ s^{-1}, to finite shear strains of up to 57. Microstructural evolution is quantified through analysis of back-scattered electron (BSE) images and electron backscatter diffraction (EBSD) data.

During deformation, polycrystalline domains of the two phases are geometrically stretched and thinned, causing an increase in the spatial density of interphase boundaries. At moderate shear strains ($\gamma > 6$), monophase domains are so severely thinned that they become 'monolayers' of only one or two grain's width. Monolayer formation is accompanied by a critical increase in the degree of grain boundary pinning and, consequently, grain size reduction below the theoretical limit established by the grain-size piezometer or deformation mechanism field boundary. Ultimately, monolayers neck and disaggregate at high strains ($17 < \gamma < 57$) to complete the phase mixing process. This 'geometric' phase mixing mechanism is consistent with observations of mylonites, where layer (i.e. foliation) formation is associated with strain localization, and layers are ultimately destroyed at the mylonite-ultramylonite transition.

Recognition of melt flux through shear zones.

N.R. Daczko[1], S. Piazolo[1,2], D. Da Silva[1], U. Meek[1], C.A. Stuart[1] & H. Ghatak[1]
[1]Department of Earth and Planetary Sciences, Macquarie University, Sydney, Australia (nathan.daczko@mq.edu.au)
[2]School of Earth and Environment, University of Leeds, Leeds, England

Parallels are drawn between hornblendite in the exposed root of a magmatic arc, in Fiordland New Zealand and biotite-rich glimmerite in an exposed middle crustal section of an intracontinental orogenic belt, in Central Australia. The hornblendite and glimmerite bodies are metres to tens-of-metres thick, elongate and hosted in shear zones. In contrast to the dynamic setting of the host shear zones, the hornblendite and glimmerite bodies preserve igneous microstructures, sharing many similarities with cumulate rocks. The hornblendite and glimmerite bodies link with precursor rocks by the progressive modification of pre-existing minerals and structures. We propose that the metasomatic replacement of variable precursor rocks formed hornblendite or glimmerite during channelled high melt-flux through the crust. The composition of the fluxing melt controls the formation of hornblendite versus glimmerite. Melt flux through shear zones in the lower crust of the New Zealand arc rocks is inferred to involve flux of arc magma, in comparison to flux of S-type magma through the middle crustal shear zones of Central Australia. In both systems, high melt to rock ratios and the chemical interaction between the migrating melt and host rock induced dissolution of pre-existing minerals in the host and growth of mainly hornblende or biotite. This reaction-replacement mechanism forms hornblendite or glimmerite bodies delineating significant melt conduits. Accordingly, hornblendite, glimmerite or other basic to ultrabasic bodies may map significant mass transfer through shear zones.

Melt flux through the root of a magmatic arc under static versus dynamic conditions.

N.R. Daczko[1], S. Piazolo[1,2], C.A. Stuart[1] & U. Meek[1]
[1]Department of Earth and Planetary Sciences, Macquarie University, Sydney, Australia (nathan.daczko@mq.edu.au)
[2]School of Earth and Environment, University of Leeds, Leeds, England

Melt–rock interaction in crustal rocks is rarely documented due to a lack of criteria for identification of where melt has previously fluxed. The inherent complexity of crustal rock types and melt compositions compounds the difficultly of recognising former melt flux. We contrast four examples of both static and dynamic styles of melt flux throughout a homogeneous host rock, the Pembroke Granulite in Fiordland, New Zealand. Field relationships and microstructures demonstrate that all four examples of melt–rock interaction involved little to no crystallisation of melt within the modified rocks, and the mineral assemblages and microstructures that were produced during melt–rock interaction are common in lower crustal rocks. All four examples of melt flux include microstructures indicative of the former presence of melt and hydration involving an increase in the mode of amphibole. The static melt flux styles (two examples) involved (1) widespread growth of pargasite-bearing coronae around pyroxene throughout the entire Pembroke Granulite and (2) the development of localised tschermakite–clinozoisite gneiss and migmatite. The dynamic styles (two examples) of melt-rock interaction formed distinct minor rock types hosted within the Pembroke Granulite, including melt-bearing high-grade shear zones and hornblendite. The static melt flux styles are both inferred to involve diffuse porous melt flow as (1) low melt flux at the kilometre scale and (2) channelled high melt-flux at the metre-scale, leading to local migmatisation in the channels. By contrast, the dynamic styles of melt flux only occurred at the metre-scale and were hosted in shear zones. Significant metasomatism in some shear zones formed hornblendite and indicates an increased cumulate flux in these examples.

Implications of structural analysis, P-T pseudosection modelling and white mica $^{40}Ar/^{39}Ar$ age distributions for the interpretation of the tectonometamorphic history of Syros (Cyclades, Greece)

M. de Paz-Álvarez[1], B. Uunk[1], F. Brouwer[1] & J. Wijbrans[1]
[1]Geology & Geochemistry cluster, Vrije Universiteit Amsterdam, De Boelelaan 1085, 1081, HV Amsterdam, The Netherlands (espoopse@hotmail.com)

The island of Syros, in the Cycladic region of Greece, remains a key location for investigations aiming to understand tectonic and metamorphic subduction processes of fluid-rock interaction and metasomatism, channel flow, extrusion wedges and back-arc extension in syn-collisional environments. The present ongoing research is based on newly obtained $^{40}Ar/^{39}Ar$ phengite ages, P-T modelling of eclogite, blueschist and greenschist facies samples, and structural analysis and mapping. It provides new insights in order to unravel the complex Eocene-Miocene history of the Cycladic Blueschist Unit (CBU) in Syros. Numerous previous contributions provide a wide variety of interpretations for similar observations. An agreement on a basic input such as the peak metamorphic conditions achieved by the different identified units within the island, needed for the proposition of geological sound models, is still lacking despite considerable efforts. This research aims to estimate peak metamorphic conditions for several of them. Preliminary data suggests that they experienced peak metamorphic conditions varying between 20-25kbar and temperatures ranging 500-600ºC: this supports a recent trend in literature towards higher peak pressure conditions for eclogite metamorphism. Moreover, it suggests that the different units reached similar metamorphic conditions. Structural observations on the island scale support previous research with respect to the preservation of at least two ductile deformation events. The first, mostly recorded in the northern part of the island associated to preserved lawsonite pseudomorphs, is interpreted to record prograde burial and top-to-the-S thrusting in blueschist facies. The second, pervasively found across the island, is associated to a continuum of top-to-the-E extensional shearing that started in eclogite facies, being the blueschist structures the dominant ones. Continued greenschist overprint is found as both static and deformation-driven. It is interpreted to record syn-collisional exhumation and top-to-the-E extension: transport direction is narrowly clustered around 90º in the proximities of shear zones, and more distributed within the wall rocks. The pervasiveness of lineation development indicates a deviation from simple shear strain in the shear zones. Therefore, shear sense analysis is not as straightforward as previously assumed in the island. The occurrence of both top-to-the-E and top-to-the-W shear sense indicators has previously been interpreted as a consequence of vertical thinning and coaxial stretching. Alternatively, it can be explained in terms of flow partitioning resulting in the generation of coaxially stretched domains, or as a consequence of slip along the penetrative foliation planes, as has been previously shown theoretically and experimentally. The clear dominance of top-to-the-E shear sense is interpreted as an indication of the bulk kinematics during syn-collisional extension. Considering opposite rotations of the western and eastern Cycladic regions, the apparently orthogonal angle between transport estimates for coeval thrusting (S, in Ios) and extension (E, in Syros) decreases considerably. This supports the interpretation of the exhumation of the CBU as taking place within an extrusion wedge during a syn-collisional stage. The different shear zones identified in the island are the result of flow partitioning during the extrusion-related retrograde deformation, so that they accommodated most of the extension that led to the early exhumation.

Shear localisation in homogeneous, anisotropic materials

T. de Riese[1], P. D. Bons[1], M. Finch[1], E. Gomez-Rivas[2], A. Griera[3], M.-G. Llorens[1], H. Ran[1] & F. Steinbach[1]

[1]Department of Geosciences, University of Tübingen, Germany (tamara.de-riese@uni-tuebingen.de)
[2]School of Geosciences, University of Aberdeen, Scotland, UK
[3]Departament de Geologia, Universitat Autònoma de Barcelona, Barcelona, Spain

Shear zones on all scales are commonly observed in exposed metamorphic rocks and indicate that shear localisation is the rule rather than the exception in crustal rocks. Despite decades of research, there is ongoing debate on the mechanism(s) of shear localisation (grain size reduction, shear heating, brittle precursors, etc.). The potential role of rheological anisotropy of rocks in the formation of shear zones has received relatively little attention. Here we investigate shear localisation in anisotropic materials. A related issue is the self-similarity that is observed over a range of scales in shear zone networks (e.g. in Cap de Creus, Spain; Carreras, 2001).

We simulated the deformation of anisotropic materials with a spectral solver (Fast Fourier Transform, FFT). The FFT-model simulates visco-plastic deformation by dislocation glide, taking into account the different available slip systems and their critical resolved shear stresses. Although developed for the simulation of deformation within mineral aggregates, we here use the capability to simulate deformation of strongly nonlinear anisotropic materials to model shear localisation at arbitrary length scales. We modelled the amount and patterns of localisation of stress and strain rate as a function of lattice-preferred orientation (LPO) and anisotropy in both 2D and 3D and up to large strains.

Shear localisation is observed in all cases. We applied fractal analyses to the strain-rate distribution patterns. The results show shear localisation on all scales and (multi-)fractal distribution patterns of strain rate. The probability distribution of strain rates shows a distinct deviation from a Gaussian distribution for the highest strain rates, indicating self-organization and entailing fractal distributions. Movies of the simulations show that the distribution of both strain rate and of finite strain is much more heterogeneous than the finite strain distribution tends to indicate. The observation that shear localisation on the micro-scale (Llorens et al., 2016), due to anisotropy, appears almost inevitable raises the question whether there is a larger length scale where shear localisation is averaged out. Analyses of strain-rate and finite strain distributions indicate that these have multi-fractal characteristics. This suggests that shear localisation is to be expected at all scales, which can be explained by the fact that the reason for localisation, mechanical anisotropy, is a property with no length scale. Multi-fractal analysis will help to understand the dynamics of shear localisation in anisotropic materials, particularly since this method is suitable to describe the impact of other processes that may be involved, leading to multi-fractal statistics. This may explain how the formation of the smallest-scale shear bands up to the largest, crustal-scale shear zones is linked.

Carreras, J. (2001) Zooming on Northern Cap de Creus shear zones. Journal of Structural Geology, 23(9), 1457-1486.

Llorens, G.-M., Griera, A., Bons, P.D., Lebensohn, R.A., Evans, L.A., Jansen, D., Weikusat, I. (2016) Full-field predictions of ice dynamic recrystallisation under simple shear conditions. Earth and Planetary Science Letters 450, 233-242.

Dynamics of bimodal, diffusional and ballistic transport systems in the Earth's crust

T. de Riese[1], P. D. Bons[1] & T. Sachau[1]
[1]*Department of Geosciences, Eberhard Karls University Tübingen, Germany (tamara.de-riese@uni-tuebingen.de)*

Fluid flow is one transport system that can be regarded as "bimodal". At low hydraulic head gradients, fluid flow through pores is slow and can be termed "diffusional". Structures such as breccias and hydrothermal veins indicate high fluid velocities, which can only be achieved by localized fluid transport via hydrofractures. Hydrofracture propagation and simultaneous fluid transport can be seen as a "ballistic" transport mechanism, which is activated when transport by diffusion alone is insufficient to release local fluid overpressure. The brief activation of a ballistic system locally reduces the drive, but may cause the escape of most of the fluids. The aim of this study is to investigate the properties of the two transport modes in general and the transition between them in particular.

We developed a numerical model (based on Bak et al., 1988 and Roering et al., 2001) in order to study patterns that result from bimodal transport, i.e. coupled diffusional and ballistic transport. Interesting and rich behaviour emerges in the transition between diffusion- and ballistic-dominated behaviour. We quantified this transition from diffusional to ballistic transport using fractal analysis, and especially wavelet transforms. To assess this method with respect to its ability to describe the evolving patterns, we compared the spatial and temporal dynamics of the system with fractal analysis data of natural systems, such as hydraulic breccias (Mt Painter, Australia) and hydrothermal veins (Black Forest, Germany). The data show similarities, which is strong evidence for the usefulness of our approach.

We show that the criterion for activation of a ballistic system is mostly scale invariant, thus leading to (multi-)fractal patterns and statistics. The outcome of this study will have implications for a large range of transport related processes in the Earth's crust. Examples of such processes are the formation of hydrothermal ore deposits, the passage of hydrocarbons through low-permeability layers or the dispersion of contaminants in ground water. The results will also impact the research on tipping points in the crust, as they are often exceeded due to geothermal energy production and well stimulation.

References:

Bak, P., Tang, C., & Wiesenfeld, K. (1988). Self-organized criticality. Physical review A, 38(1), 364.

Roering, J. J., Kirchner, J. W., & Dietrich, W. E. (2001). Hillslope evolution by nonlinear, slope independent transport: Journal of Geophysical Research: Solid Earth, 106(B8), 16499-16513.

Deformation mechanisms, rheology, and the geophysically observed phenomena of slow slip and tremor

A. Fagereng[1]
[1]*School of Earth & Ocean Sciences, Cardiff University, Cardiff, United Kingdom (FagerengA@cardiff.ac.uk)*

Slow slip events (SSEs) represent transient fault slip velocities slower than earthquakes but faster than steady, average plate motion. SSEs are detected geodetically and do not emit detectable seismic waves, although they are commonly, but not always, accompanied by tectonic tremor. Tremor is defined as persistent, low-frequency (< 10 Hz) arrivals lacking impulsive body waves. Within the tremor signal are low and very low frequency earthquakes, interpreted as shear slip on faults subparallel to, and kinematically consistent with, the hosting fault. An increasingly common interpretation is that SSEs are a form of transient fault creep, and associated low frequency seismic phenomena represent shear failure of asperities embedded in the creeping fault segment. A geological analogue to the coupled phenomena of slow slip and tremor is then a continuous-discontinuous shear zone where frictional failure occurs in scattered locations within a dominantly viscous matrix.

Where slow slip and tremor spatially and temporally coincide, the total seismic moment of tremor and superimposed low frequency seismic events is negligible compared to the geodetic moment of the SSE. Thus, the geological analogue is restricted to shear zones where the majority of finite strain is accommodated by deformation consistent with an aseismic geophysical expression. Many SSEs occur at temperatures greater than 350˚C, where aseismic deformation is typically accommodated by viscous mechanisms. Also, the geodetic moment of an SSE is representative of the elastic strain in the rock volume surrounding the fault, which is converted to finite fault zone displacement by the SSE (centimetres), whereas tremor represents coincident frictional failure with small (sub-mm) slip magnitudes. This interpretation assumes that SSEs, like earthquakes, represent a form of stick-slip motion associated with elastic strain build-up and release in the surrounding elastic rock volume. If this assumption is correct, and geological analogues implying SSEs may form by viscous shearing flow are also correct, then SSE source parameters can be considered in terms of viscous deformation of a tabular shear zone. Questions that then arise include: (1) how thick is the deforming zone; (2) what are the deforming minerals; and (3) what are the active deformation mechanisms and their flow laws?

Analogous to ’characteristic earthquakes’, many SSEs repeating at the same location have approximately characteristic slip magnitude and duration. Contrary to earthquakes, however, average slip relates to neither duration nor area, and average slip velocity is, typically, considerably greater in shallow events than in deep events. Variation in SSE properties may reflect a range of answers to the questions above, and an opportunity exists in exploring the geological record for the allowable range in properties. Critically, these properties must be able to generate slow slip at temperatures ranging from less than 100˚C to more than 600˚C.

Deformation bands in Numidian sandstones of Sicily: a petrographic-structural study

E. Fazio[1], R. Punturo[1], G. Barreca[1], S. Gambino[1], R. Maniscalco[1] & R.W.H. Butler[2]
[1]Earth Science Section - Department of Biological, Geological Environmental Sciences, Catania University, Catania, Italy (punturo@unict.it)
[2]Geology and Petroleum Geology, School of Geosciences, University of Aberdeen, Aberdeen, AB24 3UE, UK

Here we consider the Numidian turbidite system (Miocene) of Sicily as analogue for a variety of deepwater hydrocarbons reservoirs. In particular, we carried out a detailed petrographic-structural investigation on sandstones cropping out near the village of Sperlinga (central Sicily - Italy). The main outcrop consists of a roughly NW-SE trending km-scale wavelength syncline fold, transversally sliced by left-lateral strike-slip faults NE-SW oriented, associated with a younger regional-scale right-lateral shear zone according to Carbone et al. (1990).
Our study shows that an intricate network of different generations of deformation bands (DBs) widely occur in the area. Petrographic observations highlight different typologies of DBs: cataclastic- shear- dilation, and compaction-type bands, suggesting a shear component mixed to a contractional one. The classic rock assemblage is given essentially by quartz (often consisting of polycrystalline clasts showing blocky extinction and preferred shape orientation), with minor amount of plagioclase, K-feldspar, chlorite, mica, zircon, glauconite.
The structural analysis and trends indicate that DBs are possibly associated with a previous low-angle thrust contact developed during the early stage of tectonic piling. Currently, the thrust damaged zone is well exposed indoors the castle of Sperlinga, where it appears strongly tilted up to exhibit subvertical boundaries trending NW-SE. The great circles of poles of DBs planes are oriented NW-SE and NE-SW sub-perpendicular and/or oblique (at about 30 degrees) to the current maximum compressional stress direction, roughly N-S oriented. Considering that Numidian outcrops in Sicily have experienced a c. 100 CW rotation since deposition (Speranza et al., 2003; Pinter et al., 2016a) we restored the succession by operating first a tilt correction (of ca. 60 degrees of the originally low-dipping angle thrust surface) and then a second rotation (back of about 100 degrees CCW) around a vertical axis. The data indicate that the turbiditic channel system, N-S oriented at the time of sedimentation (Pinter et al., 2016b), deformed under an E-W trending shortening axis consistent with Neogene thrusting in the central Mediterranean. Further investigation should reinforce our preliminary results.

References:
Carbone S., Catalano S., Grasso M., Lentini F., Monaco C., 1990. Carta geologica della Sicilia centro-orientale. S.El.Ca, Firenze.
Pinter, P.R., Butler, R.W.H., Hartley, A. J., Maniscalco, R., Baldassini, N., Di Stefano, A., 2016a. The Numidian of Sicily revisited: A thrust-influenced confined turbidite system. Mar. Pet. Geol., 78: 291–311. doi:10.1016/j.marpetgeo.2016.09.014
Pinter, P.R., Butler, R.W.H., Hartley, A.J., Maniscalco, R., 2016b. Deep-water sandstones in tectonically complex systems: the Numidian of Sicily as an example. 88° Congresso SGI, Napoli 2016. Rend. Online Soc. Geol. It., Suppl. n. 1 al Vol. 40 (2016): 501.
Speranza, F., Maniscalco, R., Grasso, M. 2003. Pattern of orogenic rotations in central-eastern Sicily: implications for the timing of spreading in the Tyrrhenian Sea. Journal of the Geological Society, 160, 183-195.

Quartz CPO analysis of mylonitic leuco-granodiorites from a ductile crustal scale shear zone (Calabria, southern Italy)

E. Fazio[1], R. Punturo[1], R. Cirrincione[1], H. Kern[2], A. Pezzino[1], H-R. Wenk[3], S. Goswami[4] & M.A. Mamtani[4]

[1]Earth Science Section - Department of Biological, Geological Environmental Sciences, Catania University, Catania, Italy (punturo@unict.it)
[2]Institute of Geosciences, CAU University of Kiel, Olshausenstr. 40, 24098 Kiel, Germany
[3]Department of Earth and Planetary Science, University of California, Berkeley, CA 94720, USA
[4]Department of Geology and Geophysics, Indian Institute of Technology, Kharagpur, West Bengal 721302, India

A microstructural investigation was carried out on leuco-granodiorite mylonites from the Montalto shear zone (Calabria, southern Italy) exhibiting different stages of deformation. The main mineral assemblage is Qtz, Pl, Kfs Wm, typical of greenschist to lower amphibolite facies conditions in the PT range 0.25– 0.55 GPa and 350–550 °C (Cirrincione et al. 2008; 2009). Occurring minerals display S–C and shear-band textures; mica-fish and ribbon-like quartz are widespread. In particular, we investigated quartz c-axis orientations in selected naturally sheared rocks by different techniques spanning from the classical universal stage (US), a computer aided polarization microscopy method (CIP), the time-of-flight (TOF) neutron diffraction analysis, and the electron backscatter diffraction (EBSD). Comparison among results obtained by different techniques give on the whole a good correlation, nevertheless we can conclude that each method provides complementary piece of information (Fazio et al., 2017) that are important for specific structural interpretations. Moreover, by means of shape porphyroclasts analysis, a sub-simple shear (40% simple shear vs 60% pure shear) was also inferred and a general tendency of an asymmetric c-maximum near to the Z direction (normal to foliation) suggesting dominant basal slip, consistent with fabric patterns related to dynamically recrystallization under greenschist facies, was recognized.

References:

Fazio E., Punturo R., Cirrincione R., Kern H., Pezzino A.,· Wenk H-R · Goswami S., Mamtani M.A. 2017. Quartz preferred orientation in naturally deformed mylonitic rocks (Montalto shear zone–Italy): a comparison of results by different techniques, their advantages and limitations. Int J Earth Sci (Geol Rundsch). DOI 10.1007/s00531-016-1424-y.

Cirrincione R, Ortolano G, Pezzino A, Punturo R (2008) Poly-orogenic multi-stage metamorphic evolution inferred via P–T pseudosections:
an example from Aspromonte Massif basement rocks (Southern Calabria, Italy). Lithos 103:466–502.

Cirrincione R, Fazio E, Fiannacca P, Ortolano G, Punturo R (2009) Microstructural investigation of naturally deformed leucogneiss from an Alpine shear zone (Southern Calabria–Italy). Pure Appl Geophys 166:995–1010.

The ephemeral development of shear bands in mylonites

M. Finch[1], P.D. Bons[1], E. Gomez-Rivas[2], A. Griera[3], G.-M., Llorens[1], H. Ran[1] & F. Steinbach[1]
[1]Dept. of Geosciences, Eberhard Karls University Tübingen, Germany (paul.bons@uni-tuebingen.de)
[2]School of Geosciences, University of Aberdeen, Scotland, UK
[3]Departament de Geologia, Universitat Autònoma de Barcelona, Spain

Shear bands are common strain-localisation structures in highly strained rocks. They are commonly used as shear-sense indicators, especially in igneous rocks (granites, gabbros) where other indicators, such as offset bedding, are commonly lacking. Although their interpretation in terms of shear sense is well established, their origin remains relatively unclear.

We used the VPFFT/ELLE code (e.g., Griera et al., 2011; 2013; Llorens et al., 2016) to investigate the development of shear bands during simple-shear deformation to high strains (up to 20). As the protolith we used three "numerical minerals": a hard one (comparable to feldspar), one of intermediate strength (comparable to quartz), and a soft one to represent mica. Only the softest mineral was assigned a strong mechanical anisotropy with a weak basal plane. We varied the strength contrasts, as well as the fraction of the "mica", keeping a 1:1 ratio of "feldspar" and "quartz".

Shear localisation in the form of shear bands develop in all cases, but at different rates and intensity. The development of C and C' shear bands is facilitated by a high fraction and/or a low viscosity of the weakest mineral. C'' shear bands develop at low strains, but their development may later be suppressed when dominant C and C' shear bands are established. Overall, synthetic C' shear bands preferentially develop when the strong mineral(s) form(s) the load-bearing framework, while C'' shear bands preferentially develop when the soft mineral(s) form(s) the framework.

Shear bands form and disappear again, and are therefore ephemeral. C' shear bands rotate slowly and, therefore, persist longer than C'' shear bands. These form at a high angle to the shear plane and experience the highest passive rotation rate. C'' are typically only active for shear strain increments less then 0.5. This explains the scarcity of C'' compared to C' shear bands in the geological record. However, movies of the numerical simulations show that C'' are much more active than the final microstructure indicates.

Shear bands are common and "textbook" structures. Our simulations, especially the movies, will shed some light on how they actually form and often disappear again.

Griera A, Bons PD, Jessell MW, Lebensohn RA, Evans L, Gomez-Rivas E. 2011 Strain localization and porphyroclast rotation. Geology 39, 275-278. (doi: 10.1130/G31549.1).
Griera A, Llorens M-G, Gomez-Rivas E, Bons PD, Jessell MW, Evans LA, Lebensohn RA. 2013 Numerical modelling of porphyroclast and porphyroblast rotation in anisotropic rocks. Tectonophysics 587, 4-29. (doi: 10.1130/G31549.1).
Llorens, M.-G., Griera, A., Bons, P.D., Lebensohn, R., Jansen, D., Evans, L.A. and Weikusat, I. 2016. Full-field predictions of ice dynamic recrystallisation under simple shear conditions, Earth and Planetary Science Letters, 450, 233-242. (doi:10.1016/j.epsl.2016.06.045).

Evolution of an inherited texture during pressure solution

J. Gardner[1], J. Wheeler[1] & E. Mariani[1]
[1]*School of Environmental Sciences, University of Liverpool, Liverpool, UK (jgardner@liv.ac.uk)*

Deformation histories are stored in the microstructures of deformed rocks. Microstructural and textural analysis can identify which deformation mechanisms were dominant during strain accommodation, and thus allow us to predict the rheology of a deforming system at specific conditions in the Earth. Our study focuses on the deformation behaviour of feldspar in metagabbroic rocks from a km-wide mid-crustal extensional shear zone in the NW Italian Alps (Gressoney Shear Zone). At these conditions, feldspar is expected to exhibit brittle or pressure solution behaviour, but not intracrystalline plasticity. However we observe microstructures suggestive of crystal plasticity (subgrain formation, high dislocation density). We attribute these features to the epitaxial replacement of Ca-bearing plagioclase to pure albite in the presence of a thin film of fluid, followed by deformation. A lattice mismatch leaves product albite with a high dislocation density, which provides a driving force for recovery and recrystallization. As recovery is controlled by the climb of dislocations it is not expected to occur in feldspar at the temperatures of the mid-crust; we speculate in this case it may occur at lower than expected temperatures due to hydrolytic weakening. Overall, this process results in a fine-grained (~50 μm) matrix of albite characterised by domains of crystallographic preferred orientation (CPO) inherited from cm-scale parent grains. A second Ca-bearing phase, epidote, is also produced.

We present the results of an electron backscatter diffraction (EBSD) study that focuses on the evolution of this inherited microstructure during continued deformation. Grain size reduction during recovery and recrystallization promotes the dominance of grain size sensitive creep (fluid-assisted diffusion creep/pressure solution). Microstructural evidence suggests that albite had the highest solubility, as it appears as coarser-grained (~100 μm) precipitate in pressure shadows and fractures, where epidote is not present. Some regions of precipitate display foam textures with quasi-equilibrium grain boundaries. These features are generally lacking in the fine-grained two-phase matrix, suggesting the presence of a second phase inhibited grain coarsening in the matrix, thus promoting continued dominance of grain size sensitive creep. The presence of commonly-observed quadruple junctions, phase mixing, and the weakening of initially very strong (i.e. inherited from a single crystal) CPO domains all suggest grain boundary sliding (GBS), which necessarily accompanies diffusion-dominated strain accommodation, played a significant role during deformation.

Our work shows that epitaxial replacement with a lattice mismatch can lead to grain size reduction, and an associated switch to a grain size sensitive deformation mechanism (in this case, fluid-assisted diffusion creep). We show how an inherited texture can evolve during diffusion creep, and what influence initial grain geometry may have on texture maintenance and/or evolution. We show the influence variable amounts of second phase can have on textural evolution, and how all these factors may influence strain localisation and the overall rheology of feldspar-rich rocks deforming at mid-crustal conditions.

Flow behaviour of the middle and lower crust: Insights from field observations and numerical modelling

R. Gardner[1], S. Piazolo[2] & N. Daczko[1]
[1]*Australian Research Council Centre of Excellence for Core to Crust Fluid Systems/GEMOC, Department of Earth and Planetary Sciences, Macquarie University, Sydney, NSW 2109, Australia (robyn.gardner@mq.edu.au)*
[2]*School of Earth and Environment, University of Leeds, Leeds, UK*

Understanding the flow behaviour of the middle and lower crust is fundamental to understanding the large-scale tectonic processes operating on Earth. These processes form the landscape we see today and, over millennia, have created the ore bodies and energy reserves we use in everyday life. Numerical modelling of large-scale tectonic processes provides insights not available from examination of field outcrops and analogue experiments due to the static nature of the outcrops, the time and scale of the geological processes, and the dynamic nature of the processes. However, significant limitations exist due to oversimplification of the flow properties, with respect to viscosity and flow regime, used in the models, particularly in view of the known heterogeneous nature of the middle to lower crust.

We use a combination of in-depth field studies and numerical modelling, to examine the effect of viscosity contrast and flow regime on the development and shape symmetry of pinch and swell structures. These structures form from the microscopic scale to the tectonic scale. A toolbox is developed to examine pinch and swell structures in the field and thereby determine the relative and absolute viscosity of mid-crustal rock units. The toolbox is applied to two natural pinch and swell examples from Milford Sound, New Zealand, at the outcrop and kilometre scale. Detailed microstructural analysis determines the flow regime, Newtonian and non-Newtonian flow regime, respectively, for use in the numerical model. The results show the differences in absolute viscosity between individual layers and between flow regimes, can be orders of magnitude in size. This implies heterogeneity of the continental crust has a significant impact on Earth's tectonic processes and therefore, must be considered in large scale geodynamic models.

The use of the proposed cross-disciplinary technique allows more accurate, scale independent, estimation of flow property values for the heterogeneous layers of the middle to lower continental crust. Using these as input to large-scale tectonic numerical models provides more accurate geodynamic models, thereby allowing improved understanding of the workings of our Earth.

Patterns of strain localization in heterogeneous, polycrystalline rocks – a numerical perspective

R. Gardner[1], S. Piazolo[2] & N.Daczko[1]
[1]*Department of Earth and Planetary Sciences, Macquarie University, Sydney, NSW 2109, Australia (robyn.gardner@mq.edu.au)*
[2]*School of Earth and Environment, University of Leeds, Leeds, UK*

Strain localisation fundamentally controls a material's rheological response to deformation, and there is well documented evidence of the major role that localization plays in governing the development of important tectonic and economic structures. Shear zone initiation and development is, therefore, widely studied at all scales. However, speculation remains regarding the mechanisms and patterns of strain localization, including the influence of the rheology and geometry of pre-existing heterogeneities, and the importance of weakening and strengthening processes.

We use the microdynamic modelling platform Elle to investigate the impact of the spatial distribution (i.e. the pre-deformation microstructure) and stress related evolution for a 20% weak phase on the bulk strength and strain localising behaviour of a material deformed in simple shear. The model is extended to simulate material weakening by allowing the strong phase to dynamically transition to weak based on a stress threshold. Material strengthening is also simulated by allowing the weak phase to strengthen based on a time threshold. Systematic testing of the stress and time thresholds are undertaken.

Our results highlight that during simple shear, if dynamic weakening with or without strengthening feedbacks is present, strain is quickly localized into an interconnected weak layer (IWL), where an increasing proportion of weak material increases the interconnections between the IWLs, thereby increasing the anastomosing character of the shear zones. The results show the geometry of a shear zone can provide relative viscosity where it crosses a lithology boundary. Shear zones are wide and anastomosing compared with narrow and concentrated where viscosity is lower and higher, respectively.

We also establish the temporal patterns of shear zones are sensitive to the dominance of the weakening or strengthening process. Consequently, shear zones are dynamic in time and space within a single deformation event and therefore, the pattern of finite strain can be an incomplete representation of the evolution of a shear zone network.

Structural and kinematic evolution of deformation profiles of dominant thrusts: Insights from Main Central thrust and Pelling thrust faults, Sikkim Himalayan FTB

P. Ghosh[1] & K. Bhattacharyya[1]
[1] *Indian Institute of Science Education and Research Kolkata, India.*
(pg14rs039@iiserkol.ac.in)

Early formed dominant thrust sheets get modified and the associated microstructures get overprinted by the formation of footwall structures during progressive deformation in a fold-thrust belt. Deformation profile of a thrust sheet is generally characterised by higher simple-shear near the base and dominantly pure-shear higher up within the sheet. To examine how the deformation profile of such dominant thrust sheets vary temporally due to the formation of footwall structures, we focus on two dominant thrusts of the Sikkim Himalayan FTB, the northernmost Main Central thrust (MCT) and its major footwall thrust, the Pelling thrust (PT). Both these thrust sheets are folded in an E-W trending antiform-synform pair by the growth of the underlying Lesser Himalayan duplex (LHD). The PT is the roof thrust of the duplex. We evaluate the operative deformation mechanisms and attempt to quantify the strain and vorticity from the deepest exposed segments of the MCT and the PT to focus on the microstructural and kinematic evolution of these two fault zones.

As a result of forelandward progression of the deformation front, foliation of the MCT is overprinted by the PT. The structural dominance of northerly plunging pucker axes and mineral lineation within the PT zone is a result of regional northerly plunge associated with the culmination of the underlying duplex. Based on the porphyroclast and matrix percentages, the protomylonite zone lies in the middle of both the fault zones, bounded by mylonite zone. The coarse grained quartzo-feldspathic gneissic protolith has undergone ~72% grain size reduction in quartz and ~50% reduction in feldspar and form quartz mylonite zone within the ~1.17km thick MCT zone. The PT protolith records ~85% and ~75% grain-size reduction in quartz and feldspar, respectively, within ~938m thick PT zone. Dislocation creep and fracturing are the dominant deformation mechanisms in quartz and feldspar, respectively. Interestingly, microfracturing is more pronounced in the MCT zone than in the underlying PT zone, while evidence of pressure solution is more dominant within the PT zone. The proportion of later formed transgranular fractures that cross-cut the earlier formed mylonitic foliation increase toward the fault zone boundaries. This indicates that the deformation continues to propagate toward the boundary, as fault rocks exhumed to the shallower level.

Quantification of 3D viscoplastic strain from quartz and feldspar suggests that the MCT fault zone records higher flattening strain than the PT fault zone. Microstructural observation suggests fracturing and pressure solution accommodate a significant amount of strain, thereby under-representing the viscoplastic strain. Two different incremental strain markers, i.e., earlier formed oblique-fabric and later formed subgrains, indicate both the MCT and the PT zones record a non-steady deformation with progressively higher pure-shear dominated deformation through time. We suggest, due to the growth of underlying footwall duplex, the simple-shear dominant deformation progressively transformed to pure-shear dominated deformation, as the deformation profile within the thrust sheets evolved through time. The PT zone records a higher pure-shear than the MCT zone. Therefore, structural geometry, microstructural observation and kinematic data suggest that the PT fault zone records the effect of footwall duplex more prominently than the MCT fault zone, as the PT acts as the roof thrust of the underlying duplex.

Hierarchical creep cavity formation in mono-mineralic quartz domains of an ultramylonite from the Redbank Shear Zone

J. Gilgannon[1,2], F. Fussies[2], L. Menegon[3], K. Regenauer-Lieb[4] & J. Buckman[5]

[1]*Institut für Geologie, Universität Bern, Bern, Switzerland (james.gilgannon@geo.unibe.ch)*
[2]*School of Geosciences, The University of Edinburgh, Edinburgh, Scotland*
[3]*School of Geography, Earth and Environmental Sciences, Plymouth University, Plymouth, England*
[4]*School of Petroleum Engineering, The University of New South Wales, Sydney, Australia*
[5]*Institute of Petroleum Engineering, Heriot-Watt University, Edinburgh, Scotland*

Deformation in the middle crust involves a complex interplay of brittle, ductile and fluid assisted processes. Recently, the middle crust has also been discovered as being the locus of slow slip events (SSE). Geophysical models of SSE often emphasize the role of fluids but are mostly theory driven and lack a robust observational microstructural basis. Here we present detailed microstructural observations of syn-kinematic porosity from a mid-crustal ultramylonite that outline the potential significance of creep cavitation in the nucleation of slow slip events.

We investigate a quartzo-feldspathic, amphibolite facies ultramylonite from the Redbank Shear Zone in central Australia. We observe syn-kinematic pores, creep cavities, in mono-mineralic quartz domains of a fine-grained ultramylonite. High resolution image analysis in conjunction with Electron Backscatter Diffraction mapping allow for the discrimination of two pore populations that we interpret to be indicative of different pore generation mechanisms: Zener-Stroh cracks and Superplastic void growth. We found that creep cavitation controls the disaggregation process of recrystallised quartz ribbons during ultramylonitisation. In initially thick and coherent quartz ribbons, pores generated by Zener-Stroh crack formation on grain-boundaries aligned with the YZ plane of finite strain. In our interpretation the newly formed pores attract fluids, which lowers the adhesion and cohesion of the grain boundaries and promotes the activity of viscous grain boundary sliding (VGBS). With decreasing quartz domain thickness and increasing quartz dispersion into the fine-grained (~1-2 μm) polyphase domains, VGBS becomes dominant and Superplastic voids grow. We suggest that creep cavity formation in mono-mineralic quartz domains evolves in tandem with creep cavity activity in the poly-mineralic domains.

These findings expand on the previous observations of the ‘Dynamic Granular Fluid Pump’ to include, under certain boundary conditions, mono-mineralic quartz domains as second textual component. The detail of these new observations provides a robust micro-structural basis for discussing porosity generated directly out of dislocation creep, via Zener-Stroh cracking. Furthermore, the observed abundance of creep cavities in the sample raises questions about the potential of ductile failure, as has previously been observed in laboratory experiments, and its role in triggering of mid-crustal shear instabilities. Currently much of our hydro-mechanical understanding of the middle crust is based on the assumption that fluid mobility is linked purely to brittle instabilities; the observations we present here suggest that we must also consider the possibility that ductile instabilities are equally capable of generating complex fluid pathways. They may thus affect the nucleation of slow slip events in this crustal domain.

A microstructural characterisation of transitioning rheological behaviour at greenschist-facies conditions

J. Gilgannon[1], M. Herwegh[1] & A. Berger[1]
[1]*Institut für Geologie, Universität Bern, Bern, Switzerland (james.gilgannon@geo.unibe.ch)*

Many aspects of the dynamics of deformation, while well studied, remain enigmatic: most specifically the mechanisms responsible for transitioning a rocks rheology. Phenomenological work on end member behaviours, load bearing frameworks (LBF) and interconnected weak layers (IWL), has provided a starting point in understanding mechanical transitions by accounting for the proportion of second phases and how this effects rheology. However, these descriptions are mostly grounded in mechanical considerations and lack information about the micro-mechanisms associated with transient stages of deformation. In our study we seek to bolster the current understanding of these transient stages of an evolving rheology with detailed micro-structural analysis. For our investigations we utilise a pristine drill core from the Doldenhorn Nappe (Central Alps) that extends to the nappe's basal thrust plane and experiences simultaneously both frictional and viscous deformations. Our main aim is to shed light on the interplay of micro-mechanisms capable of increasing the amount of secondary phases, which ultimately takes a LBF to an IWL rheology.

The role of pre-existing anisotropies in fault mechanics: experimental insights from triaxial saw-cut experiments

C. Giorgetti[1,2] , M. M. Scuderi[1,2] , T. Tesei[2] & C. Collettini[1,2]
[1]*Department of Earth Sciences, Sapienza University of Rome, Rome, Italy (carolina.giorgetti@uniroma1.it)*
[2]*HP-HT laboratory, INGV, Rome, Italy*

Fault orientation and fault rock mechanical properties exert a major control on fault reactivation. Slip along faults that lie at high angle to the maximum compressive stress requires restrictive conditions, such as very low friction coefficient and/or near-lithostatic pore fluid pressure. However, the mechanism allowing a misoriented fault to initiate is still a matter of debate. Nevertheless, misoriented faults, such as the San Andreas fault, low-angle normal faults and sub-horizontal décollements, are recognized throughout the world. On a smaller scale, field observations show that mesoscale faults in mechanical multilayers often propagate within clay-rich layers at high angle to the maximum principal stress. These observations suggest that the presence of pre-existing anisotropies, not only resulting from faulting but also due to inherited foliation or sedimentary layering, plays a key role in determining fault geometry.

To investigate this problem, we present a suite of triaxial experiments in which we deformed cylindrical samples of sandstone with pre-imposed saw-cuts with variable orientations respect to the axial stress. A layer of powdered marl or shale was placed within the saw-cut to simulate a pre-existing anisotropy. We performed: 1) conventional triaxial experiments to evaluate the failure envelope of the sandstone, and 2) biaxial experiments to evaluate the frictional strength of the marl and shale. Then, 3) we conducted triaxial experiments at constant confining pressure with saw-cuts oriented at different angles to the axial stress, from 30° (favourably oriented) up to 80° (severely misoriented). Microstructural observations on reactivated saw-cuts were conducted to investigate the deformation processes with increasing fault deformation. Finally, we compared the resulting deformation mode, i.e. saw-cut reactivation vs. new fracture development, with theoretical predictions based on sandstone strength and marl/shale friction.

Our results show a complex mechanical behaviour that results from the interplay between the stress field orientation and the contrast in mechanical properties between the gouge and the surrounding. Reactivation occurs only in saw-cuts at angles to the axial stress that are lower than 60°-70°, consistently with theoretical predictions. Preliminary laboratory data show that under dry conditions the reactivation is a multi-stage process: after an initial compaction phase and a linear-elastic phase, yielding of the fault gouge occurs. Given the same boundary conditions, yielding occurs at the same differential stress independently of saw-cut orientation. After the yielding, a second linear-elastic phase precedes stick-slips followed by stable sliding. Integrating mechanical data and microstructural investigation we suggest that the first inelastic yielding occurs when the Mohr circle is tangent to the frictional reactivation criterion, obtained from friction experiments (2). Then, stick-slip and stable sliding are associated to localization of deformation along shear planes. We infer that they occur only when the stress path of the saw-cut intersects the frictional reactivation criterion.

Full-field numerical simulations of subgrain rotation recrystallisation during shearing of dry halite polycrystals

E. Gomez-Rivas[1], A. Griera[2], M.-G. Llorens[3], P.D. Bons[3] & R.A. Lebensohn[4]

[1]School of Geosciences, University of Aberdeen, AB24 3UE Aberdeen, United Kingdom (e.gomez-rivas@abdn.ac.uk)
[2]Departament de Geologia, Universitat Autònoma de Barcelona, Bellaterra (Cerdanyola del V.), Spain
[3]Department of Geosciences, University of Tübingen, Wilhelmstr. 56, 72074 Tübingen, Germany
[4]Materials Science and Technology Division, Los Alamos National Laboratory, Los Alamos, NM 87545, USA

The study of rock deformation microstructures is essential to understand tectonic processes and rock physical properties. Dislocation creep of polycrystalline aggregates typically leads to the formation of crystal preferred orientations (CPO) and a strong anisotropic behaviour. Halite (NaCl) is a widely used mineral in experiments that aim to understand the behaviour of rocks deformed in the ductile regime because it can flow ductily and recrystallise in the solid state under relatively low stresses. At low temperature and dry conditions halite deforms by dislocation creep, with subgrain rotation being the dominant recrystallisation mechanism. This results in an anisotropic behaviour associated with the development of intracrystalline heterogeneities that result in a strong grain-size reduction with increasing deformation. However, the interplay between dislocation creep and recovery of intracrystalline defects can substantially modify the microstructure and produce a reduction of subgrains associated with the decrease of boundary and strain stored energies. Microdynamic numerical simulations are an essential tool to complement the analysis of experimental/field samples, because they allow overcoming the length- and time-scale limitations of experiments.

We present, for first time, results of full-field numerical simulations of subgrain rotation recrystallisation of halite polycrystals during simple shear deformation. We combine a full-field viscoplastic formulation based on the Fast Fourier Transform (VPFFT) with ELLE modules to simulate intracrystalline recovery driven by a reduction of the local misorientations, generated by dislocations (*e.g.*, Llorens et al., 2017). Lattice orientation and grain boundary maps reveal how this method reproduces dry halite deformation experiments.

The results show how microstructures are controlled by the competition between (i) grain fragmentation by dislocation glide and (ii) subgrain coarsening by coalescence through rotation and alignment of the lattices of neighbouring subgrains, associated with recovery. A strong grain-size reduction as a result of the formation of high-angle boundaries develops in models where recovery is not active. Subgrain coarsening associated with recovery decreases the stored strain energy and leads to microstructures dominated by grains with low intracrystalline heterogeneities. However, this does not modify CPOs. We show how the geometric mean of subgrain-boundary misorientations can be used to estimate the strain accommodated by dislocation creep using a universal scaling exponent of 2/3, as predicted by theoretical models. This strain gauge can also be applied to estimate the amount of recrystallisation using EBSD maps.

Reference: Llorens, M.-G., Griera, A., Steinbach, F., Bons, P.D., Gomez-Rivas, E., et al. Dynamic recrystallisation during deformation of polycrystalline ice: insights from numerical simulations. 2017. Philosophical Transactions of the Royal Society A, 375:20150346.

Early quartz fabrics from the Caledonides of northern Scotland: a new look at old data

D. Greenawald[1] & R. Law[2]
[1]*Geological Sciences, University of North Carolina, Chapel Hill, USA*
[2]*Geosciences, Virginia Tech, Blacksburg, USA (rdlaw@vt.edu)*

In the 1930s-1980s quartz c-axis fabrics reported from the plastically deformed and dynamically recrystallized rocks of the Caledonides in northern Scotland played a historically important role in the evolution of ideas on a range of structural/tectonic processes. These included: a) whether mineral stretching lineations develop perpendicular or parallel to tectonic transport; b) the influences of 3D strain, dynamic recrystallization and multiple phases of deformation on fabric development; c) kinematic frameworks and the role of simple shear versus pure shear (symmetric and asymmetric fabrics) in tectonic evolution of thrust sheets and mylonite zones. Influential early fabric studies included: 1) Phillips (1937) and the often overlooked PhD study by his research student (Crampton 1955) on Moine Supergroup rocks in the Moine thrust sheet and overlying thrust sheets; 2) Johnson (1957, 1960) on the zone of mylonites derived from Moine and locally Lewisian rocks at the base of the Moine thrust sheet; 3) Christie (1963) on Cambrian quartzites in the footwall to the Moine thrust.

As was the general practice in the 1930-1960s measured fabrics were almost always reported on sample coordinate projection planes oriented perpendicular to mineral lineation. Frank Coles Phillips also used horizontal geographic (i.e. map view) projection planes for his data sets when addressing the on-going contentious issues of whether mineral stretching lineations develop perpendicular or parallel to tectonic transport, and consequently was development of the Caledonides associated with westward or N-S tectonic transport (e.g. Phillips 1937). Since the mid-1970s to early 1980s it has been generally accepted that microstructural and crystal fabric shear sense indicators are most meaningfully viewed in projection planes oriented parallel to lineation and perpendicular to foliation - so called 'XZ' section planes. Certainly compared with other projection planes, such as the lineation perpendicular plane that was used before, internal and external fabric asymmetry attributes that can be used to deduce shear senses are more easily interpreted in these 'XZ' projection planes. We have therefore digitized representative examples of the historically more important quartz c-axis fabrics reported by the early fabric pioneers and re-plotted them on 'XZ' section planes, and in this poster compare them with fabrics from the same locations that have more recently been directly measured on XZ planes. We find that in general these early fabrics are similar to the more recently measured fabrics and often faithfully record known shear senses, 3D strain variation and a foreland to hinterland increase in deformation temperatures as indicated by transitions in fabric topology and opening angle.

Christie, J.M. 1963. The Moine thrust zone in the Assynt region, northwest Scotland. University of California Publications in Geological Sciences, 40, 345-440.
Crampton, C.B. 1955. Petrofabric and textural study of the Moine and Cambrian in Sutherland and Ross. Unpublished PhD thesis, University of Bristol.
Johnson, M.R.W. 1957. The structural geology of the Moine thrust zone in Coulin Forest, Wester Ross. Quarterly Journal of the Geological Society, London, 113, 241-266.
Johnson, M.R.W. 1960. The structural history of the Moine thrust zone at Lochcarron, Wester Ross. Transactions of the Royal Society of Edinburgh, 64, 139-168
Phillips, F.C. 1937. A fabric study of some Moine schists and associated rocks. Quarterly Journal of the Geological Society, London, 93, 581-620.

The influence of the deformation history on the microstructural evolution of polycrystalline olivine and how it affects the interpretation of mantle seismic anisotropy

A. Griera[1], M.-G. Llorens[2] & E. Gomez-Rivas[3]
[1]*Departament de Geologia, Universitat Autònoma de Barcelona, Bellaterra (Cerdanyola del V.), Spain (albert.griera@uab.cat)*
[2]*Department of Geosciences, Eberhard Karls University of Tübingen, Tübingen, Germany*
[3]*School of Geosciences, King's College, University of Aberdeen, Aberdeen, United Kingdom*

Relating seismic anisotropy with mantle flow requires a good understanding of the rock's microstructural evolution and the development of crystal preferred orientations (CPO), because plastic deformation of olivine is interpreted as the main cause for mantle seismic anisotropy. In this contribution, the influence of deformation history in the microstructure evolution and resulting seismic anisotropy is investigated by means of full-field numerical simulations at the microscale. We explicitly simulate the microstructural evolution of olivine polycrystalline aggregates during dynamic recrystallization up to high strain using the code VPFFT/ELLE (e.g. Griera et al., 2011; 2013; Llorens et al., 2016). Modeling results indicate that the evolution of a CPO is highly sensitive to the initial olivine fabric. When the initial fabric is formed by a random distribution of crystallographic orientations, there is a rapid alignment of the a-axes (or [100]) with the stretching direction of flow. However, when there is an initial CPO inherited from previous deformation, larger strains are required in order for the a-axes to become re-aligned with the stretching direction. Our numerical results are in agreement with field and experimental observations (e.g. Boneh and Skemer, 2014; Skemer et al., 2012). The analysis of the seismic properties reveals that an increase of the strength of the initial inherited CPO produces a reduction of the azimuthal seismic anisotropy, compared to the case with an initial random fabric. It is concluded that the deformation history significantly influences the development of fabrics. Accordingly, seismic anisotropy interpretations must be carried out with caution in regions with complex deformation histories.

References:

Boneh Y., Skemer P. 2014 The effect of deformation history on the evolution of olivine CPO. Earth and Planetary Science Letters, 406. (doi:10.1016/j.epsl.2014.09.018).

Griera A, Bons PD, Jessell MW, Lebensohn RA, Evans L, Gomez-Rivas E. 2011 Strain localization and porphyroclast rotation. Geology 39, 275-278. (doi: 10.1130/G31549.1).

Griera A, Llorens M-G, Gomez-Rivas E, Bons PD, Jessell MW, Evans LA, Lebensohn RA. 2013 Numerical modelling of porphyroclast and porphyroblast rotation in anisotropic rocks. Tectonophysics 587, 4-29. (doi: 10.1130/G31549.1).

Llorens, M.-G., Griera, A., Bons, P.D., Lebensohn, R., Jansen, D., Evans, L.A. and Weikusat, I. 2016. Full-field predictions of ice dynamic recrystallisation under simple shear conditions, Earth and Planetary Science Letters, 450, 233-242. (doi:10.1016/j.epsl.2016.06.045)

Skemer P., Warren J.M., Hirth G. (2012) The influence of deformation history on the interpretation of seismic anisotropy, Geochemistry Geophysics Geosystems, 13:3, doi:10.1029/2011GC003988

Inverted temperature fields: role of progressive deformation

D. Grujic[1], K. T. Ashley[2], M. A. Coble[3], I. Coutand[1], D. A. Kellett[4], & N. Whynot[1]
[1]Department of Earth Sciences, Dalhousie University, Halifax, NS B3H 4R2,Canada (dgrujic@dal.ca)
[2]Department of Geological Sciences, Jackson School of Geosciences, University of Texas at Austin, Austin, TX 78712, USA
[3]Department of Geological Science, Stanford University, CA 94305, USA
[3]Geological Survey of Canada, Natural Resources Canada, 601 Booth St., Ottawa, Canada

To explain the formation of an inverted metamorphic sequence we performed a study, which combined geothermometry with the thermochronology. The data are evaluated trough thermokinematic forward and inverse modeling to constrain the ranges of important geological parameters such as fault slip rates, the location and rates of localized crustal accretion, and the thermal properties of the crust. The case study was performed along a transect across the Lesser Himalayan Sequence (LHS) of the eastern Bhutan. The geothermometry included the Raman spectroscopy of carbonaceous material (RSCM) to determine the peak metamorphic temperatures and Ti-in-quartz thermobarometry to determine the deformation temperatures. The thermal kinematic modeling was performed with PECUBE software and as thermochronologic constraints we used apatite and zircon U-Th/He and fission-track data and $^{40}Ar/^{39}Ar$ dating of muscovite. The spatial pattern of peak temperatures across the LHS, acquired by RSCM indicates that there are two temperature field sequences separated by a major thrust. Internal temperature sequence shows an inverted temperature field gradient of 12 °C/km; in the external one the peak temperatures are same with the structural sequence. Thermo-kinematic modeling shows that the thermochronologic and thermobarometric data can be well fit by a two-stage evolutionary scenario: an Early-Middle Miocene phase of overthrusting of a hot hanging wall over a downgoing footwall and inversion of the synkinematic isotherms, followed by the formation of the external duplex developed by basal accretion.

The inverted metamorphic field gradient is registered by various geothermometric systems and at different temperatures ranges indicating that the processes that formed the current (i.e., finite) metamorphic field gradient have lasted over an extended time period, along the retrograde metamorphic path, and have involved various processes at different stages:

(a) Synkinematic steepening and inversion of the isotherms in the vicinity of the crustal-scale shear zone.
(b) Locking in of the peak-*T* isotherms registered by the metamorphic assemblages.
(c) On-going pervasive ductile deformation characterised by general shear.
(d) Deformation of the peak-*T*-isotherms; formation of the quartz deformation-isotherms.
(e) Deformation focusing (progressive shear zone narrowing) may offset the peak-*T* isotherms.
(f) Retrograde ductile deformation still with an inverted temperature gradient but caused by progressive cooling of successively more internal and thus hotter rocks.

Geostatistics applied to strain field analysis: application to the Variscan orogen, Pyrenees.

C. Gumiaux[1], B. Cochelin[2,3], D. Chardon[2,4], Y. Denele[2] & B. Le Bayon[3]
[1]*ISTO, University of Orléans, CNRS, BRGM, Orléans, France (charles.gumiaux@univ-orleans.fr)*
[2]*Géosciences Environnement Toulouse, University of Toulouse, Toulouse, France*
[3]*BRGM DGR/GSO, BP 36009 Orléans, France*
[4]*IRD & Université Ouaga 1 Professeur Joseph Ki-Zerbo, Ouagadougou, Burkina Fasso*

Strain field mapping allows imaging and highlighting spatial variations, both in orientation and intensity, of the finite strain in the rocks. At a given location, strain ellipsoid is characterised by structural field measurements including cleavage/foliation planes and stretching lineations for ductilely deformed domains. Based on such measurements; trajectory maps are classically used to study regional-scale spatial variations in the strain fields. However, there is a difficult "scale problem" between the weight given to measured data and the degree of data filtering/smoothing required to draw large scale tendencies. Most extrapolation techniques tend to respect as much as possible the original data values, and this may fail if one wants to extract regional-scale trends; data values can indeed be sensitive to local strain variations (e.g. competency-induced cleavage refraction, small-scale folding, boudinage), as well as to significant errors made during measurements, data digitizing from maps, or location of data points.

Here we develop a geostatistical approach for best-fit interpolation of orientation data applied to cleavage orientation measurements. The analytical procedure comprises two main steps: (i) the analysis of the spatial variations of the data by calculating angle variograms, and (ii) the kriging interpolation between individual angles via their direction cosines. Indeed, angles values are of circular type data and none of the classical statistical/geostatistical tools can be directly applied before being transposed. In a first stage, angle variogram analysis allows quantifying the natural spatial correlation between scattered data values. In particular, the “range parameter” value estimates the maximum correlation distance in between data point values that corresponds to the scale of the tectonic phenomenon leading to the variations observed in the strain field. Another parameter, the "nugget effect", allows measuring the proportion of the significant part of the signal and background noise from the data. The latter includes errors that can be made during measurements and/or further computation processes but also some share of “local” effects in data variations that cannot be taken into account at the scale considered. As nugget effect value can vary, from the same data set, when considering various extensions of the study area, geostatistics can be used for multi-scale analysis and imaging of the finite strain fields.

Application of this approach is exemplified from the study of late Variscan deformation of the Paleozoic crust of the Pyrenees. There, the abnormally hot foreland crust of the orogen has been squeezed, from ~310 to ~290 Ma, at the core of the Iberian-Armorican arc. The ~300 km long study area allows for the observation of both upper and lower crust levels. Using the geostatistical approach, strain fields from different massifs and regions – at various scales – are modelled and compared to evaluate the contrasting behaviour of the different structural levels of the crust, and their mechanical coupling, during late-orogenic shortening.

Stress-driven versus fluid-driven slip: using experiments to explore differences in modes of earthquake rupture

K.S. Hayward[1] & S. F. Cox[1]
[1]*Research School of Earth Sciences, Australian National University, Canberra, Australia (kathryn.hayward@anu.edu.au)*

In upper seismogenic crust, rock failure is controlled by the evolution of stress states and pore fluid pressures. Classic mainshock-aftershock earthquakes occur as a result of increases in shear stress acting on a fault, either through tectonic loading or small stress changes that occur in response to slip on nearby faults. Although changes in fluid pressure within the fault zones may enhance or impede rupture, if fault slip is dominantly driven by a relative increase in shear stress it is referred to here as a 'stress-driven' failure. In contrast, some types of earthquake swarms (e.g. injection-driven swarms) occur in geological settings where overpressured fluids are injected in large volumes into low-permeability rock. In response to local increases in pore-fluid pressures, faults repeatedly slip in sequences of hundreds to thousands of generally small ($-2 < M_w < 4$), low displacement ruptures. As these ruptures are induced by changes in fluid pressure rather than through tectonic loading, they are referred to here as 'fluid-driven' failures. Although these two examples of fault rupture style represent end-members of fault behaviour, they serve as the basis for the experiments discussed here.

We have used a Paterson triaxial apparatus to explore the mechanics and microstructures associated with the reactivation of faults under high normal stress using either changes in axial load or fluid pressure to drive slip on existing faults at room temperature. A pure quartz-sandstone with porosity between 6-8% was used as a starting material. Pre-ground fault surfaces were oriented between 30° and 60° to the maximum shortening direction, representing both favourably and unfavourably oriented faults. Faults were reactivated under both dry and fluid-saturated conditions, with the former experiments involving an increase of axial load at constant rate until failure (stress-driven failure). Under saturated conditions we reactivated faults by maintaining a constant axial load and increasing pore fluid pressure until slip occurred (fluid-driven failure).

Unlike the injection-driven earthquake swarms observed in nature, our experiments cannot achieve either high fluid volumes or distributed areas of fluid overpressure due to apparatus and experimental limitations. However, the results reveal notable differences between stress-driven and fluid-driven reactivation, both in terms of rupture style and the formation of microstructures at the slip interface. Compared with stress-driven failure, fluid-driven reactivation results in shorter displacements and smaller stress drops. Microstructures formed during the fluid-driven events are characterised by a notable absence of damage to the fault surface and adjacent areas, suggesting limited asperity contact. However, as effective normal stress increases (e.g. >500MPa) asperities come into contact and the interface is partially welded by a thin layer of frictional melt.

Although the role that fluids play in nucleating fault rupture by reducing the effective normal stress is mechanically simple, the influence that fluids have on dynamic weakening processes remains poorly understood. These experiments provide new insights into the mechanisms operating at an asperity scale on the fault surface. Observations will be compared with theoretically described mechanisms such as thermal pressurization or elastohydrodynamic and boundary lubrication.

Capturing the first milliseconds of earthquake slip

K.S. Hayward[1], P. W. F. Forsyth[2], B.J.J. Slagmolen[2], D.A. Shaddock[2] & S.F. Cox[1]
[1]Research School of Earth Sciences, Australian National University, Canberra, Australia (kathryn.hayward@anu.edu.au)
[2]Research School of Physics and Engineering, Australian National University, Canberra, Australia

The Paterson-type triaxial apparatus was originally built to investigate the strength, deformation and rheological properties of geological materials within a viscous flow regime (Paterson, 1970). A key feature of this apparatus is its mechanical sensitivity arising from the use of a gas confining medium and internal load cell, allowing exploration of confining pressures (P_c) up to 300MPa, pore fluid pressures equivalent to (P_c – 30MPa) and differential stresses of up to ~1GPa. Although study of earthquake slip was not the original intent of the apparatus, its mechanical sensitivity and the ability to store elastic strain energy that is released into a sample upon failure makes it valuable for use in the study of small seismic events during stick-slip. These rapid slip events can be produced on pre-ground 'fault surfaces' at pressure and temperature conditions equivalent to those estimated for the crustal seismogenic regime.

Traditionally mechanical measurements on the Paterson apparatus have involved the use of sensors such as pressure transducers, strain gauges and displacement transducers. These types of sensor produce a voltage output that is sampled at frequencies up to 1000Hz and recorded at a rate of 1-100 samples per second. Fundamental limitations in sensor response time, signal conditioning requirements, and electromagnetic interference prevent data acquisition rates being increased to levels sufficient to capture seismic slip events.

This poster presents a new sensor that we have designed and built for measuring slip displacement at sampling speeds sufficient to capture fault rupture (estimated to be equivalent to the shear wave velocity of the sample (e.g. ~3500m.s^{-1}). We utilise a 1550nm fibre-based Mach-Zehnder optical heterodyne system coupled with a digital phase lock loop to provide non-continuous, triggered acquisition at a rate of 1 million samples per second. The use of an optical interferometer alleviates the effect of electromagnetic interference, allows flexibility in measurement configuration and achieves a system capable of a large dynamic range (multiple centimetres of axial displacement), high displacement resolution (10^{-9}m/$\sqrt{Hz}$ above $2Hz$), and high velocity tracking capabilities (up to ~30m.s^{-1}). We have adopted a novel approach to measurement, with multiple beam paths allowing isolation of sample and machine responses to slip events. Presently two beam paths are located on the exterior of apparatus, with optical collimators mounted at the top and bottom of the pressure vessel. The laser beam is reflected off mirrors attached to the apparatus yoke providing a path that varies during deformation as the upper yoke moves relative to the pressure vessel. A third beam path is located internally within the piston assembly above the sample. A micro-collimator, located within the pore-fluid conduit, reflects the beam off an optically flat, highly polished tungsten carbide disc at the top of in the sample assembly, allowing the first direct measurements of the sample displacement during rupture propagation.

Early results of this system have revealed new insights into the first milliseconds of fault slip. High spatial and temporal resolution of the data has shown that multiple slips can occur during what would previously be defined as a single event. We have also been able to correlate fault behaviour and slip velocities with different microstructural phenomena (*Hayward et al.*, 2016).

FracPaQ: a MATLAB™ toolbox for the quantification of fracture patterns

D. Healy[1*], R. Rizzo[1], D. Cornwell[1], N. Farrell[1], H. Watkins[1], N. Timms[2] & E. Gomez-Rivas[1]
[1]School of Geosciences, University of Aberdeen, Aberdeen AB24 3UE UK (d.healy@abdn.ac.uk)
[2]Department of Applied Geology, Curtin University, Perth WA 6845 Australia

The patterns of fractures in deformed rocks are rarely uniform or random. Fracture orientations, sizes, shapes and spatial distributions often exhibit some kind of order. In detail, there may be relationships among the different fracture attributes e.g. small fractures dominated by one orientation, larger fractures by another. These relationships are important because the mechanical (e.g. strength, anisotropy) and transport (e.g. fluids, heat) properties of rock depend on these fracture patterns and fracture attributes. This presentation describes an open source toolbox to quantify fracture patterns, including distributions in fracture attributes and their spatial variation.

Software has been developed to quantify fracture patterns from 2-D digital images, such as thin section micrographs, geological maps, outcrop or aerial photographs or satellite images. The toolbox comprises a suite of MATLAB™ scripts based on published quantitative methods for the analysis of fracture attributes: orientations, lengths, intensity, density and connectivity. An estimate of permeability in 2-D is made using a parallel plate model. The software provides an objective and consistent methodology for quantifying fracture patterns and their variations in 2-D across a wide range of length scales.

Our current focus for the application of the software is on quantifying crack and fracture patterns in and around fault zones. There is a large body of published work on the quantification of relatively simple joint patterns, but fault zones present a bigger, and arguably more important, challenge. The methods presented are inherently scale independent, and a key task will be to analyse and integrate quantitative fracture pattern data from micro- to macro-scales. New features in this release include multi-scale analyses based on a wavelet method to look for scale transitions, support for multi-colour traces in the input file processed as separate fracture sets, and combining fracture traces from multiple 2-D images to derive the statistically equivalent 3-D fracture pattern expressed as a 2nd rank crack tensor.

The mechanical behaviour and failure modes of volcanic rocks

M. Heap[1], J. Farquharson[1], M. Violay[2], P. Baud[1], F. Wadsworth[3], J. Vasseur[3], Y. Lavallée[4] & T. Reuschlé[1]

[1]*Géophysique Expérimentale, Institut de Physique de Globe de Strasbourg (UMR 7516 CNRS, Université de Strasbourg/EOST), 5 rue René Descartes, Strasbourg 67084, France (heap@unistra.fr)*

[2]*Laboratory of Experimental Rock Mechanics, École Polytechnique Fédérale de Lausanne, Station 18, CH-1015, Lausanne, Switzerland*

[3]*Earth and Environmental Sciences, Ludwig-Maximilians-Universität, Theresienstr. 41, 80333 Munich, Germany*

[4]*Earth, Ocean and Ecological Sciences, University of Liverpool, Liverpool, UK*

Volcanic structures are constructed from the products of successive effusive and explosive eruptions. The modelling of volcanic systems, and the interpretation of geophysical signals, relies on a detailed understanding of how edifice rock responds to the dynamic pressures, stresses, and temperatures that characterise volcanic systems. We investigate here mechanical behaviour, failure modes, operative micromechanical mechanisms, and strain localisation in volcanic rocks using triaxial deformation experiments (performed at a range of pressures and temperatures) on porous andesite (porosity from 0.08 to 0.25).

Room-temperature triaxial experiments (effective pressures from 0 to 70 MPa) show that at shallow depths in the edifice (<1 km), both low- and high-porosity andesite dilate and fail by shear fracturing (i.e., brittle). However, deeper in the edifice (>1 km), while low-porosity (porosity < 0.1) andesite remains dilatant, the failure of high-porosity andesite is compactant (i.e., ductile). Although inelastic compaction is typically characterised by the absence of strain localisation, we observe compactive localisation features manifest as subplanar surfaces of collapsed pores. In this regime, porosity is only reduced within the bands of crushed pores; the porosity outside the bands remains unchanged. High-temperature triaxial experiments (effective pressure = 40 MPa) show that the micromechanism facilitating compaction is localised cataclastic pore collapse at all temperatures below the glass transition of the amorphous groundmass glass, Tg (the transition whereat the glass within the groundmass transitions from a glass to an undercooled liquid, found to be at about 750 °C for the studied andesite). However, the micromechanism driving compaction above the threshold Tg is the distributed viscous flow of the melt phase. In this regime, porosity loss is distributed and accommodated by the widespread flattening and closure of pores. We find that viscous flow is much more efficient at reducing porosity than cataclastic pore collapse, and that it requires stresses much lower than those required to form bands of crushed pores.

The failure mode (brittle or ductile) influences the evolution of rock physical properties. Brittle behaviour will lead to increases to porosity and permeability. Indeed, we find that a throughgoing tensile fracture increases sample permeability. Ductile behaviour will result in reductions to porosity and permeability, the magnitude of which will depend on the micromechanism (viscous flow or cataclastic pore collapse) and therefore temperature. We find that room temperature inelastic compaction to an axial strain of 4.5% reduces sample permeability by an order of magnitude, but anticipate that the huge reduction in porosity due to viscous flow (porosity reduced from 0.26 to 0.06) could reduce permeability by up to four or five orders of magnitude. Taken together, our experiments highlight that changes in pressure and temperature can result in changes to the failure mode and deformation micromechanism that can drastically alter the mechanical, physical, and hydraulic properties of the rocks forming the volcanic edifice.

Re-measuring Recrystallized Grain Sizes in Quartz Shearing Experiments

R. Heilbronner[1,2], R. Kilian[1] & J. Tullis[3]
[1]*Geological Institute, Basel University, Switzerland,*
[2]*Department of Geosciences, Tromsø University, Norway,*
[3]*Department of Geological Sciences, Brown University, USA*

For a series of shearing experiments on Black Hills quartzite, the recrystallized grain size was re-measured using EBSD maps obtained with the ZEISS Merlin SEM and AZtec acquisition software recently installed at Tromsø University. The experiments were carried out at Brown University at temperatures from 850° to 915°, confining pressures of 1.5 to 1.58 GPa, a shear strain rate of 10-5 s-1, and with and without 0.2 wt% water added. Deformation was in the dislocation creep regime, and the resulting shear stresses τ were between 100 and 320 MPa (Δσ between 200 and 640 MPa).

In the original papers (Heilbronner & Tullis, 2002, 2006), grain size determinations were made using c-axis orientation images (CIP method). However, the spatial resolution of polarization microscopy was not good enough to obtain reliable measurements for the very small recrystallized grain sizes of regime 1 and 2. For regime 3, equivalent diameters could be measured with sufficient accuracy and by considering grain boundary density, a dependence of the recrystallized grain size on c-axis orientation was detected.

When re-examining the three dislocation creep regimes, two or three samples with bulk shear strains of γ = 2 - 7 were analyzed. Careful re-calculation of the flow stresses with updated software confirms the published data. The determination of the recrystallized grain sizes confirms the approximate measurements made using CIP for regime 3 and the texture dependence of the recrystallized grain size in the one case investigated in 2006. - Interestingly, for a second sample deformed under almost identical conditions, but to higher strain, such a texture dependence cannot be observed. What can be observed, however, is that in both samples, small recrystallized grain sizes correlate with high grain kernel average misorientation (GAM). Many samples show gradients of GAM and corresponding gradients of grain size. Within zones of constant GAM, the texture dependence of grain size varies according to the active deformation mechanisms, evolving over relatively large strains before a stable grain size is developed.

In order to compare the results to the quartz piezometer of Stipp & Tullis (2003), the RMS of the 2-D equivalent diameter of the recrystallized grains was plotted against the differential stress, Δσ (2·τ). Overall, a clear dependence of grain size on flow stress was found, independent of the amount of finite shear strain the sample had incurred. However, the resulting piezometer relationship shows that under shearing conditions the flow stresses are higher (or the grain sizes larger) than would be predicted by the Stipp &Tullis piezometer. Whether the discrepancy is due to the different kinematic frame work (coaxial versus non-coaxial), the difference in finite strain, i.e., total amount of recrystallization, or due to different experimental conditions that may have led to the activation of different deformation mechanisms or different combinations of mechanisms, is still under investigation.

Deformation behaviour of feldspar in greenschist facies pegmatitic mylonites from the Austroalpine basement to the south of the western Tauern window, Eastern Alps

F. Hentschel[1], C. Hsu[1] & C.A. Trepmann[1]

[1]*Department of Earth and Environmental Sciences, Ludwig-Maximilians University, Munich, Germany, (claudia.trepmann@lmu.de)*

The goal of this study is to correlate different feldspar microstructures to specific deformation mechanisms. As plagioclase and K-Feldspar are abundant in the continental crust, knowledge about their deformation behaviour is crucial for our understanding of the long-term rheology of the crust. Experiments and natural studies have long shown that the interaction of brittle, dissolution-precipitation and crystal-plastic mechanisms are very important for the feldspar deformation behaviour over a large temperature range. But a correlation of specific microstructures to the different deformation mechanisms is still unclear. In this study we use the deformation record of pegmatites from the Austroalpine basement south of the western Tauern Window. The pegmatites are Permian in age and constitute an almost Ca-free system, mainly containing albitic plagioclase, K-feldspar, quartz and white mica. In addition, tourmaline, magmatic and alpine garnet as well as accessory phases like apatite, monazite and xenotime occur. Growth of secondary garnet and replacement of monazite and xenotime by allanite and epidote indicate that the pegmatites experienced middle greenschist facies conditions during Alpine tectonometamorphism. Deformed pegmatites show clasts of feldspar and mica suspended in a finer grained matrix. The matrix consists of alternating almost monocrystalline albite- and quartz-ribbons. Based on the microstructure two types of matrix with quartz and albite ribbons can be distinguished. The first type is characterized by elongate and fine-grained (<10 µm) recrystallized quartz ribbons with marked y-maximum of c-axes and ribbons of coarser (50-100 µm) lense-shaped feldspar aggregates. In the second type, quartz in ribbons is much coarser grained (a few tens of µm) and feldspar grains are isometric with an average diameter of 25 µm. In both cases feldspar has a non-existent to weak CPO. This weak CPO can hardly be explained by dislocation glide with any known glide system and is probably inherited from the original host, indicating replacement. Both plagioclase and K-feldspar porphyroclasts show replacement by new plagioclase grains at the rim or along fractures. A weak host-control on the orientation of new grains can be observed for the replacement of plagioclase clasts but not for the replacement of K-feldspar. So far, no difference in the An-content between old and new plagioclase could be observed but in one case new grains can show Ca-rich rims. Strain shadows can occur around either type of feldspar porphyroclasts. These are composed of polymineralic aggregates of feldspar and quartz. Feldspar porphyroclasts can show evidence of crystal-plastic deformation by mechanical twins that are bent and undulatory extinction. New feldspar grains are devoid of any intracrystalline deformation microstructures. We interpret polycrystalline strain shadows and polycrystalline matrix to be due to precipitation from the fluid phase. Replacement of K-feldspar by albite is interpreted to be driven by chemical gradients and probably favoured by fracturing and crystal-plastic deformation. Replacement of plagioclase clasts by secondary plagioclase is interpreted to be mainly driven by reduction in strain energy. The isometric shape of new grains in albite ribbons of the type 2 pegmatites suggests that they are also formed by replacement of primary albite. The isometric shape of new grains indicates growth at relatively low stress, consistent with the coarse quartz ribbons. In contrast, the lens shaped elongate albite matrix, is suggesting growth during ongoing deformation, consistent with the fine-grained quartz ribbons.

Permeability evolution in crystalline basement fault zones

A.D. Hollinsworth[1], D. Koehn[1] & T.J. Dempster[1]
[1]*School of Geographical and Earth Sciences, University of Glasgow, Glasgow, Scotland*

Fault zones are important sites for crustal fluid flow, specifically where they cross-cut low permeability host rocks such as granites and gneisses. Fluids migrating through fault zones can cause rheology changes, mineral precipitation and pore space closure, and may alter the physical and chemical properties of the host rock and deformation products. It is therefore essential to consider the evolution of permeability in fault zones at a range of pressure-temperature conditions to understand fluid migration throughout a fault's history, and how fluid-rock interaction modifies permeability and rheological characteristics.
Field localities in the Rwenzori Mountains, western Uganda and the Outer Hebrides, north-west Scotland, have been selected for field work and sample collection. Here Archaean-age TTG gneisses have been faulted within the upper 15km of the crust and have experienced fluid ingress.

The Rwenzori Mountains are an anomalously uplifted horst-block located in a transfer zone in the western rift of the East African Rift System. The north-western ridge is characterised by a tectonically simple western flank, where the partially mineralised Bwamba Fault has detached from the Congo craton. Mineralisation is associated with hydrothermal fluids heated by a thermal body beneath the Semliki rift, and has resulted in substantial iron oxide precipitation within porous cataclasites. Non-mineralised faults further north contain foliated gouges and show evidence of leaking fluids. These faults serve as an analogue for faults associated with the Lake Albert oil and gas prospects.

The Outer Hebrides Fault Zone (OHFZ) was largely active during the Caledonian Orogeny (ca. 430-400 Ma) at a deeper crustal level than the Ugandan rift faults. Initial dry conditions were followed by fluid ingress during deformation that controlled its rheological behaviour. The transition also altered the existing permeability. The OHFZ is a natural laboratory in which to study brittle fault rocks, and younger Mesozoic age faults may provide analogues for the West Shetland basin.

Samples have been collected from both of these localities, and will be examined by optical and scanning electron microscopy. X-Ray micro-tomography will also be used to analyse the permeability characteristics of the fault rocks. Our understanding of fault zone permeability is crucial for a number of research areas, including earthquake geoscience, economic mineral formation, and hydrocarbon systems. As a result, this research has relevance to a variety of industry sectors, including oil and gas (and ccs), nuclear waste disposal, geothermal and mining.

Stylolite-controlled diagenesis of a mudstone carbonate reservoir: examples from the Ca2 Stassfurt carbonate (Central European Basin, NW Germany)

E. Humphrey[1], E. Gomez-Rivas[1], D. Koehn[2], P. Bons[3], J.D. Martín-Martín[4] & J. Schoenherr[5]
[1]*School of Geosciences, University of Aberdeen, AB24 3UE Aberdeen, United Kingdom*
[2]*School of Geographical and Earth Sciences, University of Glasgow, G12 8QQ Glasgow, United Kingdom*
[3]*Department of Geosciences, University of Tübingen, Wilhelmstr. 56, 72074 Tübingen, Germany*
[4]*Departament de Mineralogia, Petrologia i Geologia Aplicada, Universitat de Barcelona, 08028 Barcelona, Spain*
[5]*ExxonMobil Production Deutschland GmbH, Riethorst 12, 30659 Hannover, Germany*

Stylolites are rough dissolution surfaces that form as a consequence of intergranular pressure-solution resulting from burial compaction or tectonic stress. Despite being ubiquitous in most carbonate rocks, their potential impact on structural diagenesis and fluid flow has not been systematically addressed. The Zechstein-2-Carbonate (Ca2) is a diagenetically complex reservoir in the Lower Saxony Basin and Pompeckj block, and represents one of the most prolific gas reservoirs in NW Germany. In the study area, located on the Pompeckj block, the Ca2 features a variety of structures, including fractures, veins and networks of stylolites with different morphologies, and diagenetic products that formed during different times. Though the diagenetic history of the Ca2 has been previously studied, little attention has been paid to the presence of stylolite networks and their influence on the diagenetic evolution of the reservoir. This investigation focuses on evaluating the relationship between stylolites, fractures/veins and spatial variations in petrophysical properties. We utilise drill core provided by ExxonMobil Production Deutschland GmbH to carry out a combined analysis of cross-cutting relationships between different structures and diagenetic products, petrography and geochemistry of cements and replacive phases, and a statistical quantification of stylolite networks, focusing on quantifying their occurrence, morphology and sealing capacity.

The results indicate that several episodes of pressure-solution occurred, producing both bedding-parallel and tectonic stylolites at different stages. In the study area, the Ca2 deposited in the slope environment and is dominantly a carbonate mudstone that was initially dolomitised under shallow burial conditions, followed by the development of bedding-parallel stylolites during burial. Calcitising fluids percolated from neighbouring evaporite units causing dedolomitisation. Some of the stylolites locally acted as barriers to prevent the vertical migration of the calcitising fluids, resulting in a layer cake geometry of relatively porous dolomite and calcitised dolomite with lower porosity. During inversion, horizontal stylolites were reopened to act as fluid conduits to enable the lateral migration of fluids that precipitated metal sulfides. This indicates that stylolites are able to act as both barriers and conduits for fluid flow depending on variations in the stress regime of the basin. Stylolites present a range of sealing capacities depending on their morphology and teeth frequency, and can result in partial leakage and subsequent invasive calcitisation in their vicinity (Koehn et al., 2016). This study highlights the importance of understanding the impact of stylolites on structural diagenesis in carbonate reservoirs to establish spatial and petrophysical variations in reservoir quality.

Reference: Koehn, D., Pataki-Rood, M., Beaudoin, N., Chung, P., Bons, P.D. and Gomez-Rivas, E. 2016. A new stylolite classification scheme to estimate compaction and local permeability variations. Sedimentary Geology, 346, 60–71.

The anatomy of ‘hot-on-cold’ shear zones: insights from quartzites of the Main Central Thrust in the Alaknanda region (Garhwal Himalaya)

N. J. R. Hunter[1], R. F. Weinberg[1], C. J. L. Wilson[1], V. Luzin[2] & S. Misra[3]
[1]School of Earth, Atmosphere and Environment, Monash University, Victoria, 3800, Australia (nicholas.hunter@monash.edu)
[2]Australian Center For Neutron Scattering, Australian Nuclear Science and Technology Organization (ANSTO), Lucas Heights, NSW, 2234, Australia
[3]Department of Earth Sciences, Indian Institute of Technology Kanpur, Uttar Pradesh 208016, India

Crustal shear zones exhumed at the surface provide a window into the mechanics of the Earth’s interior. However, difficulties remain in quantifying their dynamic properties due to the numerous macro- and grain-scale factors controlling natural deformation. The complex interplay between such factors has meant that a number of inconsistencies remain between the knowledge derived from controlled laboratory deformations and that from empirical observations in nature. We present a methodological framework for quantifying the deformation characteristics in shear zones, using the microstructural and crystallographic orientations of quartz. The Main Central Thrust (MCT) in the Alaknanda Valley (NW Himalaya) is used as a ‘natural laboratory’, due to its abundant pure quartzite units situated along a gradient of increasing strain and temperature. Using a combination of microstructural analysis and neutron diffraction, we show that quartzites up-sequence are characterised by (i) systematic increases in grain lobateness and coarseness, indicating the transition from sub-grain rotation (SGR) to grain boundary migration (GBM) dynamic recrystallisation; and (ii) a concomitant shift in crystallographic preferred orientation (CPO) from oblique (top-to-the-SSW) girdles to a strong single *Y*-maximum, indicating the increasing role of prismatic-<*a*> slip.

In this presentation, we present novel techniques through which various deformation characteristics (temperature, strain geometry, strain distribution) can be quantitatively described across the shear zone. Our results suggest the MCT can be characterised as a ~3km wide zone of non-coaxial deformation where maximum strain, estimated using bulk CPO intensities, coincides with a sharp change in peak metamorphic temperatures, from ~450ºC in the footwall to 750−800ºC in the hanging wall. We propose that these systematic microstructural and CPO transitions may typify the deformational behaviour of quartz in ‘hot-on-cold’ crustal thrusts.

Seismic expression of fault deformation Zones using multi-attributes: limits and challenges

D. Iacopini[1] & R. Butler[1]
[1]*Department of Geology and Petroleum Geology, University of Aberdeen, UK (d.iacopini@abdn.ac.uk)*

Mapping and understanding distributed deformation is a major challenge for the structural interpretation of seismic data. Conventional workflows for seismic interpretation commonly represent faults as discrete planar discontinuities across which stratal reflections are offset. Although this approach can greatly facilitate the creation of maps of stratal surfaces and hence the formulation of seismic stratigraphic models, this simplification can hamper understanding of subsurface structural geology. We show here that volumes of seismic signal disturbance with low signal/noise ratio are systematically observed within 3D seismic datasets around fault systems. These seismic disturbance zones (SDZ) are commonly characterized by complex perturbations of the signal and occur at the sub-seismic to seismic scale (Iacopini et al., 2011, 2012). They may store important information on deformation distributed around those larger scale structures that may be readily interpreted in conventional amplitude displays of seismic data scale. We first show how existing forward modelling seem to support the SDZ expression observed using multi attributes (Botter et al., 2014). We then introduce a method to detect fault-related disturbance zones and to discriminate between this and other noise sources such as those associated with the seismic acquisition (footprint noise). Two case studies, from the Taranaki basin and deep-water Niger delta are presented. These resolve structures within SDZs using tensor and semblance attributes along with conventional seismic mapping. We shows that, through seismic image processing (Cohen et al., 2006) and the use of cross-plot functions, it is possible to extract SDZs, to treat them as geobodies and explore their internal seismic texture (Iacopini et al., 2016). A seismic image processing workflow to map the signal properties within the fault SDZ and reconstruct unsupervised seismic facies by using cluster analysis methods is described. Pitfall and limits of the methodology are proposed and a possible strategy beyond the backscattered image processing is discussed.

References:

Botter, C., Cardozo, N., Hardy, S., Leconte, I., Escalona, 2014. From mechanical modeling to seismic imaging of faults: a synthetic workflow to study the impact of faults on seismic. Mar. Pet. Geol. 57, 187-207

Cohen, I., Coult, N., Vassiliou, A., 2006. Detection and extraction of fault surfaces in 3D seismic data. Geophysics 71, 21-27.

Iacopini, D., Butler, R.W.H., 2011. Imaging deformation in submarine thrust belts using seismic attributes. Earth Planet. Sci. Lett. 302, 414-422.

Iacopini, D., Butler, R.W.H., Purves, S., 2012. Seismic imaging of thrust faults and structural damage: a visualization workflow for deepwater thrust belts. First Break 30, 39-46.

Iacopini, D., Butler, RWH., Purves, S., McArdle, N. & De Freslon, N. (2016). 'Exploring the seismic expression of fault zones in 3D seismic volumes'. Journal of Structural Geology, vol 89, pp. 54-73.

Long, J.J., Imber, J., 2010. Geometrically coherent continuous deformation in the volume surrounding a seismically imaged normal fault-array. J. Struct. Geol. 32, 222-234.

On the relationship between mantle dynamics and the configuration of subduction-related continental margins

J. Idárraga-García[1] & C.A. Vargas[2]
[1]PhD. Program in Geosciences, Universidad Nacional de Colombia, Bogota, Colombia
[2]Department of Geosciences, Universidad Nacional de Colombia, Bogota, Colombia
(cavargasj@unal.edu.co)

In this work, we present evidence of the possible control exerted by the dynamics of the sub-slab mantle on the shallow morpho-tectonic configuration of continental margins. For this, we have established a number of relationships between *S*-wave splitting delay times, which is the main parameter that characterizes the dynamics and deformation in the mantle beneath subducting slabs, and a series of parameters that describe the geometric configuration of continental margins, mainly of the accretionary wedge, in 15 subduction zones around the world. In subduction systems exhibiting perpendicular-to-trench flow patterns in the sub-slab mantle, we established that the splitting strength in the sub-slab mantle (as represented by delay times) has a direct relationship with the slab dip under the frontal accretionary prism, the terrain slope of the outer accretionary wedge, and the taper angle of the prism, while there is an inverse relationship with the thickness of the trench sedimentary infill. In contrast, in subduction zones with trench-parallel mantle flow in the sub-slab domain, a strong inverse correlation was found between the deformation in the sub-slab mantle (as represented by delay times) and the dip of the slab below the frontal accretionary prism. We hypothesize that subduction-related drag flow, in conjunction with a high coupling between the slab and the mantle beneath it, exerts a control on the basal friction and, hence, on the geometric configuration and evolution of continental margins, mainly those of the accretionary prisms.

What controls deformation in a bent three-dimensional orogen? An example from the Bolivian Andes

L. Kaislaniemi[1] & D. Whipp[1]
[1]*University of Helsinki, Department of Geosciences and Geography, Helsinki, Finland*

The Bolivian orocline is a change in the orientation of the central Andes from N-S south of ~18°S in central Bolivia to roughly NW-SE in the north. This bend coincides with ~50 % reduction in the width of the orogen east of the Altiplano, an approximately eight-fold increase in the yearly precipitation, and the presence of a basement arch that reduces the thickness of relatively weak Paleozoic sediments upon which the orogen detaches [1, 2]. This has led to uncertainty about whether the growth of the orogen is controlled primarily by climate (erosion) or tectonics (strength of the basal detachment) [3].

The study of the deformation in such oroclines is complicated by the fact that they are inherently three-dimensional and cannot be reduced to 2-D vertical cross-sections to reconstruct deformation. We study deformation in a curved orogen using 3D numerical models to better understand how along-strike variations in rainfall and basal detachment strength affect orogen deformation and growth of the Subandean zone, the frontal part of the Andean fold-thrust belt.

We calculate the visco-plastic deformation in the retro-wedge of a curved Andean-style orogen using the finite element software DOUAR [4] coupled to the surface process model FastScape [5]. Model design comprises the crust in a 1000x1000x50 km box, including the fold-and-thrust belt east of the Altiplano and the basement of the western edge of the Amazonian craton. A basal detachment zone with a change in its strike is prescribed as an initially strain-softened (weak) region. Strain softening also allows development of new faults elsewhere and evolution of the geometry of the detachment zone. The effects of varying rock strength in the detachment zone and in the overlaying rocks, orocline bending angle, and varying erosion rates (precipitation) along the orogen are considered to determine the primary control(s) on the geometry and evolution of curved orogens.

Our models successfully replicate the first-order surface kinematics of the Bolivian Andes as measured by GPS and paleomagnetic studies. Preliminary results show that variations in the precipitation affect the topographic expression such that higher erosion rates lead to decrease in the width of the orogen. However, the subsurface structure of the orogen is largely unaffected by variations in precipitation, and is instead controlled by the strength of the detachment zone: A weaker basal detachment allows deformation to propagate towards the foreland and produces a wider retroarc thrust belt, whereas a strong basal detachment concentrates deformation in a single zone of thrusting.

References:
[1] McQuarrie N. Bulletin of the Geological Society of America, 114(8), 950-963, 2002.
[2] Barnes J. B., et al. Geology, 40, 1135-1138, 2012.
[3] Whipple K. X., Gasparini N. M. Lithosphere, 6(4), 251-268, 2014.
[4] Braun J., et al. Physics of the Earth and Planetary Interiors, 171(14), 76-91, 2008.
[5] Braun J., Willett S. D. Geomorphology, 180-181, 170-179, 2013.
[6] Dewey J. F., Lamb S. H. Tectonophysics, 205, 79-95, 1992.

Emplacement mechanisms of block-and-matrix serpentinite in the California Coast Ranges from 35 to 39° N: Largely cold intrusions facilitated by weak rheology governed by dissolution and growth processes under hydrothermal conditions

C. Kellner[1] & S. Kirby[1]
[1]*U.S. Geological Survey, Menlo Park, CA, USA, skirby@usgs.gov*

We review the large geological literature on serpentinite emplacement mechanisms based on field relations described in dozens of articles on specific serpentinite localities in California. Many of these papers focused on the numerous mercury mines that were associated with serpentinite bodies and their partial ametasomatism to silica-carbonate rocks and mercury metallization by carbonated hydrothermal alteration. USGS geologists and others had access to extensive underground mercury mine workings and this access afforded these authors three-dimensional information on the geometries and contact relations of fresh serpentinites with host rocks (e.g., Taff, 1935; Ross, 1935; 1940a & b; Bailey, 1942, 1946, 1951; Bailey and Everhart, 1948, 1964; Bailey and Myers, 1942; Bailey, Irwin, Porter and Jones, 1964; Wells, 1951; Coleman, 1957; Page, B.M., 1966; Page, B.J., 1967; Page, De Vito, and Coleman, 1999; Coleman and Keith 1971; Coleman and Keith 1971; Page, B.M., 1966; Page, B.J., 1967; Murata, et. al., 1979; Page, De Vito, and Coleman, 1999). These cited authors unequivocal view was that members of this class of serpentinite bodies were emplaced as serpentinites by “cold-intrusion” as sills, dikes, plugs, and along faults (aka serpentinite protrusions or serpentinite piercement structures. Their criteria for cold intrusion emplacement interpretations as sills, dikes, and plugs: (1) Sheared along all contacts, often heavily weathered and eroded. Contacts locally metasomatized to silica carbonate rock by carbonated water. (2) Sills show branching or pinch-and-swell structure. (3) Dikes often parallel to and coincident with active faults. (4) Many of the larger bodies are rootless, resembling salt domes that pinch off from their diapiric sources. (5) Lack evidence of high-temperature contact metamorphism. Other geologists with field experience outside California have shared this view (e.g., B.N. Benson, 1918, 1924; F. J. Turner, 1948; F.J.Turner & J. Verhoogen, 1951; J. P. Lockwood, 1972). Many of these classic papers have evidently have largely been forgotten. A recent paper posits a large mantle source of water from the former forearc during the Mesozoic and Paleogene subduction era and after the transition to transpressive continental-transform kinematics of the San Andreas Fault System (Kirby, Wang, and Brocher, Earth Planets and Space 2014; Kirby, 2015 AGU Abstract). This model gives insights into both the source of these serpentinite bodies and their rheological mobilization by a water flux released from the former forearc mantle through the crust. A companion presentation (Kirby et al., 2017) shows extensive field and thin-section mircrostructural evidence for dissolution and growth as the mechanisms governing the rheology of these rocks. Other weak lithologies that share intrusion contact relations with their host rocks are some magamas, salt diapirs, and fluid charged muds.

Microstructures and crystallographic preferred orientations from the exhumation of the high-pressure Adula Nappe (Switzerland)

R. Keppler[1], M. Stipp[2] & N. Froitzheim[1]
[1]Steinmann Institute, Poppelsdorfer Schloss, 53115 Bonn (rkep@uni-bonn.de)
[2]Geomar Helmholtz Zentrum für Ozeanforschung, Wischhofstr. 1-3, 24148 Kiel

The Adula Nappe represents a basement nappe in the eastern Central Alps. It was originally part of the distal European continental margin and entered a south-dipping subduction zone, where it experienced high- to ultrahigh pressure peak conditions at about 38 Ma. Afterwards the unit underwent several deformation phases. The Zapport phase started right after peak conditions and accomplished the largest part of the exhumational deformation associated with a pressure drop of 13–9 kbars in the Northern Adula Nappe and 20–10 kbars in the central part. Despite extensive research during the last decades, the internal deformation of the Adula Nappe during exhumation is not completely understood. Especially the large pressure-temperature gradient from 12–17 kbar/500–600 C° in the north to 30 kbar/800–850 C° in the south is a topic of debate. This phenomenon either originates from internal, heterogeneous deformation of the Adula Nappe during its exhumation, or it was caused by tectonic overpressure, which would indicate that the Adula Nappe was not as deeply subducted as previously assumed.

In this study, we sampled quartzites, micaschists, para- and orthogneisses in a close-meshed net throughout the entire Adula Nappe. Only samples showing Zapport deformation without any significant younger overprint were collected. Crystallographic preferred orientations (CPOs) of all mineral phases in the samples were measured with time-of-flight neutron diffraction at the SKAT diffractometer at JINR, Dubna, Russia. With this method, it is possible to investigate the CPO of all phases in polymineralic samples, despite overlapping Bragg reflections in the spectra.

Quartz CPOs show a great variability. Most of the c-axis patterns yield an asymmetry charateristic of a top-to-the-north sense of shear, although there are a few top-to-the-south samples. Most c-axes patterns exhibit peripheral maxima at an angle to the foliation normal pointing to dominant basal <a> slip, especially in the northern Adula Nappe. The samples from the central Adula nappe show also maxima between Z and Y of the c-axis pole figure indicative of rhomb-, π- and prism <a> slip. These maxima are usually combined with asymmetric crossed or single girdles of quartz c-axes. A few samples yield small circle distributions suggesting a flattening component. Maxima range from 1.3 to 9 multiples of random distribution (m.r.d.) independently of rock type, CPO pattern or location. For comparison, mica exhibits a pronounced alignment of its basal plane within the foliation and high m.r.d. in all samples, even in the ones with very weak quartz CPO. In some of the orthogneiss samples even plagioclase shows a weak CPO with an alignment of its (010) plane within the foliation. From the variability of the quartz c-axis patterns, which appear to be independent from lithology, we can infer dominant top-to-the-north directed shear at the exhumational front of the northern Adula Nappe during Zapport deformation. This corresponds to previous field and microstructural investigations. The patterns of the central Adula Nappe are more complex with a multiple slip system activity and indicate plane as well as flattening strain. Further sampling and CPO as well as microstructural analysis will provide a more comprehensive view on the Zapport deformation phase and the exhumation of the Adula Nappe.

Dispersion axes of deformed quartz grains - mapping, interpretation and applications

R. Kilian[1]
[1]*Geological Institute, Basel University, Switzerland (ruediger.kilian@unibas.ch)*

The kinematics of flow of a polycrystalline aggregate deforming by dislocation creep can be interpreted from dislocation induced microstructural and textural features such as the misorientation characteristics of subgrain boundaries (e.g. Bestmann & Prior, 2003) or bulk textures (Michels et al., 2015). Less commonly, the continuous orientation change (lattice bending) within deformed grains is analysed in a quantitative way. In both cases, it is assumed that intragranular deformation is related to the global kinematics of flow of the rock.

While it is fairly easy to measure today, the interpretation of subgrain boundaries in terms of deformation history comes with several difficulties. For example, at low-grade conditions, subgrain boundaries are not readily developed and not every low angle boundary might represent a subgrain boundary. Or, the extent of subgrain development may depend on the orientation of the grain within a given kinematic reference frame; some orientations seem to be more prone to subgrain boundary formation while differently oriented grains can be highly stretched and record a continuous lattice bending. To allow a kinematic interpretation, it is usually assumed that low angle angle boundaries are tilt boundaries, which are formed during dynamic recovery by the strain producing dislocation type. Hence, interpretations purely based on the character of low angle boundaries might be biased and depend on a set of vaguely tested assumptions.

In this contribution, intragranular orientation changes are analysed based on their dispersion axes which are derived from orientation fibres of individual grains or subvolumes within grains. In addition to the directions of dispersion axes, a measure for the extend of lattice bending is derived and it is possible to identify and discriminate dispersions originating from multiple rotation axes.

Results from quartzites, deformed experimentally in progressive general and pure shear are compared to natural quartz mylonites. The distribution of dispersion axes can be related to the global kinematics of flow and a mapping of dispersion axes shows a spatial correlation of mean axis directions with high strain zones in experimentally deformed samples. Using this approach the analysis can be made independent of low angle boundaries and very high resolution EBSD data is not necessary as long as grains are sufficiently resolved. There are strong indications that the results are also robust in rocks where dislocation glide is dominant and subgrains boundaries are rare.

The contribution of EBSD maps from experimental samples by Andrew Cross, David Prior, Michael Stipp, Jan Tullis and Renée Heilbronner is gratefully acknowledged.

References:
Bestmann, M., Prior, D.J., 2003, Intragranular dynamic recrystallization in naturally deformed calcite marble: Diffusion accommodated grain boundary sliding as a result of subgrain rotation recrystallization: JSG, v. 25, doi:10.1016/S0191-8141 (03)00006-3.
Michels, Z., Kruckenberg, S., Davis, J., Tikoff, B., 2015, Determining vorticity axes from grain-scale dispersion of crystallographic orientations, Geology,doi:10.1130/G36868.1.

Microstructures of natural ice from Northern Victoria Land, Antarctica

D. Kim[1], D. Prior[2], Y. Han[1], C. Qi[3], L. Craw[1], C-K. Lee[1], K. Lilly[2], J.I. Lee[1] & S.D. Hur[1]
[1]Korea Polar Research Institute (KOPRI), Incheon, Korea (dkim@kopri.re.kr)
[2]University of Otago, Dunedin, New Zealand
[3]University of Pennsylvania, Philadelphia, United States

As polycrystalline ice 1h deforms plastically, it develops an anisotropic, sometimes inhomogeneous by impurity, microstructure, with a strong crystallographic preferred orientation (CPO). As the kinematics and conditions (temperature, stress and strain) of deformation vary, deformed ice exhibits different microstructures. These deformation-induced microstructures of natural ice provide records of the deformation histories and constraints on the future flow rate of natural ice bodies. In order to investigate the formation of microstructures of ice during deformation, we analysed natural ice samples from Styx, Nansen and Larsen Glaciers, Northern Victoria Land, Antarctica using electron backscatter diffraction (EBSD) technique. The CPOs of ice samples from Styx Glacier (a snow accumulation site) are characterized by single maxima of c-axes with random to girdled distributions of (11-20) and (10-10). The fabric strength progressively increases with increasing depth. The results show the successful formation of ice fabric by the accumulation of ice (pure shear), indicating that Styx Glacier successively preserve the evidences of paleoclimate. In Nansen Glacier (a blue-ice region), c-axes of ice samples are characterized by double cluster, which can be formed by simple shear. Ices from Larsen Glacier (a blue-ice region) display a strong vertical girdle of c-axes with horizontal concentrations of (11-20) and (10-10). This pattern suggests the ice experienced tensile deformation normal to the direction of the c-axes girdle. Based on those results, we discuss diverse CPOs of ice formed by different kinematics in nature.

Orogenic block-and-matrix serpentinites in the Franciscan mélange of California: petrographic and field evidence of multi-stage serpentinization and dissolution-and-growth rheology during cold intrusion through the crust from the Coast-Range mantle

S. Kirby[1], M. Uno[2], M. Lewis[1,3] & C. Kellner[1]
[1]*U.S. Geological Survey, Menlo Park, CA 94025, USA; skirby@usgs.gov*
[2]*Department of Environmental Sciences, Tohoku University, Sendai, Japan*
[3]*Division of Geological & Planetary Sciences, California Institute of Technology, USA*

Part of the California Coast Ranges is comprised of the Franciscan mélange, an assemblage of marine sedimentary, igneous, and metamorphic rocks juxtaposed tectonically during the terrane accretion and post-subduction San Andreas Fault System tectonics. Among those rocks are ultramafics largely composed of serpentinites bodies that represent altered peridotites as well as tectonic blocks of Franciscan igneous and sedimentary rocks. We have sampled and investigated the field relations of 21 of these serpentinite bodies in the San Francisco Bay Area [Uno and Kirby, 2017; Lewis and Kirby, 2015 AGU Abstract; Kellner and Kirby, 2016 AGU Abstract] and reviewed the extensive literature on emplacement mechanisms for an additional four bodies in the Coast Ranges from 35 to 39° N. ALL of these bodies are considered by the authors of these papers as having been *cold-intruded* (T < 500°C) into the host Franciscan Mélange under hydrothermal conditions [*E.g.,* Ross, 1935; Ross, 1940a & b, Bailey, 1942, 1946, 1948, 1951; Bailey and Myers, 1942; Bailey, 1964; Bailey and Myers, 1942; Bailey, Irwin, and Jones, 1964; Wells, 1951; Coleman, 1957; Page, 1967; *Page et al.* 1999). These rocks were emplaced as serpentinities and caused little or no contact metamorphism of their host rocks. Many of these serpentinite bodies host blocks of blueschist and/or eclogite. Their ascent from depth is part of the process of bringing their host serpentinites from the forearc mantle.

Petrographic examination of polished thin sections cut from more than 200 of our serpentinite blocks show the following features: A) Multiple stages of serpentinization ranging from (i) antigorite/lizardite/brucite/magnetite in partially serpentinized peridotite block cores (ii) to rims of lizardite plus magnetite (iii) to sheared lizardite skins; B) Abundant evidence of hydrothermal fluids forming multiple vein systems as well as the (i) -> (ii) serpentinization reaction; C) Lizardite skins that show evidence of dissolution and growth processes during ascent of these rocks from their presumed mantle origin. These skins show evidence of shear deformation parallel to the skin and are near universal for blocks ranging in diameter from about 7 meters down to ~10 cm. Smaller blocks (*phacoids*) tend to be lens-shaped, also have sheared skins, and display a rough foliation surrounding the large blocks. Based on these observations, the main deformation process that has occurred is dissolution and growth localized at or near block surfaces and somewhat resembles grain-boundary sliding in fine-grained materials at higher temperatures where diffusive mass transport largely controls the rheology rather than crystal plasticity within blocks. Also individual blocks where skins have been scraped away sometimes show “corrugated” features beneath the sheared lizardite skins, indicating that serpentinite rim material that has been removed by dissolution. Rim structures are also truncated by such dissolution. We illustrate the macro- and microstructures of these samples and suggest future laboratory investigations to better understand this process. We also discuss possible sources of hydrothermal fluids and the ultramafic peridotite protoliths of these serpentinites.

Structural Disorder of Graphite and Implications for Graphite Thermometry

M. Kirilova[1], V. Toy[1], J. Rooney[2], K. Gordon[2], C. Giorgetti[3] & C. Collettini[3]
[1]*Department of Geology, University of Otago, PO Box 56, Dunedin 9054, New Zealand*
[2]*Department of Chemistry, University of Otago, PO Box 56, Dunedin 9054, New Zealand*
[3]*Dipartimento di Scienze della Terra, Università degli Studi La Sapienza, Rome, Italy*

Graphitization, or the transformation of organic matter into crystalline graphite, is induced by compositional and structural changes during diagenesis and metamorphism. The irreversible nature of this process has allowed the degree of graphite crystallinity to be calibrated as an indicator of the peak temperatures reached during progressive metamorphism. However, discrepancies between temperatures indicated by the graphite crystallinity vs. other thermometers have been documented in numerous fault zones, such as the Alpine Fault rocks, New Zealand (Kirilova et al, in review) and the Hidaka metamorphic belt, Japan (Nakamura et al., 2015). We hypothesise this is because the calibrated graphite thermometers disregard the effects of mechanical modifications of the graphite structure. To examine this possibility, we have carried out laboratory deformation experiments, combined with Raman microspectroscopy to investigate the impacts of structural disordering of graphite on the graphite 'thermometry'.

Our experiments were performed in the Brittle Rock Deformation Versatile Apparatus (BRAVA) at INGV, Rome. We systematically sheared highly crystalline graphite powder at room temperature, normal stresses of 5 MPa and 25 MP and sliding velocities of 1 µm/s, 10 µm/s and 100 µm/s to total displacements of 20 mm, 10 mm and 5 mm. We then analysed the degree of graphite crystallinity in the resulting material by Raman microspectroscopy. Our results show consistent decrease of graphite crystallinity with increasing shear strain; spectra area ratios (R2) drop from ~0.1 in the initial material to ~0.5 in the deformed powder. We infer this is due to mechanical modification and thus conclude that graphite thermometers are unreliable in brittely deformed rocks. Temperatures derived from the thermometer in deformed rocks should be treated as minimum estimates of temperatures experienced by them.

References:
Kirilova, M., Toy, V., Timms, N., Little, T.,Halfpenny, A., Menzies. C., Craw, D., DFDP-1 Science Team, DFDP-2 Science Team (in review.). Transformation of graphite by tectonic and hydrothermal processes in an active plate boundary fault zone,Alpine Fault, New Zealand
Nakamura, Y., Oohashi, K., Toyoshima, T., Satish-Kumar, M. & Akai, J. 2015. Strain-induced amorphization of graphite in fault zones of the Hidaka metamorphic belt, Hokkaido, Japan. Journal of Structural Geology 72: 142 – 161.

Stress and veins at stylolite tips, the anti-crack problem

D. Koehn[1], N. Beaudoin[1] & Z. Robinson[1]
[1]*School of Geographical and Earth Sciences, University of Glasgow, Glasgow, UK (Daniel.koehn@glasgow.ac.uk)*

In this contribution we discuss how stylolites behave when their tips are offset and interact with each other to form overlap zones or local veins between the tips. Stylolites develop during pressure solution as a function of localized dissolution that is driven by stress or chemical gradients. There has been a debate in the literature as to why and how these surfaces develop and propagate. The two end-member cases are stress driven propagation in a similar way to cracks but with the opposite stresses (compaction versus extension) or chemical driven localization due to the collection of material that enhances dissolution and thus propagation. The study of stylolite tips that overlap in a very similar fashion to overlapping extensional cracks may shed light on this problem. We studied natural examples from stylolite and vein bearing rocks form Italy in detail with a special emphasis on stylolite tip propagation using microscopy, EBSD analysis and X-ray tomography. In addition we performed static and dynamic numerical simulations of two overlapping compacting layers to understand stress fields and developing fractures between the tips. Our results show that stress at stylolite tips interact in orientation and magnitude, predicting a stress pattern consistent with observed cracks between the tips and stylolite rotation in the transition zone

Stylolite classification to estimate compaction and permeability variations

D. Koehn[1], N. Beaudoin[1], M.P. Rood[2], P.D. Bons[3] & E. Gomez-Rivas[4]
[1]*School of Geographical and Earth Sciences, University of Glasgow, Glasgow, UK (Daniel.koehn@glasgow.ac.uk)*
[2]*Department of Earth Science and Engineering, Imperial College London, UK*
[3]*Department of Geosciences, Eberhard Karls University Tübingen*
[4] *School of Geosciences, University of Aberdeen, UK*

Stylolites are rough dissolution seams that develop in sedimentary basins during chemical compaction. They can develop very variable shapes forming waves, spikes or distinct rectangular teeth, and these characteristics may change along a single stylolite. In order to estimate chemical compaction at stylolites classifications have been put forward that can be used when analyzing drill-core or outcrop data. However, these classifications are not necessarily consistent nor are they build on a real growth theory of the roughness. Stylolites typically have three different end-members of noise: background noise on the small-scale (small grains or secondary phases), noise on the larger-scale (large grains or fossils) and noise in the form of sedimentary layers. How these different noises interact and which noise is dominant determines which class of stylolites form. Based on numerical modeling of roughness development and analysis of a range of natural stylolites we present an advanced classification and separate stylolites into four classes: (1) rectangular layer type, (2) seismogram pinning type, (3) suture/sharp peak type and (4) simple wave-like type. Rectangular layer type stylolites are the most appropriate for chemical compaction estimates because they grow linearly and record most of the actual compaction. Seismogram pinning type stylolites also provide good tracking capabilities, with the largest teeth tracking most of the compaction. Suture/sharp peak type stylolites grow in a non-linear fashion and thus do not record most of the actual compaction. However, when a non-linear growth law is used, the compaction estimates are similar to those making use of the rectangular layer type stylolites. Simple wave-like stylolites are not useful for compaction estimates, since their growth is highly non-linear with a very low growth exponent. We present examples of how stylolites should be used to estimate compaction and show that data from drill-cores from the Zechstein in northern Germany indicates that conventional compaction estimates at stylolites underestimate the compaction by an order of magnitude. We also discuss how different stylolites influence the local permeability.

Shear zone in calcite: AMS and microstructure

V. Kusbach[1], Z. Roxerová[1], M. Machek[1], M. Racek[2] & P. F. Silva[3]
[1]*Institute of Geophysics AS CR, v. v. i., Prague, Czech Republic (kusbach@ig.cas.cz)*
[2]*UPSG PrF UK, Prague, Czech Republic*
[3]*IDL, Lisbon, Portugal*

The measurement of anisotropy of magnetic susceptibility (AMS) becomes one of the most popular structural techniques to determine anisotropic fabric in rocks with lack of macroscopically visible structures. Therefore understanding of the AMS formation and its textural response in rocks under deformation is crucial. Although despite AMS is well-established method and the strain-AMS relationship has been long time under investigation, there are still questions to solve especially in terms of microstructure-AMS relation.

Therefore we studied two structural profiles across subvertical thin shear zone in marble from quarry in Estremoz (Portugal) to clarify a relationship between AMS and strain in natural rocks. The mesoscopic fabric can be described as changing from the subhorizontal coarse-grained foliation towards the wider shear zone center with subvertical fine-grained foliation. In microstructure, the shear zone records dynamic recrystallization of calcite aggregate which resulted in development of porphyroclastic microstructure with increasing proportion of fine-grained recrystallized matrix towards the shear zone center. Two distinct crystallographic preferred orientations of calcite were recorded. One related with porphyroclasts, characterized by subvertical orientation of calcite <c> axes and another associated with recrystallized matrix showing subhorizontal calcite <c> axes orientation.

The magnetic susceptibility ranges from -8E-06 SI to 9E-06 SI, with the average -4E-06 SI. The majority of the rock mass is diamagnetic, corresponding well with the thermomagnetic curves, with local paramagnetic accumulations in form of thin bands. The AMS of the both profiles exhibits in the low strain margins subvertical magnetic foliation bearing vertical lineation. With increasing strain, the AMS starts to rotate towards the shear zone and become inclinated to ~45° associated with steep lineation as well. We interpret the AMS fabric pattern which is perpendicular to the mineral one as a type of inverse AMS fabric, due to high iron content in major part of calcite grains. The magnetic and microstructural description of the shear zone is accompanied by numerical modeling of AMS based on CPO and different proportion of porphyroclasts, matrix and mica for purposes of deciphering the influence of present microstructural features on AMS.

Quantifying variation in effective normal stress responsible for gold mineralization: comparing vein orientation data from mineralized and non-mineralized zones of Dharwar Craton (Southern India)

S. Lahiri[1], V. Rana[1] & M.A. Mamtani[1]
[1]*Department of Geology & Geophysics, Indian Institute of Technology, Kharagpur-721302, India (sivaji.lahiri@gg.iitkgp.ernet.in)*

It is well-established that the emplacement of veins and mineralization depends on the extent to which fluid pressure (P_f) fluctuation influences reactivation of pre-existing planar structural elements (fractures/foliation) in the host rock. Vein orientation data can help in evaluating relative stress/P_f, and the variation in stress state can be analyzed by plotting the 3D Mohr circle for high P_f ($>\sigma_2$) and low P_f ($<\sigma_2$) conditions (e.g., Mondal and Mamtani, 2013 and references therein). Variation in the stress state can also be quantified by scaling the 3D Mohr circle using absolute P_f value (fluid inclusion studies), and intrinsic rock mass quality data (Lahiri and Mamtani, 2016 and reference therein). This helps (a) identify the orientations of structural elements that are most susceptible to dilation/reactivation during P_f fluctuation and (b) quantify effective normal stress (= normal stress - P_f) for high P_f and low P_f conditions. Since separation of minerals (e.g., gold) from the fluid is known to take place during the sudden drop in P_f, scaling of the 3D Mohr circle can help evaluate variation in effective normal stress (σ'_n) that prevailed during mineralization. A further step in evaluating paleostress associated with mineralization would be to compare variation in σ'_n between mineralized and non-mineralized zones of a particular province. It is this aspect that the present authors have targeted in this study by analyzing quartz vein orientations from the mineralized and non-mineralized zones of Gadag region (Dharwar Craton, Southern India). The region is a known province of gold mineralization that occurs in quartz lodes having dominantly NW-SE orientation. The host rocks are metabasalts and gold mineralization is known to have occurred at ca. 2.5 Ga. In the present study, 157 veins from the mineralized zone and 162 veins from non-mineralized zone are analyzed following the above approach involving scaling of the 3D Mohr circle. 14 veins with a mean orientation of 150^o are identified to have been continuously active during high P_f and low P_f conditions. This orientation is similar to that of the gold bearing lodes in the mineralized zone and σ'_n is calculated to be -11.5 MPa for $P_f>\sigma_2$ and -1MPa for $P_f<\sigma_2$. In contrast, for the non-mineralized region, 7 veins with a mean orientation of 154^o are recognized to be continuously under dilation during the P_f fluctuation cycle, and σ'_n is calculated to be -5.4 MPa for $P_f>\sigma_2$ and -1 MPa for $P_f<\sigma_2$. Thus, it is noted that the change in σ'_n during dilation/reactivation of NE-SW structural elements in the mineralized zone was 10.5 MPa, while it was only 4.4 MPa in the area outside the mineralized part (non-mineralized zone). It is concluded that the present approach provides considerably refined data to quantify the exact variation in effective normal stress that can lead to mineralization in an area.

References:

Lahiri, S. and Mamtani, M.A. (2016). Scaling the 3-D Mohr circle and quantification of paleostress during fluid pressure fluctuation – Application to understand gold mineralization in quartz veins of Gadag (southern India). Journal of Structural Geology, 88, 63-72.

Mondal, T.K., and Mamtani, M.A. (2013). 3-D Mohr circle construction using vein orientation data from Gadag (southern India) – implications to recognize fluid pressure fluctuation. Journal of Structural Geology, 56, 45-56.

Acknowledgments: SL thanks IIT Kharagpur for Institute Research Scholarship. VR and MAM thank MoES (India) for financial assistance (Project No. MoES/P.O(Geosci)/1/2013).

Chemical-mechanical feedback and fracture size and spacing patterns

S.E. Laubach[1], J.E. Olson[2], R.H. Lander[3] & J.N. Hooker[4]
[1]Jackson School of Geosciences, The University of Texas at Austin, Austin TX, USA (steve.laubach@beg.utexas.edu)
[2]Petroleum & Geosystems Engineering, The University of Texas at Austin, Austin TX, USA
[3]Geocosm, University, Durango CO, USA
[2]Oxford University, Oxford, UK

Core and outcrops studies—including outcrop studies in NW Scotland—suggest that cement accumulation in fractures affects the size distribution, spatial arrangement, strength, porosity, and permeability of fracture arrays. The mechanism for modifying fracture size patterns may be variable resistance to fracture reopening that depends on the completeness and strength of cement bridges formed during fracture growth. Here we show how natural fracture pattern reconstructions motivate development of models that couple mechanical and diagenetic effects. Crystal growth models that predict cement accumulation patterns and volumes in fractures incorporated into geomechanical models of fracture pattern evolution show how evolving rock mechanical properties and the mechanical interaction of cement accumulation and fracture growth can influence pattern geometry and fluid flow attributes. But for fully testing predictions of fracture size and spatial arrangements, models require validation in special outcrops, where fractures have diagnostic features that show they are like those in the deep subsurface. Localized quartz deposits in otherwise open fractures contain crack-seal textures and fluid inclusion assemblages, allowing fracture temperature histories to be reconstructed and compared with burial histories. Using thermal history as a proxy for time allows inference of duration and rates at which fractures open, and thus comparison of fracture growth models with natural examples. This presentation focuses on outcrop and horizontal core data sets, highlighting examples where the interaction between cement deposition and fracture widening correlates with differences in many key fracture pattern attributes, including length, height, and aperture. Fractures impact the mechanics and fluid flow of the upper crust, and accurate knowledge of fracture attributes is an increasingly central issue in recovering water and hydrocarbon supplies and geothermal energy, in predicting flow of pollutants underground, in predicting the effectiveness of subsurface engineered structures such as hydraulic fractures, and in understanding large-scale crustal behavior. Yet inherent sampling and imaging limitations mean we typically cannot measure subsurface fracture attributes, and our research shows that many outcrop fractures are misleading guides to the subsurface. Fracture mechanics has been central to interpreting opening-mode fractures in rock, but our results show that mechanics must be coupled with geochemical principles to understand how fracture porosity, spacing, size and connectivity evolve.

Shear senses and deformation temperatures indicated by quartz c-axis fabrics and microstructures in a NW-SE transect across the Moine and Sgurr Beag thrust sheets of northern Scotland

R. Law[1], S. Mazza[1], R. Thigpen[2], C. Mako[1], K. Ashley[3] & M. Krabbendam[4]
[1]*Geosciences, Virginia Tech, Blacksburg, USA (rdlaw@vt.edu)*
[2]*Earth & Environmental Sciences, University of Kentucky, Lexington, USA*
[3]*Jackson School of Geosciences, University of Texas, Austin, USA*
[4]*British Geological Survey, Edinburgh, Scotland*

Quartz c-axis fabrics and deformation microstructures are reported from dynamically recrystallized psammites exposed on a 45 km long NW to SE transect (Loch Broom to Garve/Rogie Falls) across the Moine and Sgurr Beag thrust sheets. At the NW end, the psammites are cut by a platy mylonitic foliation that dips gently to the ESE parallel to the underlying Moine thrust. The mylonites define a ~ 4 km thick planar zone of intense shearing, in which gently plunging mineral stretching lineations change in trend from E to SSE traced structurally upwards and to the SE. At the base of this zone quartz is recrystallized by subgrain rotation and minor grain boundary bulging, while feldspar grains are fractured. Traced upwards through the zone, recrystallized quartz grain size increases, feldspars are deformed plastically, grain boundary migration recrystallization microstructures develop in both quartz and feldspar, and shape fabrics become less platy and more granular. Above this zone of platy mylonites, the metasedimentary rocks of the Moine and overlying Sgurr Beag thrust sheets are buckled in to a series of km-scale W-vergent folds defined by stratigraphic units, with N-S trending, gently plunging hinges and hinge planes that progressively become more steeply dipping traced eastwards along the transect (Krabbendam et al., 2011). These folds are thought to detach on the underlying Moine thrust. Mineral stretching lineations in this fold zone are sub-parallel to the N-S gently plunging fold hinges and in fold hinge zones it can be demonstrated that the associated tectonic foliation is deformed around these km-scale folds. Both quartz and feldspar from the Moine and Sgurr Beag thrust sheets in this zone are characterized grain boundary migration recrystallization.

In the planar mylonite zone above the Moine thrust microstructures and quartz c-axis fabrics indicate a top to the WNW to NW shear sense, with deformation temperatures indicated by fabric opening angles increasing from ~ 460 °C at the base to ~ 550 °C at the top. In the overlying fold zone to the east, microstructures and quartz c-axis fabrics indicate a remarkably consistent pattern of top to the N shearing after unfolding the km-scale right way-up and inverted fold limbs back to the horizontal. In both domains c-axis fabrics clearly demonstrate that the mineral lineations are parallel to the maximum principal stretching direction. Deformation temperatures indicated by fabric opening angles from the Moine and Sgurr Beag thrust sheets within this fold zone range from ~550 °C (Moine thrust sheet at Braemore Junction) in the west to ~ 630 °C in the east (Sgurr Beag thrust sheet at Rogie Falls). Top to the WNW shearing in the mylonites in the immediate hanging wall to the Moine thrust at the NW end of the transect is clearly of Scandian (mid-Silurian age). However, the higher temperature top to the N shearing, preserved in the overlying fold zone to the east, could be of older Grampian (Ordovician) or Knoydartian (Precambrian) age.

Krabbendam, M., Strachan, R.A., Leslie, A.G., Goodenough, K.M. and Bonsor, H.C. 2011. The internal structure of the Moine nappe complex and the stratigraphy of the Morar Group in the Fannichs-Beinn Dearg area. NW Highlands. Scottish Journal of Geology, 47, 1-20.

An association between subgrain boundaries, Dauphiné twinning, and partial melting in migmatites

J.S.F. Levine[1] & J.M. Rahl[2]
[1]*Appalachian State University, Boone, NC, USA (levinejs@appstate.edu)*
[2]*Washington and Lee University, Lexington, VA, USA*

Migmatitic samples from both the Wet Mountains of central Colorado and the Llano Uplift of central Texas provide microstructural evidence for partial melting along grain boundaries as well as subgrain boundaries within quartz and plagioclase. Partially melted grain and subgrain boundaries have cuspate edges surrounded by melt pseudomorphs with a different composition than the surrounding material. Subgrain boundaries associated with former melt in quartz can be identified both optically and through electron backscatter diffraction (EBSD) analysis. Within samples from both locations, optically identified subgrain boundaries are characterized by a slight but noticeable change in extinction. Subgrain boundaries characterized via EBSD have misorientations ranging from ~1-5° but usually between 1-2°.
Many optically-identified subgrain boundaries are also associated with a 60° misorientation around the c-axis, diagnostic of Dauphiné twinning. In some locations, these Dauphiné twins were found associated with melt pseudomorphs along optically identified subgrain boundaries. However, twins were also found along optically-identified subgrain boundaries within the interior of grains free of former melt, indicating that the association between subgrain boundaries and Dauphiné twins does not require the presence of partially molten material.
Previous work suggests Dauphiné twins may form through three primary mechanisms, during cooling as a result of the beta-alpha transition in quartz, mechanically due to an applied compressive stress, and as a result of static grain growth. Although these migmatitic rocks did reach temperatures in the beta-quartz stability field, it seems unlikely that this was the main cause of Dauphiné twinning because the twins are not uniformly developed. Instead, due to heterogeneous twin development, we hypothesize that Dauphiné twins developed in appropriately oriented quartz grains as a response to stress and may have been further augmented by static grain growth. The association of Dauphiné twins along subgrain boundaries may further support the idea of twin development due to static grain growth because the twins commonly nucleate on dislocations or impurities, both of which are components of subgrain boundaries. Additionally, it has been shown that whichever Dauphiné twin is more stable is the one that has the higher strain energy, and thus it would also be favorable for twins to nucleate onto a location of higher strain energy. Ongoing work seeks to systematically document the potentially complex relationships between partial melting, subgrain boundaries, and Dauphiné twins throughout migmatitic samples.

The effect of gradient in crustal thickness in relief development in the Cantabrian Mountains (N Iberia)

S. Llana-Fúnez[1], L. Rodríguez-Rodríguez[1], D. Ballesteros[1], P. Valenzuela[1], L.M. Díaz[1], P. Cadenas[1], G. Fernández-Viejo[1], M.J. Domínguez-Cuesta[1], M. Jiménez-Sánchez[1], M. Meléndez-Asensio[2] & C. López-Fernández[1]

[1]Geocantabrica Research Group, Department of Geology, University of Oviedo, Oviedo, Spain (llanasergio@uniovi.es)

[2]Instituto Geológico y Minero de España (IGME), Oviedo, Spain

The active boundary between Europe and Africa during the Eocene and Oligocene convergence was located at the northern edge of Iberia and led to the formation of the Pyrenees and, to the west, the Cantabrian Mountains. Since the Neogene, when the active boundary migrated to southern Iberia, the Cantabrian Mountains entered into an erosive phase. The westerly bulk trend of this orogen in the study section was controlled by the W-E orientation of Alpine thrusts and other structures that accommodated the N-S shortening in relation to Eocene-Oligocene plate convergence. As a consequence of Alpine orogenesis in the Cantabrian Mountains, the thickness of the crust increased along the orogenic belt from an average 30 km in Galicia and western half of Asturias to 45-50 km in the Asturias-Cantabria segment, to the east. The aim of this contribution is to study the relief along this linear segment of the orogen, approximately 230 km long, with a gradient in crustal thickness.

Based on a GIS-analysis using 5 and 25 m-resolution DEM by the Spanish National Geographical Institute, we identify several elements in the Cantabrian Mountains landscape informative about relief evolution and its relation to Alpine tectonics. As expected, major Alpine tectonic structures control the location and orientation of the main water divide of the mountain range, but also the orientation of some local water divides, e.g. associated to the Llanera (thrust) fault or the Ventaniella (strike-slip) fault. There is also an expected strong lithological control in the development of local relief, particularly in specific areas dominated either by limestone massifs or by Variscan syn-orogenic detritic rock sequences. A DEM swath profile along the main watershed shows for 100 km a progressive increase in mean altitude from the west to a steady mean altitude of 1,500 m, slightly offset with known crustal difference in thickness along the profile. Another feature in the landscape that reflects some lateral difference along the length of the orogen is the presence near the coast of an elevated wave-cut platform slightly dipping west. Regarding the fluvial network, most longitudinal river profiles running from the main watershed to the sea lack knick points, indicating that the current drainage in most parts postdates tectonic activity. A preliminary analysis of river incision through traverse and longitudinal DEM swath profiles shows river incision increasing towards the east. Both the increase of mean altitudes and river incision to the east are consistent with an expected increase in uplift and erosion associated to the thickening of the crust in the same direction. One of the ultimate aims of the work is to quantify cumulative erosion along the Cantabrian Mountains to provide a first order approximation to long-term erosion rates in different rocks during the erosive phase in response to its location within the mountain belt.

Fault rocks at the base of the Somiedo Nappe (Variscan Orogen, NW Spain)

S. Llana-Fúnez[1], J.L. Alonso[1], N. Caldera[1] & M.A. Lopez-Sanchez[1]
[1]*Department of Geology, University of Oviedo, Oviedo, Spain (llanasergio@uniovi.es)*

The Somiedo Nappe is one of the major tectonic units within the Cantabrian Zone (NW Iberia). This zone represents the foreland-fold-and-thrust belt of the Variscan Orogen in Iberia. The late stage of the Variscan orogeny originated the Ibero-Armorican Arc, with the Cantabrian Zone at its core. The development of this arcuate megastructure not only produced large rigid body rotations but the overprinting of some of previous Variscan structures. During the Eocene-Oligocene, the convergence between Europe and Africa localised in the north of the Iberian Peninsula to form the Pyrenees and the Cantabrian Mountains, both oriented east-west. The Alpine shortening was directed north-south and produced the reworking of some of earlier Variscan thrusts. Current topography in the Cantabrian Mountains, where the study area is located, relates to Alpine tectonics, which also exhumed deep parts of the Variscan foreland-fold-and-thrust belt.

The base of the Somiedo Nappe contains micritic Cambrian dolomites (Lancara Fm), which overlie Carboniferous shales and limestones (San Emiliano Fm). The cumulative displacement during its emplacement and partial reactivation during out of sequence Variscan thrusting is estimated to be up to 30 km according to balanced cross sections. The current studied locations lie in an open valley with a westerly trend very likely associated to the Alpine thrusting. The fault zone at the base of the nappe contains fault rocks in two distinctive structural levels. In a lower level, cataclasites are cohesive and fine grained. We found a discrete band 10-20 mm in thickness made of very fine grained cataclastic rocks at the base of the Lancara Fm. This band presents a planar basal contact and an irregular top with frequent injection structures. The upper level has metric bands of cataclastic rocks, less cohesive, and developed also on carbonate rocks. Within the cataclasites, particle size distribution for a size range between 30 and 250 μm follows an exponential law in frequency-size log-log scale with an exponent of about 2.25, approaching the exponent expected for a particle distribution formed by fracturing.

The lower level does not present evidences of reworking, contrary to what it is observed in the upper level, where thin flat slip surfaces are relatively frequent. In general, minor structures in the fault zone at the base of the nappe, or in immediately above it, such as minor folds and secondary striated faults, indicate two distinct directions for tectonic transport once late Variscan folding is restored: a dominant top to the northeast, and a secondary indicating north-south shortening.

There are two main findings to be highlighted from this work. First, is that our observations support the preservation of kinematic criteria associated to the original emplacement of Variscan thrusts, and separately to the late overprint with northerly kinematics associated to a less intense Alpine fracturing. Second, grain comminution in cataclasites reduces grain size locally to sizes below 1 μm. SEM observations in a fault mirror within the less cohesive cataclasites show a polygonal microstructure indicative of some recrystallization during slip.

Effect of vorticity on polycrystalline ice deformation

M-G. Llorens[1,2], A. Griera[3], F. Steinbach[1,2], P.D. Bons[1], E. Gomez-Rivas[4], D. Jansen[2], J. Roessiger[1], R.A. Lebensohn[5] & I. Weikusat[1,2]

[1]*Department of Geosciences, Eberhard Karls University Tübingen, Germany. (maria-gema.llorens-verde@uni-tuebingen.de)*

[2]*Alfred Wegener Institute for Polar and Marine Research, Bremerhaven, Germany*

[3]*Departament de Geologia, Universitat Autònoma de Barcelona, Spain*

[4]*School of Geosciences, University of Aberdeen, UK*

[5]*Material Science and Technology Division. Los Alamos National Laboratory, USA*

Understanding ice sheet dynamics requires a good knowledge of how dynamic recrystallisation controls ice microstructures and rheology at different boundary conditions. In polar ice sheets, pure shear flattening typically occurs at the top of the sheets, while simple shearing dominates near their base. We present a series of two-dimensional microdynamic numerical simulations that couple ice deformation with dynamic recrystallisation of various intensities, paying special attention to the effect of boundary conditions. The viscoplastic full-field numerical modelling approach (VPFFT) (Lebensohn, 2001) is used to calculate the response of a polycrystalline aggregate that deforms purely by dislocation glide. This code is coupled with the ELLE microstructural modelling platform that includes recrystallisation in the aggregate by intracrystalline recovery, nucleation by polygonisation, as well as grain boundary migration driven by the reduction of surface and strain energies (Llorens et al., 2016a, 2016b, 2016c). The results reveal that regardless the amount of DRX and ice flow a single c-axes maximum develops all simulations. This maximum is oriented approximately perpendicular to the maximum finite shortening direction and rotates in simple shear towards the normal to the shear plane. This leads to a distinctly different behaviour in pure and simple shear. In pure shear, the lattice preferred orientation (LPO) and shape-preferred orientation (SPO) are increasingly unfavourable for deformation, leading to hardening and an increased activity of non-basal slip. The opposite happens in simple shear, where the imposed vorticity causes rotation of the LPO and SPO to a favourable orientation, leading to strain softening. An increase of recrystallisation enhances the activity of the non-basal slip, due to the reduction of deformation localisation. In pure shear conditions, the pyramidal slip activity is thus even more enhanced and can become higher than the basal-slip activity. Our results further show that subgrain boundaries can be developed by the activity of the non-basal slip systems. The implementation of the polygonisation routine reduces grain size and SPO, but does not significantly change the final LPO, because newly nucleated grains approximately keep the c-axis orientations of their parental grains. However, it enables the establishment of an equilibrium grain size, and therefore the differential stress reaches a steady-state.

References:

Lebensohn. 2001 N-site modelling of a 3D viscoplastic polycrystal using fast Fourier transform. Acta Materialia, 49(14), 2723–2737.

Llorens, et al., 2016a. Dynamic recrystallisation of ice aggregates during co-axial viscoplastic deformation: a numerical approach. Journal of Glaciology, 62(232), 359-377.

Llorens, et al., 2016b. Full-field predictions of ice dynamic recrystallisation under simple shear conditions, Earth and Planetary Science Letters, 450, 233-242.

Llorens, et al., 2016c. Dynamic recrystallisation during deformation of polycrystalline ice: insights from numerical simulations, Philosophical Transactions of the Royal Society A, 375 (2086), 20150346.

Mud Volcanoes eruptions in response to the August-October 2016 Central Italy seismic sequence

D. Maestrelli[1,2], M. Bonini[3], D. Delle Donne[4], L. Piccardi[3] & F. Sani[2]
[1]*Dipartimento di Scienze della Terra, Università di Pisa, Pisa, Italy (daniele.maestrelli@for.unipi.it)*
[2]*Dipartimento di Scienze della Terra, Università di Firenze, Firenze, Italy*
[3] *Consiglio Nazionale delle Ricerche, IGG, UOS Firenze, Firenze, Italy*
[4]*Dipartimento di Scienze della Terra e del Mare, Università di Palermo, Palermo, Italy*

On 24th August 2016 a M_w 6.0 earthquake stroke the central Italy, causing several casualties and the almost complete destruction of historical towns, particularly Amatrice and Accumoli (identified as the epicentral area). Only two months later, on 26th October a new destructive seismic event (M_w 5.9) hit 3 kilometres west of Visso, and on 30th October was followed by a M_w 6.5 event, with epicentral area localised 6 kilometres North of Norcia. These seismic events resulted in a widely distributed range of coseismic effects, such as ground fracturing, sediment liquefaction, landslides, and rock falls. A number of mud volcanoes located to the east, along the Apennine foothills, in the Ascoli Piceno and Fermo provinces (Marche), erupted or showed a markedly increased activity. We investigate the role of this seismic sequence in the triggering of mud volcanoes eruptions.

The mud volcanoes which experienced a strong reactivation (or even formed immediately after the seismic events) are located in the Monteleone di Fermo area, while some others, even closer to the epicentral areas apparently did not responded to the earthquakes. The interpretation of seismic sections, acquired by ENI, shows that these mud volcanoes are related to deep buried anticlines, which are expectedly trapping pressurised fluids at their core. Fieldwork, carried out before and immediately after the seismic events, allowed us to identify the fracture systems responsible for the fluid emission at surface, mainly mud and water, with rare traces of hydrocarbons. We used field data to speculate about the influence of static/dynamic stress on the reactivation of these mud volcanoes. Magnitude of the earthquakes and the epicentral distances of the eruptive events are in good agreement with previously published triggering thresholds, accounting for a major role of dynamic stresses. Nonetheless, due to the vicinity to the epicentral areas, the contribution of static stresses to the triggering cannot be excluded. We therefore performed Coulomb stress models (by means of the “Coulomb” software) to evaluate the possible role of static stresses using as input the earthquakes focal mechanisms and our fieldwork data. The results indicate that static stresses associated with these earthquakes were relatively large but not properly oriented to contribute to the triggering the mud volcanoes eruptions (i.e., the static stresses clamped the inferred feeder dikes). This finding confirms the primary role of dynamic stresses on mud volcano triggering. Furthermore, Peak Ground Velocities (PGV) show values higher than 8 cm/s, similar to the PGV associated with other responses. PGV maps show that the Monteleone di Fermo mud volcanoes are located in a favourable zone for reactivation, while other mud volcanoes, even if closer to the epicentral area, did not experience seismic triggering.

A further M_w 5.5 earthquake hit in the Aquila province on 18th January 2017, south to the former ones. At the moment this abstract is being written (23rd January 2017), more than 48,200 seismic events have been recorded since 24th August 2016. Thus, new or renewed mud volcano triggering is possible, even if not yet reported (also due to the deep snow cover).

Detecting localized shear zones versus distributed tectonic fabrics with crustal seismic anisotropy using examples from western North America and the European Alps

K.H. Mahan[1], V. Schulte-Pelkum[1], C. Condit[1], T. Leydier[2], P. Goncalves[2], A. Raju[1], S.J. Brownlee[3] & O.F. Orlandini[1]
[1]Department of Geological Sciences, University of Colorado, Boulder, USA (kevin.mahan@colorado.edu)
[2]Laboratoire Chrono-Environnement, Université de Bourgogne Franche-Comté, Besançon, France
[3]Department of Geology, Wayne State University, Detroit, USA

A range of promising tools are available for using seismic anisotropy to image deep crustal deformation but they also present challenges, especially with respect to potential biases in both the detection methods themselves as well as in competing processes for localized versus distributed deformation. We address some of these issues from the geophysical perspective by employing azimuthally dependent amplitude and polarity variations in teleseismic receiver functions combined with a compilation of published rock elasticity tensors from middle and deep crustal rocks, and from the geological perspective through studies of shear zone deformation processes. Examples are highlighted at regional and outcrop scales from western North America and the European Alps.

In regionally observed patterns, strikes of seismically detected fabric from receiver functions in California show a strong alignment with current strike-slip motion between the Pacific and North American plates, with high signal strength near faults and from depths below the brittle-ductile transition suggesting these faults have deep ductile roots. In contrast, despite NE-striking shear zones being the most prominent features portrayed on Proterozoic tectonic maps of the southwestern USA, receiver function anisotropy from the central Rocky Mountain region appears to more prominently reflect broadly distributed Proterozoic fabric domains that preceded late-stage localized shear zones. Possible causes for the discrepancy fall into two categories: those that involve bias in seismic sampling, and deformation processes that lead either to weaker anisotropy in the shear zones compared to adjacent domains or to a symmetry that is different from that conventionally assumed. Most of these explanations imply that the seismically sampled domains contain important structural information that is distinct from the shear zones.

The second set of examples stem from studies of outcrop-scale shear zones in upper amphibolite-facies (0.9-1.0 GPa, 700 °C) metagabbro from Precambrian exposures in Montana (USA) and in greenschist-facies (0.7-0.8 GPa, 450-500 °C) metagranites from the External Crystalline Massifs of the European Central Alps. The shear zones are characterized by strain gradients from undeformed coarse-grained protoliths to very fine grained ultramylonite, and by microstructures dominated by CPO-producing deformation mechanisms in the protomylonite and CPO-weakening mechanisms such as dissolution-precipitation creep and grain boundary sliding in the ultramylonite. In the mafic mylonites, the result is a lower seismic anisotropy (~2%) in the core of the shear zones despite a well-developed hornblende shape-preferred orientation. Preliminary observations of these examples suggest that marginal gradients may contribute as much or more to the bulk anisotropy signal compared to the higher strained cores of these structures. If true, a similar effect could explain some otherwise puzzling anisotropy studies of larger scale shear zones such as from the Himalaya where anisotropy tilt proximal to the Main Himalayan Thrust is notably steeper than expected.

Restored cross sections in complex deformation zones: usefulness and limitations

A. Margalef[1] & J.M. Casas[2]
[1]*Snow and Mountain Research Center of Andorra, Institut d'Estudis Andorrans, Sant Julià de Lòria, Andorra (amargalef.cenma@iea.ad)*
[2]*Departament de Dinàmica de la Terra i de l'Oceà-Institut de Recerca Geomodels, Universitat de Barcelona, Barcelona, Spain*

Several restored cross sections through pre-Variscan rocks from the Pyrenees are presented for the first time. The study area is located in the southern part of Andorra (Central Pyrenees), where pre-Variscan rocks are affected by a polyphasic Variscan deformation, which has produced several systems of thrusts and synfoliar folds. Deformation took place during Namurian (330-319 Ma) in low-grade metamorphic conditions, prior to the emplacement of the granodioritic batholiths (305-290 Ma). The methodology used is described and its usefulness and limitations in zones with polyphasic deformation and strong internal deformation are discussed.

To better visualize and reconstruct the fold geometry, data were integrated into a 3D environment, which also facilitates the construction of geological cross sections. Cross sections are perpendicular to the main megastructures and each section was divided into several cylindrical domains. An appropriate projection vector was chosen in each domain for each mesostructure (S0, S1, S2, S3). This procedure is used to avoid errors derived from the projection of complex structures using an average projection vector. This is a time-consuming procedure, and in-house developed routines for CAD-type tools were used to project data and calculate apparent dip values. Some preliminary cross sections have been built and then restored, corrected and reconstructed several times in order to obtain a geometrically feasible restored cross section, which in turn will be compatible with field observations. Two restoration methodologies have been used: rigid body restoration for thrusts and normal faults, and flexural slip restoration to restore folds; both were applied in the reverse order in which deformational structures were formed. This methodology has allowed us to differentiate the contribution of each deformational episode in the current geometry, as well as to propose a geometrically valid evolution for a region with complex structure and several subtractive-type thrusts. In the study area, Silurian slates act as a detachment level that generate a deformation partition: above this level, thrusts and associated folds predominate, whereas they are not well developed below the detachment level. Cross sections revealed that this partition is linked to a different amount of shortening: minimum shortening in Devonian materials above this level is about 60%, while in infra-Silurian materials the shortening is about 48%. One of the critical points is that internal deformation related to fold and foliation systems has been considered homogeneous above and below the detachment level, and it has not been taken into account in the restoration. Thus, the minimum amount of shortening can differ from the real value. Furthermore, the study area presents a fairly rugged relief and, in some places, a pretty dense vegetation cover that conditions the spatial distribution of the available data and thus leads to limitations in its number and location. This fact has not allowed us to apply more complex methods, so simpler restorations have been applied, but still permitting us a reasonable approximation to the structure of a complex deformation zone.

The role of twinning in microstructure evolution during the static recrystallization of cold-worked Carrara marble

E. Mariani[1], S.J. Covey-Crump[2], J. Wheeler[1], D. Wallis[3] and D.J. Prior[4]
[1]*School of Environmental Sciences, University of Liverpool, Liverpool, UK (mariani@liverpool.ac.uk)*
[2]*School of Earth, Atmospheric and Environmental Sciences, University of Manchester, Manchester, UK*
[3]*Department of Earth Sciences, University of Oxford, Oxford, UK*
[4]*Department of Geology, University of Otago, Dunedin, New Zealand*

In the Earth's crust and mantle syn-tectonic (dynamic) and post-tectonic (static) recrystallization of rocks can modify grain sizes, shapes and crystallographic orientations. This affects physical properties and anisotropies and is important for the interpretation of the mechanical behaviour of rocks in major fault zones along plate boundaries and geological terrains in mountain belts.

To improve our understanding of static recrystallization mechanisms, we carried out quantitative microstructural analyses of cold-worked and then annealed Carrara marble, using electron backscatter diffraction (EBSD) in a field emission gun (FEG) scanning electron microscope (SEM).

Initially samples were experimentally deformed to 8%, 17% and 27% strain, at 420 °C, 170 MPa confining pressure and a strain-rate of $3x10^{-4}$ s^{-1}. In all samples deformation twinning contributed to the accommodation of strain. Subsequent annealing was carried out at temperatures between 500 °C and 700 °C, and for periods from 3 hours to 35 days. The thirty two samples analysed show that, at all conditions, the strength of crystallographic preferred orientation (CPO) decreases with the progress of static recrystallization. This is linked with a progressive switch from e-twin to c-axis maxima, and may be interpreted as follows:

1) New recrystallized grains inherit CPOs from both twin and original old grains. If old grains have a c-axis maxima in the stress direction due to slip systems (other than e-twinning, e.g. basal <a>) active during deformation, then the new grains will inherit it.
2) The c-axis maxima results entirely from dispersion of orientations around e-twin orientations, with the highest density around c, positioned centrally with respect to the three possible e-twin orientations.

Twinning is one of the least understood microphysical processes that accommodate strain in rocks. The elastic strain field that develops at twinning intersections and in neighbouring grains around twin boundary terminations may be dissipated by local lattice distortion via the generation of new dislocations. This in turn must determine where recrystallization begins and how it evolves. High-Resolution EBSD is used to investigate the unexplored relationship between elastic and plastic strain around twin boundaries in calcite.

Recovery and sub-grain rotation recrystallization of both parent and twin grains are active recrystallization mechanisms that form new pristine grains along grain boundaries and twin lamellae. These processes result in recrystallized grains with a distinctive misorientation angle distribution make-up, with predominantly high misorientation angle relationships with each other and both low and high angle relationships with their parent grains. The distribution of high misorientation angles is controlled by twinning relationships.

High energy, high angle boundaries are readily formed, leading to the onset of rapid grain boundary migration which, together with orientation pinning mechanisms, forms irregularly-shaped recrystallized grains.

An experimental study on the brittle-viscous transition in mafic rocks and the importance of strain dependent rheology

S. Marti[1], R. Heilbronner[1], H. Stünitz[2,3], O. Plümper[4] & M. Drury[4]
[1]*Department of Environmental Science, Basel University, Basel, Switzerland (sina.marti@unibas.ch)*
[2]*Department of Geoscience, UiT the Arctic University of Norway, Tromsø, Norway*
[3]*Institut des Sciences de la Terre d'Orléans (ISTO), Université d'Orléans, Orléans, France*
[4]*Department of Earth Sciences, Utrecht University, Utrecht, Netherlands*

Strength envelopes (rheological profiles) suggest that rocks support the highest differential stresses at the transition from dominantly brittle to dominantly viscous deformation, i.e., at the 'brittle-to-viscous transition' (BVT). However, our understanding of the dynamics of fault rocks and active deformation mechanisms is still incomplete, especially if it comes to the BVT, where both time dependent viscous mechanisms and relatively time insensitive brittle mechanism significantly contribute to accommodate displacement.

Here we present results of an experimental study that was undertaken with the aim of identifying the processes of initiation and maintenance of fault- and shear zones over the BVT in mafic rocks. Experiments are performed on 'wet' plagioclase - pyroxene mixtures, at elevated pressures (0.5, 1.0 and 1.5GPa) and temperatures (300 - 800°C) with a Griggs-type solid medium deformation apparatus. At the experimental displacement rates (~ 1e-8 - 1e-9 ms^{-1}) resulting in 'bulk' shear strain rates of ~ 2e-5 to 2e-6 s^{-1}, a transition from dominantly brittle to brittle-viscous to dominantly viscous is observed between the temperatures 600 to 800°C. In all experiments, strain localizes into a network of shear bands. The geometry of the latter, together with the modes of deformation within the shear bands and the surrounding low strain lenses, determine the bulk rheological response.

In our mafic sample material, the main processes enabling viscous deformation are 1) efficient solution-mass transport, 2) reaction and nucleation, leading to strong grain size refinement and 3) shear band interconnection. Due to the time dependence of viscous processes, they in turn result in a time dependent brittle-to-viscous transition, and in the case of constant displacement rate experiments, this implies a strain dependent transition. Up to experiments performed at 800°C, shear band initiation is enhanced by dilatant / brittle deformation. Subsequently, reaction and nucleation lead to strong and localized grain size refinement along this initial shear loci, giving way to viscous deformation by grain boundary sliding accommodated solution mass transport creep.

Beside the increasing dominance of viscous mechanism with increasing T, our experimental results document a change from brittle to viscous dominated rheology as a function of strain, i.e. microstructural evolution. In the competition between time insensitive brittle and time sensitive viscous mechanism, non-steady state events in fault/shear zone dynamics are likely to trigger a temporary, brittle mechanical response, until microstructural evolution enables again efficient viscous creep and thus a viscous rheology.

Neotectonic history and landslides in the Main Ethiopian Rift (MER) and Afar triple junction revealed by analysis of remote sensing data and field mapping

K. Martínek[1,2], K. Verner[2,1] , D. Buriánek[2], L. Alemayehu Megerssa[1,2] & T. Hroch[2]
[1]Institute of Geology and Palaeontology, Faculty of Science, Charles University, Albertov 6, Prague, 12843, Czech Republic (karel.j.martinek@gmail.com)
[2]Czech Geological Survey, Klárov 3, 118 21 Prague, Czech Republic

This study presents several case studies across large area of the Main Ethiopian Rift (MER) and Afar triple junction - the central part of the Afar Depression in northeastern Ethiopia that represents a junction of three regional rift systems. These regional structures accommodate the active extension between the Nubia, Arabia and Somalia plates since the Late Miocene. Morphotectonic analysis of remotely sensed data was used to understand fault geometries in regional scale. Field structural mapping of brittle structures was carried out in mesoscopic scale. High correlation of newly identified linear indices derived from morphotectonic analysis with field structural data was found. New petrological and geochronological data of various volcanic products (32 - 0.9 My) are also presented.

The superposition of different sets of brittle structures were identified across the area in all mapped volcanic formations (e. g. regional normal faults to oblique slip faults, shear joints and extensional joints). The origin of these brittle structures have been related with the relatively younger evolution of two dissimilar rift zones. The southern part of the Afar area predominantly exhibit N-S to NE-SW trending faults and shear joints associated with NNE-SSW trending Main Ethiopian Rift System. Identified kinematic indicators reveal a normal movement. In the central part of the Afar area these steep faults sharply change strike to the ~NW-SE direction. Towards the northeast these faults dip steeply to the NE or SW and contain steeply to moderately plunging slickenslides. Indicators of normal or oblique left-lateral movement become dominant. On several localities across the Afar area these faults appear to be relatively younger than previous one forming the main escarpments of the Tendaho and Dobi grabens.

Early Oligocene stages (ca ~32 My) of rifting are characteristic by dominant normal faulting with paleostress orientation WNW-ESE perpendicular to the main rift normal faults oriented NNE-SSW to NE-SW. During late stages of rifting paleostress rotated anticlockwise to present-day WSW-ENE orientation which caused in addition to N-S to NNE-SSW normal faulting also important sinistral faulting along conjugate faults. Dextral conjugate faulting occur locally in the southern part of MER (e.g. Arba Minch area), which reflects different geometry of the main rift. Faults formed during these late stages show smaller vertical displacement and form less prominent geomorphic features. Slope instabilities are commonly located along the active fault zones; steep slopes, rock/mineral alteration and rheological weakening together with seasonal heavy rainfall and occasional seismic events are the main trigger for landslides, rockfalls and other slope instabilities.

Krkonoše Piedmont Basin inversion: Mesozoic – Cenozoic cooling, exhumation and deformation history based on detrital apatite fission track analysis and field structural data

K. Martínek[1,2], K. Verner[2,1] & M. Svojtka[3]
[1]*Institute of Geology and Palaeontology, Faculty of Science, Charles University, Albertov 6, Prague, 12843, Czech Republic (karel.j.martinek@gmail.com)*
[2]*Czech Geological Survey, Klárov 3, 118 21 Prague, Czech Republic*
[3] *Institute of Geology of the CAS, v. v. i., Rozvojová 269, CZ-165 00 Prague 6, Czech Republic*

Permo-Carboniferous Krkonoše Piedmont Basin (KPB) belongs to a system of post-Variscan extensional / transtensional basins of the Bohemian Massif, Czech Republic. The age of the KPB red bed fill spans between Asturian to Lower Triassic (ca. 307 – 240 Ma). The older parts of the KPB, deposited in extensional half-graben setting, underwent partial deformation as early as during the formation of the strike-slip pull-apart Trutnov-Náchod sub-basin (TNSB, Late Rotliegend – Triassic age), which is superimposed in the eastern part of KPB. The regional thermal history of the KPB has been assessed using detrital apatite fission track analysis. The 14 outcrop samples range stratigraphically from Variscan crystalline basement through the deposits of Pennsylvanian and Permian to Triassic. Fission track data reveal significant cooling events in Mesozoic and Cenozoic. Field structural mapping focused on major fault and fracture zones. Kinematic indicators preserve almost entirely the latest (Cenozoic) phases of brittle deformation. These phases are also well expressed by present-day geomorphic features.

Detrital apatite fission track data yield ages indicating Upper Permian annealing over 120°C of the Palaeozoic rocks followed by Middle Triassic partial annealing (over 80°C). An overall burial is suggested deeper than 3 km, assuming thermal gradient of 30°C/km. Burial events (0.1 – 0.2 km/Ma) were found in latest Pennsylvanian and Early Permian in the central and western parts of the basin. Late Permian and Triassic burial events were identified in eastern part of the KPB – in TNSB. The latter burial events followed basin reactivation from extensional to strike-slip regime. Time-temperature modelling reveals four significant cooling/uplift periods, which are generally moving through time from west to east. (I.) In Late Triassic - Middle Jurassic (220 - 160 Ma) we infer activity on the Škodějov and Pilníkov faults, and the uplift of Nová Paka Anticline, and Zvičina and Chotěvice blocks. (II.) In Cretaceous (130 - 90 Ma) we infer activity on the South Krkonoše Fault, uplift of Trutnov-Úpice block. (III.) During the latest Cretaceous - Paleocene (80 - 60 Ma) we infer activity on the South Krkonoše Fault, uplift of Trutnov-Úpice block, and rapid uplift of Náchod block. (IV.) Miocene - Pliocene rapid uplift (20 - 2 Ma) is a common feature for all studied samples. Most of the post-depositional uplift and deformation was governed by reactivated older fault zones in dextral transpressional zone connected with Elbe Zone. The results highlight the importance of regional, episodic postorogenic exhumation of Palaeozoic fold belts, where previous studies have suggested relatively long-term stability, and brings important data on timing of the basin`s deformation events, which were previously hypothesized on the basis of undirect evidence.

Microstructural indicators of channelled melt flow through the lower crust

U. Meek[1], N. Daczko[1] & S. Piazolo[1,2]
[1]Department of Earth and Planetary Sciences, Macquarie University, Sydney, Australia (uvana.meek@students.mq.edu.au)
[2]School of Earth and Environment, University of Leeds, Leeds, UK

Here we report and interpret microstructural features of a lower crustal mass transfer zone. The mass transfer zone is characterized by a 30-40m wide hornblendite unit which cuts granulite facies gabbroic gneiss. Field observations argue against an igneous cumulate origin for hornblendite, instead previous work shows that the gabbroic gneiss has been fluxed by a hydrous gabbroic melt that caused extensive melt-rock interaction (Daczko et al. 2016).

In the conceptional model of these zones, the host rock (in this case, two-pyroxene-pargasite gabbroic gneiss) is modified by flux of externally-derived melt, causing reaction-replacement. The migrating melt invokes dissolution of host rock phases that are out of equilibrium with the fluxing melt (in this study, plagioclase + pyroxene), enhancing porosity and permeability and therefore melt flow. New phases crystallise from the migrating melt (in this study, mainly hornblende ± clinozoisite and garnet). As a result, this body represents an “imposter cumulate”.

This study focusses on recognizing microstructural indicators with which it is possible to differentiate between an igneous cumulate body and an “imposter cumulate” in lower crustal systems. The microstructural features are described and characterised using thin section microscopy (optical and SEM), along with EBSD mapping of key features. The contact character of ultramafic versus host rock is the most important feature identified. At a microstructural (1-10 μm) scale, the replacement involves dissolution and precipitation of phases. The key texture involves partially dissolved phases that have irregular grain boundaries, as the new precipitating phase replaces them. Other features of channelled melt flow through the lower crust may include (i) the presence of local microstructures typical of the former presence of melt (namely low dihedral angles along grain boundaries that are pseudomorphs of former melt, melt pockets, local pegmatitic domains), and (ii) a high modal abundance of one (or two) phases as a reaction product from melt.

Utilizing these indicators along with careful field analysis will help to identify, melt transfer zones, that so far have been largely under-recognized.

Reference:
Daczko, N.R., Piazolo, S., Meek, U., Stuart, C.A. and Elliott, V., 2016. Hornblendite delineates zones of mass transfer through the lower crust. Scientific Reports, 6, 31369, doi:10.1038/srep31369, 1-6. [http://www.nature.com/articles/srep31369]

The Rotliegend fracture patterns: a transition between continuous and discontinuous geomechanical behaviour

F.F. Menezes[1] & C. Lempp[1]
[1]*Engineering geology, Institute for Geosciences and Geography, Martin-Luther-University Halle-Wittenberg, University, Halle, Germany (flora.menezes@student.uni-halle.de)*

Is it possible to use fracture patterns from triaxial tested sandstone specimens as a model to understand strain accommodation in rock masses? Using fracture patterns and geomechanical properties, this study describes the mechanical behaviour of a Rotliegend sandstone during brittle deformation, at the transition between continuous and discontinuous behaviour. Cylinder specimens with edge lengths of about 140 mm and a diameter of 70 mm were prepared from layered rock blocks of Rotliegend, which were obtained in a quarry (named Bebertal) 28km northwest from Magdeburg (Germany). This variety of Rotliegend consists of a fine to medium grain, red-brownish sandstone, massive and mostly horizontally stratified. Joints and layers of clay or fine gravels were often observed in core samples. Core samples were drilled perpendicular to bedding and tested under water saturated conditions. Conventional triaxial compressions tests were carried out under varying confining and pore pressures, with a controlled rate of deformation (0,0008 mm/s). The evaluation of shear parameters was calculated according to the Mohr-Coulomb failure criterion by using the data obtained from triaxial compression tests. Friction angle and cohesion from 34 specimens were associated with their corresponding elasticity modulus, mechanical work, dilatancy tendency and fracture pattern. Based on this analysis, it was possible to distinguish between a continuous or discontinuous behaviour for the Rotliegend sandstone from Bebertal, as well as an association of fracture patterns with geomechanical properties. Fracture patterns could be classified under progressive or punctual deformation: a progressive deformation is recognized by the development of a complex fracture pattern with many conjugated shear fractures. A punctual or simple deformation is related to a sudden loss of cohesion in the specimen which happens at the first load-step of a triaxial test. After that, there were no considerable periods of large lateral or axial deformation, although pressure still increases. In this case, the fracture pattern is represented as a unique penetrative shear fracture, sometimes attended by tensile or wedged joints. Progressive deformation paths show higher cohesion (60 %) and do more mechanical work (20 %) than punctual fracture pattern. Effective mechanical work and rock strength were normalized as indices (ratio between load- and reload-steps) and mutually related in an index-diagram. With this diagram it is possible to recognize a clustering of shear parameters and fracture patterns. Moreover, it was observed that an apparent continuous behaviour occurred at a specific confining pressure from about 40MPa. This unusual, continuous behaviour was simulated on the basis of a Finite-Elements-Method software called ADINA. Simulation results showed that, to reach the same compressive strength and elastic modulus as by compression tests, the Poisson's ratio should be ca. 0,13. This value does not correspond precisely to the minimal manifestation of lateral strain in our experimental tests, but it suits physical properties of hard sandstones (ρ=2,45g/cm³) with low porosity (ca. 8 %) and restricted permeability, such as the Bebertal sandstone. In order to propose a new approach to estimate dilatancy paths for hard sandstones, the volumetric strain was calculated by using volume changes from axial strain and pore fluid volume, similarly obtained from triaxial compression tests.

Geomechanical behaviour changes of a Bunter Sandstone due to $scCO_2$ injection effects

F.F. Menezes[1], C. Lempp[1], A. Neumann[1,2], K. Svensson[2] & H. Pöllmann[2]
[1]*Engineering geology, Institute for Geosciences and Geography, Martin-Luther-University Halle-Wittenberg, Halle, Germany (flora.menezes@geo.uni-halle.de)*
[2]*Mineralogy and Geochemistry, Institute for Geosciences and Geography, Martin-Luther-University Halle-Wittenberg, Halle, Germany*

Cluster (www.bgr.bund.de/CLUSTER) is a research project funded by the German Federal Ministry for Economic Affairs and Energy (BMWi), that investigates the impact of CO_2 streams and mass flow for different scenarios along the CO_2 capture and storage chain (CCS). This work describes geomechanical behaviour changes in a reservoir rock caused by supercritical (sc) CO_2 by taking into consideration the variability of boundary conditions in storage location (e.g. effective stress changes, storage period, presence of fractures, CO_2 streams composition). An analogue, possible reservoir formation that was investigated was the Trendelburger bed which is comprised of a fine to middle grained sandstone and is classified in mineralogy as a subarkose within the Buntsandstein group (Solling formation). This hard and compact silica cemented sandstone (ρ = 2,3 g/cm³) has an average effective porosity of 12 % and permeability of 900 mD, although physical rock parameters show that a considerable variation occurs naturally in this formation. Multiple triaxial compression tests were conducted on rock specimens saturated either with water or brine. Pore and confining pressures were also varied. Core samples with length and diameter of about 140 mm and 70 mm respectively were prepared from low, angular, inclined-bedding rock blocks, which were obtained from a quarry in Bad Karlshafen (Germany). In order to analyze directional dependency of geomechanical parameters, core samples were drilled parallel and perpendicular to bedding. The geomechanical behaviour from the Trendelburg bed was investigated with rock specimens under three different physical conditions: (1) an unloaded, untested core sample; (2) a preloaded specimen with shear fractures; and (3) an altered specimen used before at an autoclave experiment. Autoclave experiments were carried out under representative reservoir conditions (T = 60 °C, p = 16 MPa) by exposing rock specimens to $scCO_2$ and synthetic formation brine for five weeks. The experimental results show that permeability, ultrasonic velocity, fracture pattern and strength properties are direction-dependent. Rock specimens with longitudinal bedding planes are more permeable and have higher Young's modulus and strength than the ones with transverse bedding planes. However, after failure (discontinuum), rock specimens with transverse planes showed higher residual strength and higher cohesion values. An influence of $scCO_2$ on geomechanical properties and mineralogical state could firstly be detected after a long-term reaction in autoclave experiments. The influence of $scCO_2$ on the deformability of the Trendelburger bed is reflected due to the reduction of Young's modulus (ca. 17 %), a loss of cohesion (60 %), as well as a decrease in tensile and compressive strength (30 % and 20 %). Micrographs made before and after $scCO_2$ treatment show how mineral phases were dissolved and therefore how pore spaces became connected. A systematic relation between mechanical work, triaxial strength and shear parameters was identified at the transition from elastic to plastic deformation and is represented at an index graph. This relation is associated with a mechanical change of fracture patterns during shearing. Additional triaxial compression tests are planned to be conducted with CO_2 in combination with impurities such as NO_x and SO_x. This will allow supplementary statements about geomechanical behaviour and property changes in the context of CO_2-storage.

Pre Late Mesozoic deformations' phases of Wrangel Island's northern part

A. Moiseev[1], S. Sokolov[1], M. Tuchkova[1], V. Verzhbitskii[2] & N. Malyshev[2]
[1]Geological institute RAS, Moscow, Russia (moartem@yandex.ru)
[2]Open Joint Stock Company "Rosneft", Moscow, Russia

Wrangel Island is located on the continental shelf of the Russian Arctic, between the East Siberian and Chukchi seas. The northern and southern parts of the island are presented with undeformed Quaternary and Late Cretaceous-Cenozoic (?) sediments. The central part is latitudinal mountains belt builds up by carbonate and clastic rocks from the Late Proterozoic to Triassic. Wrangel Island' pre-Cretaceous complexes are involved in fold-thrust deformation north vergency (Tilman et al, 1970; Kos'ko et al, 1993; Verzhbitskii et al, 2015). Deformation caused by collision Chukchi microcontinent with structures of Siberia's active margin at the end of the Early Cretaceous (Parfenov et al., 1993; Sokolov, 2010).

It was distinguished another strike of folded Silurian-Lower Devonian sediments after 2006 field work (Verzhbitskii et al., 2014, 2015), that suggesting a manifestation Ellesmerian orogeny. All previous structural studies mostly were focused in the southern and western parts of the island. Our structural observations carry out during 2014 fieldwork, with funding from the Open Joint Stock Company "Rosneft". We investigated the least studied areas of the island. They were accumulated along the sublatitudinal crossing the northern part: 1 - Creek Dublitskogo – Cape Pillar; 2 – river Krasniy Flag; 3 –Pervay mountain - the southern branch of Kit mountain; 4 - river Lemingovaya; 5 –Drem-Head mountains. Information was obtained from the mesostructural analysis of natural outcrop. We found out and studied different structural paragenesis and deformation's phases. Kinematic indicators were measured. Structural thin sections were studied in some cases.

Subsequent to the results of research, it was made following conclusions:
1. Observations in the Silurian-Devonian rocks around Drem-Head mountains confirmed the existence of Ellesmerian orogeny in the Wrangel Island's complexes. The structures have a constant eastern vergency. The superimposed relationship with the younger late Cimmerian structures were investigated within Krasniy Flag river's outrops. This indicates structural similarity complexes of Wrangel Island with the ones of Canadian Arctic Island, Arctic Alaska, Svalbard and Greenland.
2. Between Ellesmerian and Late Cimmerian phases might need to distinguish additional phase of sublatitudinal compression. It can be associated with Early Jurassic phase of deformations, which are known in Chukotka (about 200 MA) and Alaska (Grantz et al, 1978; Tuchkova et al, 2007; Golionko et al, 2017).
3. Structural parageneses (a – kink-band, slaty cleavage, C-S structures, quartz, chlorite in strain shadows and so on) of Late Cimmerian stage of folding have been formed from the lower to the upper limits of greenschist metamorphism.
4. Postcollisional stage submeridional compression was confirmed (Verzhbitskii et al, 2015). It was distinguish within Late Carboniferous - Early Permian near Cape Uering. Defarmations presents with recumbent folds

This research was supported by Russian Scientific Fund Grant N 16-17-10251. We thank Open Joint Stock Company "Rosneft" for financial support in field work on Wrangel Island and subsequent analytical researches.

Influence of boundary conditions on the nucleation of shear zones around material heterogeneities

L. Nardini[1], L. Morales[2], E. Rybacki[1] & G. Dresen[1,3]
[1]*GFZ German Research Centre for Geosciences, Section 4.2, Potsdam, Germany (nardini@gfz-potsdam.de)*
[2]*ETH, Scientific Centre for Optical and Electron Microscopy (ScopeM), Zürich, Switzerland*
[3]*Institut für Erd- und Umweltwissenschaften, Universität Potsdam, Potsdam, Germany*

Shear zones are regions of localized deformation that occur at different crustal levels. They are often associated with material and/or structural heterogeneities. Although a lot of work has been performed about the temperature effects on the initiation and maintenance of shear zones, not much is known about the role of pressure on shear zone development. Here we present the initial results of a detailed experimental investigation on the influence of pressure on the nucleation process occurring in carbonates. We conducted a series of triaxial deformation experiments in a Paterson-type deformation apparatus on copper-jacketed Carrara marble cylinders with two flat weak inclusions of Solnhofen limestone lying on the same plane and oriented at 45° to the cylinders' longitudinal axes to simulate the presence of material heterogeneities in a homogeneous matrix. The experiments were conducted at constant strain rate and temperature ($7.2*10^{-5}$ s^{-1} and 900 °C), with varying confining pressures between 30 and 300 MPa. The samples were deformed at bulk strains of 2, 5 and 10% axial strain. Pure Carrara marble without inclusions is up to a factor 2 stronger than inclusion-bearing samples deformed under the same boundary conditions, and peak stresses increase with increasing confining pressure. The strain distribution between matrix and inclusions was estimated from markers on the copper jackets, showing local strains in front of the inclusions of up to about 10 times larger than the applied bulk strain, which rapidly decrease with distance from the inclusion tips. The extent and geometry of the process zone, defined as the area of intense intragranular deformation between the two inclusions, displays a strong dependence on confining pressure. At similar bulk strain, the width of the process zone at high confining pressure is by a factor of up to 1.5 larger than at low pressure. With increasing total bulk strain, the process zone also appears to be broadening irrespective of the confinement applied. At low confining pressures we observed the formation of a large number of intergranular elongated voids in the process zone, associated with marked grain size reduction. In addition, with increasing bulk strain the voids increase in size and an incipiently interconnected network of finely grained bands is formed. The results suggest that material heterogeneity-induced localization within the process zone changes from brittle to ductile deformation with increasing pressure, even when the matrix deforms in the ductile field.

Microstructure and Rheology of Samples of Primorsky Fault Core

A.A. Ostapchuk[1,2], E.M. Gorbunova[1] & V.V. Efremov[2]
[1]*Institute of Geosphere Dynamics of Russian Academy of Sciences, Moscow, Russia (ostapchuk@idg.chph.ras.ru)*
[2]*Moscow Institute of Physics and Technology (State University), Dolgoprudny, Moscow Region, Russia*

Excessive stresses are accumulated within the area of rock discontinuity relax in different fault slip modes. Low-frequency and very low-frequency earthquakes, as well as slow slip events have been classified recently.

Important information concerning peculiarities of fault evolution at the macro-scale can be provided by studying mineralogical and petrographic makeup of fault core and micro-crack systems with different genesis. In this work the results of investigation of samples gathered at the core of the exhumed segment of Primorsky Fault (Baykal rift zone). The petrographic analysis of thin section of the samples and shear deformation experiments on slider-model setup were carried out.

Analysis of microstructure of the thin sections have shown that there are narrow zones in the exhumed fault core where the strain exceeds the average one several times and explicit manifest of dynamic impact on minerals during tectonic slip. For example, samples of mirror of secondary fault include phenocrysts of feldspar, which are broken with cleavage cracks and show undulatory extinction.

In laboratory experiments the behavior of model fault filled with powdered rock samples were studied. The entire spectrum of deformation modes has been realized: stable sliding, stick-slip, transient slip modes. It is shown that realization of certain deformation mode is governed not so much by gouge strength as by its structure on meso-scale.

Moreover, it is established that the spatial heterogeneity of contact properties has a strong effect on the deformation mode, which, in turn, can explain the spatial and temporal variations of the slip behaviors of a local segment of a fault, for example, due to specific geological and physical processes taking place in them. The findings can be useful for understanding of the geomechanics of fault.

This work was supported by the Russian Foundation for Basic Research (project no. 17-05-01271).

Reactive Melt Migration in the Upper Mantle

M. Pec[1], B.K. Holtzman[2] M.E. Zimmerman[3] & D.L. Kohlstedt[3]
[1]*Department of Earth, Atmospheric and Planetary Sciences, Massachusetts Institute of Technology, Cambridge, MA, U.S.A (mpec@mit.edu)*
[2]*Lamont-Doherty Earth Observatory, Columbia University, New York, NY, U.S.A*
[3]*Department of Earth Sciences, University of Minnesota, Minneapolis, MN, U.S.A*

The formation of oceanic plates requires that large volumes of melt are extracted from the mantle and emplaced along a narrow spreading centre. Several lines of evidence suggest that melt extraction is rapid and therefore, necessitates high-permeability pathways. Such pathways may form as a result of melt-rock reactions. If a melt-rock reaction increases local permeability, subsequent flow is increased as well as promoting further reaction. This positive-feedback process can lead to the development of high-permeability channels that emerge from the background flow.
Anastomosing tabular dunite bodies within peridotitic massifs are thought to represent residual channels that formed by reactive flow. The conditions under which such channels can emerge are treated by the reaction infiltration instability (RII) theory.
Here we report the results of a series of Darcy type experiments designed to study the development of channels due to RII in mantle lithologies. We sandwiched a partially molten rock between a melt source and a porous sink and annealed it at high pressure (P = 300 MPa) and high temperatures (T = 1200° or 1250°C) with a controlled pressure gradient (∇P = 0-100 MPa/mm) for up to 5 hours. The partially molten rock is formed from 50:50 mixtures of San Carlos olivine (Ol, ~Fo_{90}) and either clinopyroxene (Cpx) or orthopyroxene (Opx) plus 4, 10 or 20 vol% of alkali basalt. The source and sink are disks of alkali basalt and porous alumina, respectively.

During the experiments, melt, undersaturated in silica, from the source dissolved the pyroxene and precipitated an iron-rich Ol (~Fo_{82}) thereby forming a pyroxene-free reaction layer at the melt source – partially-molten rock interface. The melt fraction, as well as the grain size, in the reaction layer was significantly larger than that in the starting material, confirming that the reaction increases the local permeability of the partially-molten rock, one of the pre-requisites for RII to form. The same reaction occurs in experiments performed with Ol:Cpx as well as with Ol:Opx mixtures. In experiments annealed under a small pressure gradient (and hence slow background melt flow velocity) the reaction layer is roughly planar. However, if the porous flow melt velocity exceeds ~0.1 µm/s, the reaction layer locally protrudes into the partially molten rock forming finger-like, melt-rich channels. This channel development is accompanied by an abrupt increase in effective permeability of the partially molten rock as recorded by the pore-pressure volumometer. Three-dimensional reconstructions using micro-CT images reveal that the morphology and spacing of the channels depends on the initial melt fraction of the partially molten rock. With 20 vol% melt, multiple and voluminous channels develop. At lower melt contents, fewer and thinner channels develop. The exact mineralogy (Ol:Cpx or Ol:Opx) does not seem to influence the channel morphology.

Our experiments demonstrate that melt-rock reactions can lead to melt channelization and an associated significant increase in permeability for mantle lithologies. The morphology of the channels appears to depend on the permeability perturbations present in the starting rock sample. The observed lithological transformations broadly agree with those observed in nature.

Atoms on the move: Deformation-induced trace element redistribution in zircon revealed using atom probe tomography

S. Piazolo[1,2], A. La Fontaine[3], P. Trimby[3], S. Harley[4], L. Yang[3], R. Armstrong[5], C. Corcoran[1] & J.M. Cairney[3]
[1]*Department of Earth and Planetary Sciences, Macquarie University, Sydney, Australia*
[2]*School of Earth and Environment, University of Leeds, Leeds, UK*
[3]*Australian Centre for Microscopy & Microanalysis, University of Sydney, Australia*
[4]*School of Geosciences, University of Edinburgh, Edinburgh EH9 3JW, UK*
[5]*Research School of Earth Sciences, The Australian National University, Australia*

One of the fundamental assumptions when using mineral chemistry signatures to decipher geological processes is that trace elements diffuse negligible distances through the pristine crystal lattice in minerals. For example, the reliable use of the mineral zircon ($ZrSiO_4$) as a U-Th-Pb geochronometer and trace element monitor requires minimal radiogenic isotope and trace element mobility. Here, using atom probe tomography, we document the effects of crystal-plastic deformation on atomic-scale elemental distributions in a number of zircons deformed at a range of geological conditions. In all cases, zircons reveal trace element distributions that are significantly influenced by element mobility at the sub-micron to micron scale. Dislocations that move through the lattice accumulate U and other trace elements where the effectiveness of accumulation is element dependent. Pipe diffusion along dislocation arrays connehcted to a chemical or structural sink results in continuous removal of selected elements (e.g. Pb), even after deformation has ceased (Piazolo *et al.* 2016). However, in disconnected dislocations trace elements remain locked. As a result, not only absolute elemental content but also element ratios can be markedly changed by crystal-plastic deformation. Our findings have important implications for the use of zircon as a geochronometer, and highlight the importance of deformation and deformation structures on trace element redistribution in minerals and engineering materials.

Reference:
Piazolo, S., La Fontaine, A., Trimby, P., Harley, S., Yang, L., Armstrong, R. & Cairney, J. M. (2016) Deformation-induced trace element redistribution in zircon revealed using atom probe tomography. *Nature Communications* 7:10490, doi: 10.1038/ncomms10490.

Earthquakes at depth: Insights from high resolution orientation and chemical analysis

S. Piazolo[1,2], P. Trimby[3,4], N.R. Daczko[1] & C. Kong[4]
[1]*Department of Earth and Planetary Sciences, Macquarie University, Sydney, Australia*
[2]*School of Earth and Environment, University of Leeds, Leeds, UK*
[3]*Australian Centre for Microscopy & Microanalysis, University of Sydney, Australia*
[4]*Electron Microscope Unit, University of New South Wales, Australia*

We report the first nanoscale orientation and chemical analysis of a lower crustal pseudotachylite. The pseudotachylite stems from Pembroke Valley, South Island, New Zealand. The Pembroke Valley exposes a 15 km^2 low strain zone within the Median Batholith, a composite regional batholith of Carboniferous to Early Cretaceous age. The pseudotachylite cuts high-P gabbroic gneiss which represents part of the deep magmatic arc (<14 kbar with temperatures of ~825 °C; Daczko et al. 2001). Rapid exhumation was facilitated by the significantly younger, Alpine aged fault zone still active today. Exhumation-related deformation was highly localized, preserving the lower crustal assemblage and microstructures throughout most of the Pembroke Granulite. Pseudotachylite is commonly observed in the Pembroke Valley and exhibits features very similar to those of the "classic" pseudotachylite from Barra, Outer Hebrides (Sibson, 1970). Typical features include rotation of pseudotachylite bound "clasts", variable thickness of pseudotachylite ranging from < 1mm to 2 cm width, mutually cross-cutting "generations" of pseudotachylite. No dominant movement surface or displacement direction could be identified.

Ar-Ar age dating constrains the age of the pseudotachylite to be unrelated to the active Alpine Fault zone, but overlapping in time with deep magmatic arc processes. This result is supported by high resolution analysis of the pseudotachylite using Transmission Kikutchi Diffraction Analysis (Trimby, 2012) performed on FIB foils within a state-of-the-art scanning electron microscope. In-depth analysis allows resolution of 10 nm and shows that the pseudotachylite vein is characterized by the presence of nanometre to micron sized newly grown clinozoisite, garnet and hornblende. Interestingly, the near amorphous vein matrix exhibits areas of cryptocrystalline plagioclase.

The newly grown phases suggest that the pseudotachylite formed at deep crustal levels (>8 kbar, ~820 °C). Details of the processes responsible for pseudotachylite formation and mineral assemblage growth are discussed in the light of the data presented.

References:
Daczko, N. R., G. L. Clarke, and K. A. Klepeis (2001), Transformation of two-pyroxene hornblende granulite to garnet granulite involving simultaneous melting and fracturing of the lower crust, Fiordland, New Zealand, J. Metamorph. Geol., 19(5), 549–562.
Sibson, R. H. (1975). Generation of pseudotachylyte by ancient seismic faulting. Geophysical Journal International, 43(3), 775–794.
Trimby, P. W. (2012). Orientation mapping of nanostructured materials using transmission Kikuchi diffraction in the scanning electron microscope. Ultramicroscopy, 120, 16–24.

Simulation of induced seismicity associated with fluid injection in single fractures: influence on the fracture slip regime

G. Piris[1], A. Griera[1], E. Gomez-Rivas[2], I. Herms[3] & X. Goula[3]
[1]*Departament de Geologia, Universitat Autònoma de Barcelona, Bellaterra (Cerdanyola del V.), Spain (albert.griera@uab.cat)*
[2]*School of Geosciences, King's College, University of Aberdeen, Aberdeen, United Kingdom*
[3] *Institut Cartogràfic i Geològic de Catalunya (ICGC), Barcelona, Spain*

The so-called Enhanced Geothermal Systems (EGS) are characterized by a stimulation phase that aims to increase fluid flow and heat transfer between wells by increasing the permeability and transmissibility of the reservoir. This is achieved by injecting fluids at high-pressure in order to increase the apertures of existing fractures, enhance their sliding and/or generate new ones. However, this technique induces low-magnitude seismicity that occasionally results in damage at the Earth's surface. Numerical simulations able to reproduce the hydro-thermo-mechanical behaviour of geological reservoirs are an essential tool for the evaluation and forecasting of induced seismicity in such systems. In this study, the numerical code CFRAC (e.g. McClure, 2012) is used to systematically evaluate how the orientation of fractures with respect to the maximum compressive stress (α) influences seismicity, the injection rate and the fracture sliding behaviour. The results show that three main seismic regimes can be distinguished.

The first type are orientations that do not require a large fluid overpressure patch on the fracture before the onset and nucleation of a seismic event. A small perturbation of strength is enough to produce a critical load and fracture reactivation. The size of the rupture surface is larger than the size of the pressurised patch, and therefore, slip along the fracture can expand outside of the pressurised front leading to situations of uncontrolled rupture propagation. The fractures oriented between α =40º and α=14º follow this behaviour.

The second type of response is defined by fracture orientations that require longer injection times before the onset of fracture slip. In this case, the onset of dynamic slip requires that a large part of the fracture is first uniformly pressurised. Seismic events in this case are not located near the injection point, but into the pressurised front. They are characterised by high slip velocities and surface run-outs that can expand outside of the pressurised region, but are still able to produce rupture surface along the whole fracture distance. The fracture orientation ranges between 5º≤ α <14º and 40º≤ α ≤45º.

Finally, a third case with the fracture oriented $\alpha \leq 5º$ can be defined. In this case, dynamic slip is not observed and fracture propagation is arrested due to the increase of the dynamic friction coefficient during the raise of the slip velocity. The accommodation of loading, and therefore the accommodation of a finite displacement along the fracture, takes place by means of slow motion events (i.e. low-magnitude seismicity) or by aseismic flow.

References:
McClure, M. W. (2012): Modeling and Characterization of Hydraulic Stimulation and Induced Seismicity in Geothermal and Shale Gas Reservoirs, PhD dissertation, Stanford University, Stanford, California, 349 p.

Viscous Flow Controls Slip Zone Thickness and Weakening during Coseismic slip in Calcite Gouges.

G. Pozzi[1], N. De Paola[1], S.B. Nielsen[1] & R.E. Holdsworth[1]
[1]Department of Earth Sciences, Durham University, Durham, UK (giacomo.pozzi@durham.ac.uk)

Viscous flow at high strain rates is a well-known deformation mechanism occurring in metals, but has only recently been associated with the behaviour of natural fault materials during earthquakes. In particular, microstructures attributed to grain boundary sliding have been recognised in high velocity (> 0.1 m/s) shear experiments on carbonates where the recrystallized materials commonly have a nanometric grainsize.

We designed and performed a set of friction experiments on a rotary shear apparatus using pure calcite microgouge (60 μm < D < 90 μm) and nanogouge (D ~ 200 nm). Experiments were run at different velocities, from sub-seismic (< 0.1 m/s) to seismic (up to 1.4 m/s), and arrested at different amounts of slip to document the evolution of microstructures and link these to the evolution of the mechanical behaviour observed.

Mechanical data show a characteristic four stage evolution of the friction coefficient when the material is sheared at seismic velocities (v > 0.1 m/s): I) an increase from initial Byerlee's values, f = 0.6 - 0.7, up to peak values, f = 0.8 - 0.9; II) a sudden decrease to low values, f < 0.4; III) the attainment of low steady-state values, f = 0.05 - 0.3; and IV) a sudden increase to final value, f < 0.6, upon sample deceleration. The latter stage is not recognised in initially nanometric gouge experiments.

Microstructural analysis of samples recovered after each stage used backscattered SEM imaging on polished cross-sections through the principal slip zones (PSZs). During stage I, initially widespread brittle deformation (Riedel shear bands) localises into a horizontal Y shear band producing intense cataclastic comminution (< 200 nm). By stage II, the Y shear band develops sharp boundaries showing patches of sintered material in the regions immediately adjacent to the PSZ. On reaching stage III, the former Y-shear band has become a well-developed nanograin recrystallized PSZ sharply bounded by two continuous planar mirror surfaces (MSs). It is characterised by an equigranular texture with triple junctions, low porosity and oblique shape preferred orientations. A sintering gradient is also developed centred on the PSZ and propagating outwards into the surrounding deactivated layers. At stage IV) fracturing and reworking of the material occurs and is limited to the PSZ, possibly due to restrengthening and thermal cracking upon deceleration and cooling.

MSs are interpreted here as the equilibrium boundaries between the PSZ where viscous grain boundary sliding occurs, and the outer deactivated layers that are dominated by quasi-static grain growth. The thickness of the PSZ is a function of the grain size, temperature, velocity and available flow stress. The evidence of rheological decoupling is best preserved in stage III microstructures of nanogouge experiments where MSs are marked by an abrupt grain size change.

Our findings illustrate the critical role that extreme comminution and localisation play in the onset of seismic weakening in carbonate gouges. Under steady state conditions (stage III), the viscous PSZ thickness is therefore an important physical parameter that controls dynamic weakening behaviour.

Microstructure, CPO and rheology of ice: scaling from the laboratory to ice sheets and ice shelves

D.J. Prior[1], L. Craw[1], W.B. Durham[2], J. Eccles[3], D. Goldsby[4], C. Hulbe[5], D. Kim[6], C. Qi[4], D. Peyroux[1], M. Seidemann[1] & M. Vaughan[1]

[1]*Department of Geology, University of Otago, Dunedin, New Zealand (david.prior@otago.ac.nz)*
[2]*Earth and Planetary Sciences, MIT, Cambridge, MA, USA*
[3]*School of Environment, University of Auckland, Auckland, New Zealand*
[4]*Department of Earth and Environmental Science, University of Pennsylvania, Philadelphia, USA*
[5]*School of Surveying, University of Otago, Dunedin, New Zealand*
[6]*Korea Polar Research Institute, Incheon, Korea*

Deformed polycrystalline ice has very strong crystallographic preferred orientations (CPO) with associated elastic and viscous anisotropy. When the loading that drives ice sheet flow changes, for example following an ice shelf collapse, the rate of response will depend upon the inherited CPO and its subsequent evolution in the new stress configuration. Lateral and vertical contrasts in mechanical properties occur where bodies of ice with different CPOs are juxtaposed. Ice shelves (where the ice sheet has moved offshore and is floating) such as the Ross Ice Shelf (RIS) provide good examples. Feeder glaciers with different CPO converge to create an ice shelf with lateral heterogeneity that controls subsequent mechanical behaviour, including break up. The mechanical response of the Earth's ice sheet systems to climate forcing depends, in part, on the evolution of the CPO. Thus, there is a need to improve our quantitative understanding of CPO evolution in ice and its impact on rheology.

Cryo-EBSD data from new axial compression experiments demonstrate that ice deformation microstructures change as a function of both temperature and differential stress/strain rate. At high T and low stress, strain induced grain boundary migration (SIGBM) is fast. The CPO is dominated by grains with high resolved stresses on the basal (easy slip) plane. In axial compression, poles to the basal plane are arranged in a cone around the compression axis. At lower T and higher stress, deformation is dominated by lattice rotation, polygonization and grain rotation. Low T axial compression experiments have the poles to the basal plane clustered parallel to compression. Polar terrestrial ice sheets deform at rates at least two orders of magnitude slower than any lab experiment, so CPO prediction requires scaling relationships. We will present a preliminary scaling relationship for CPOs in axial compression. Most natural deformation however has significant simple shear or constriction and we will show results from some new experiments with these kinematic components.
To validate scaling relationships to natural strain rate conditions, we measure CPOs from naturally deformed ice. We will present cryo-EBSD data from Antarctic glacier samples: some of these natural CPOs are explicable within the framework of existing experiments, others are not and require new experimental effort. We will also show ultrasonic measurements of *P*- and *S*-wave velocity anisotropy from natural samples and associated with some laboratory deformation experiments. The coincidence of measured velocity patterns with those calculated from the CPO gives us confidence to use seismic investigations to provide proxy CPO data on the scale of the thickness of ice sheets. We will present new data from an active source survey that used two seismometers frozen into the 220 m thick McMurdo ice shelf at depths of 39 m and 189 m. *P*- and *S*-wave velocities and *S*-wave splitting along different ray-paths enable us to constrain the bulk CPO in a way that would be much more difficult using only surface receivers. Future investigations using this approach should improve our ability to assess CPO and relate this to rheology at natural strain rates in ice sheets.

The nature of petrophysical anisotropy in the continental crust: a case study from the Serre Massif (Calabria, Italy)

R. Punturo[1], M.A. Mamtani[2], E. Fazio[3] & R. Cirrincione[1]

[1]*Department of Biological, Geological and Environmental Sciences, Catania University, Catania, Italy (punturo@unict.it)*

[2]*Department of Geology and Geophysics, Indian Institute of Technology, Kharagpur 721302, West Bengal, India*

In this study the relationships between fabric, seismic and magnetic anisotropy have been determined on a suite of lithotypes that are representative of a continental type crust exposed in the Serre Massif (Southern Italy). In particular, we selected two main lithotypes viz. granitoids (granodiorite/tonalite) and a metagabbro, which are respectively considered to be representative of upper/middle crust and the lower crust., By taking into account the fabric elements of the rock (e.g. lineation, foliation) we measured, seismic properties up to 400 MPa confining pressure with a triaxial multi-anvil apparatus as well as we carried out calculations on the basis of modal content and mineral composition. In granitoids, intrinsic (i.e. fracture-free) seismic velocities are around 6.2 km/s for compressional waves, whereas average Vs are ~ 3.6 km/s. In the same rocks, the Poisson's ratio ranges from 0.240 to 0.257, in accordance with the modal proportions of feldspars. In metagabbro, average Vp is 6.9 km/s and average Vs is 3.7 km/s. Results showed that velocity distribution within the studied lithotypes depends on progressive alignment of anisotropic mineral such as biotite, amphibole and pyroxene, which define the rock fabric. Indeed, at 400 MPa, after all of the microcracks are closed, the maxima seismic velocity values are localised within the foliation plane. Seismic anisotropy (Vp- and Vs- related) has been compared with magnetic anisotropy (K_m, the bulk magnetic susceptibility, that ranges between 136 and 15800 x 10^{-6} SI units), highlighting the different role of the constituting minerals over the petrophysical properties as a function of rock fabric. K_m of the granitic rocks is < 300 x 10^{-6} SI units indicating that paramagnetic mineral phases such as biotite and amphibole control the intensity of magnetic anisotropy. Moreover, a positive correlation between measured seismic and magnetic anisotropy has been recognized in these granites. This indicates that the modal proportions as well as arrangement of biotite and amphibole contributes to the petrophysical and textural crustal anisotropy in the middle crust.. In contrast to the above, in the metagabbro, which represents the lower crust, has a very high K_m (15800 x 10^{-6} SI units). Magnetomineralogical investigations reveal that the minor mineral ferromagnetic *s.l* minerals (magnetite and pyrrhotite) play an important role in controlling the AMS of the metagabbro despite the fact that the main minerals present in the sample are paramagnetic. Obtained results yielded useful constraints for the comprehension of the petrophysical behavior of the continental crust and also for integrating and constructing the geophysical models of the lithosphere structure beneath southern Calabria.

Kinematic analysis of quartzite mylonite from the Ruby-East Humboldt extensional shear zone, Elko County, Nevada

J.M. Rahl[1] & A.J. McGrew[2]
[1]*Washington and Lee University, Lexington, VA, USA (rahlj@wlu.edu)*
[2]*University of Dayton, Dayton, OH, USA*

Detailed SEM-EBSD investigation of quartzite mylonite from Secret Creek Gorge in the Ruby-East Humboldt extensional shear zone reveals a complex kinematic history recorded by domainal quartz crystallographic preferred orientations (CPOs). Prior work indicates that mylonitic WNW-directed shear occurred in equilibrium with meteoric fluids during cooling from ~630º to 450 ºC at shear stresses of 19-32 MPa and strain rates of 10^{-10} to 10^{-13} s^{-1}. Our analysis includes over 2.4 million observations mapped to a ~6.5 mm x 11 mm area. A kinked single girdle quartz c-axis distribution shows two strong maxima oriented approximately ±25º to Y along the shear plane normal. A modal analysis identifies at least 6 distinctly oriented subpopulations, some of which form paired Dauphiné twins; most modes share a strong <a> axis maximum inclined ~25º counterclockwise from the shear direction, while only few grains show <a> axes parallel to the shear direction as expected for simple shear.

For each mode, Schmid factors have been calculated to assess the potential activity of known quartz slip systems for the full range of principal stress orientations associated with kinematic vorticities ranging from pure shear to simple shear. Although the critical resolved shear stress to activate each system is unknown, the analysis indicates that most grains are best-oriented for slip on either r<a> or z<a>. Other systems well-oriented for slip vary between modes, but most commonly include prism<a+c>, prism<a>, □<a>, or □'<a>. The dominant crystallographic slip direction (the a-axis) from the bulk shear plane together with the potential activation of antithetic slip systems suggests a departure from end-member simple shear into the subsimple shear regime. We infer that activity of synthetic slip systems in the <a> direction on r, z, □, and □ planes is balanced by antithetic slip on the prism <a> and <a+c> systems. Combined, these slip systems produce a stable (irrotational) configuration to maintain subsimple shear to high strain values at a kinematic vorticity $W_k \approx 0.88$. The orientation of highly-stretched ribbon grains (~5º to the shear plane) suggests significant finite strain (R_{xz} ~ 17).

CPO mapping reveals significant spatial partitioning into ~1.0-1.5 mm thick domains parallel to foliation. The modes with shear-parallel a-axes are clustered together and have c-axes that plunge S-SW relative to foliation in the geographic reference frame; in contrast, ribbon grains show the dominant a-axis alignment ~25º counterclockwise to the shear direction and are mostly restricted to domains associated with c-axis maxima plunging N-NE. These spatial asymmetries suggest a triclinic aspect to the deformation, posing a challenge to two-dimensional strain compatibility. We suggest the inferred triclinicity may relate to large-scale boundary conditions, as Secret Creek gorge is located in a step-over zone between the Ruby Mountains to the East Humboldt Range shear systems.

Deformation of conglomerates with layered pebbles under simple shear: a numerical approach

H. Ran[1, 2], P.D. Bons[1], G. Wang[2], M. Finch[1], F. Steinbach[1], A. Griera[3], S. Ran[4] & X. Liang[2]
[1]*Department of Geosciences, Eberhard Karls University of Tuebingen, Tuebingen, Germany*
hao.ran@uni-tuebingen.de
[2]*School of Earth Sciences and Resources, China University of Geosciences, Beijng, China*
[3]*Departament de Geologia, Universitat Autònoma de Barcelona, Barcelona, Spain*
[4]*Tianjin Center, China Geological Survey, Tianjin, China*

Deformed conglomerates have been subject of many studies in structural geology, in particular for their potential suitability as finite strain and vorticity gauges. Most studies considered two end-member cases: rigid pebbles in a viscous matrix versus passively deforming pebbles, assuming their viscosity equals that of the matrix. Pebbles in a matrix record both the deformation history of a conglomerate and that of the source rock from which the pebbles were derived. For example, some pebbles in the Sijizhuang Formation (Wutai area, North China Craton) are internally folded, while most are not. This has been interpreted as evidence for a folding event in the Trans-North China Orogen that preceded deposition and subsequent deformation of the Sijizhuang Formation conglomerates.

We used the 2-dimensional modelling platform Elle, coupled to the full field crystal visco-plasticity code (VPFFT), to simulate deformation of conglomerates to high simple-shear strains. We varied the relative effective viscosities, using a power-law viscosity with n=3, of pebbles and matrix, as well as the area fraction, initial shape and orientation of the pebbles. The results show that there is a narrow range where the behaviour of the pebbles shifts from almost rigid to passive inclusions. The shift depends strongly on the area fraction occupied by the pebbles, due to crowding effects at high fractions. When pebbles are softer than the matrix, they become difficult to discern as pebbles and become the seeds for C and C' shear bands.

Deforming layered pebbles may develop internal folds. Internal folding, however, requires a narrow range of viscosity contrast between pebble and matrix to allow enough strain to develop folds, but still keep the pebble recognisable as such. Internal folding is furthermore facilitated by a layering initially at around 110° relative to the shear plane, sufficiently thin internal layers to achieve fold wavelengths smaller than the diameter of the pebble, and a high area fraction of pebbles. The difficulty in achieving internal folds within pebbles may explain the scarcity of internally folded pebbles in the Sijizhuang Formation conglomerates. Our simulations thus indicate that the few pebbles with folds must not necessarily indicate a previous deformation event, but may have formed during deformation of the conglomerate itself. This alternative interpretation has significant impact on the geotectonic history of the Trans-North China Orogen, as it may "remove" a whole cycle of burial, metamorphism, deformation and exhumation preceding the deposition of the conglomerate.

Microstructure and mechanical behaviour of experimentally sheared quartz gouge at the brittle-to-viscous transition

B. Richter[1], H. Stünitz[2,3] & R. Heilbronner[1,2]
[1]*Geological Institute, Basel University, Basel, Switzerland (bettina.richter@unibas.ch)*
[2]*Department of Geology, Tromsø University, Tromsø, Norway*
[3]*Institut des Sciences de la Terre d'Orléans (ISTO), Université d'Orléans, Orléans, France*

In order to study the deformation processes and microstructure development across the brittle-to-viscous transition and to derive corresponding stress exponents and activation energies, we performed a set of shear experiments on quartz gouge in a solid medium deformation apparatus. The starting material was a crushed dry quartz single crystal (sieved grain size < 100 µm) with 0.2 wt% water added. The experiments were conducted at elevated temperatures (500 °C to 1000 °C) and pressures (0.5 GPa, 1.0 GPa or 1.5 GPa) with shear strain rates between ~$3.5 \cdot 10^{-6}$ s^{-1} to ~$2 \cdot 10^{-3}$ s^{-1}.

At high confining pressures, the strength of the sample decreases with increasing temperature (from shear stress τ = 1600 MPa to 75 MPa). The most abrupt decrease occurred between 650 °C and 700 °C at a shear strain rate of ~2.5 x 10^{-5} s^{-1}. For T < 700 °C, the friction coefficient, µ, calculated as τ/σ_{mean}, is ~ 0.45 and decreases only slightly with temperature. For T ≥ 700 °C, µ shows a strong temperature dependence (µ = 0.3 to 0.05). At the same time, the positive pressure dependence of strength for T ≲ 650 °C changes towards an inverse pressure dependence at T > 700 °C.

Strain rate stepping experiments reveal power law breakdown at low temperatures (~ 650 °C). At low temperatures (T = 650 °C), the average stress exponent is n = 6.4 ± 1.3. At high temperatures (800 °C ≤ T ≤ 1000 °C), a stress exponent of n = 1.9 ± 0.7 and an activation energy of Q = 170 ± 72 kJ/mol indicate a combination of diffusion and dislocation creep.

Heterogeneous deformation - shear bands with Riedel geometry - is typical for low temperature and low confining pressure (0.5 GPa). High confining pressures inhibit frictional sliding and cataclasis dominates. With increasing temperature, viscous deformation processes become more important. Stress-induced-dissolution-precipitation is triggered along Riedel shears. Further temperature increase causes pervasive recrystallisation and creates a distinct foliation by dominating dislocation creep. The recrystallised grain size (modal value of 3D diameter) constantly increases from 1.8 µm at 700 °C to 10.1 µm at 1000 °C. At 900 °C to 1000 °C, recrystallisation is already almost complete at a shear strain γ ~ 3. At low temperatures, the crystallographic preferred orientation (CPO) is dominated by large clasts and a random c-axes orientation is developed. The accompanying stress-induced-dissolution-precipitation causes weak textures with a peripheral c-axis maximum. At intermediate temperatures, dominating dislocation creep creates a strong CPO with a single peripheral maximum rotated with the sense of shear; at high temperatures, the c-axes form a single central maximum.

Across the brittle-to-viscous transition, two main deformation mechanisms are partitioned into different grain size fractions of the quartz gouge: diffusion accommodated grain boundary sliding favours the very fine-grained material while dislocation creep tends to select the coarse-grained material.

Structural style and kinematic analysis of Cenozoic inversion structures in the Celtic Sea basins, offshore Ireland

P. Rodríguez-Salgado[1,2], C. Childs[1,2], P.M. Shannon[1,3] & JJ. Walsh[1,2]
[1]*Irish Centre for Research in Applied Geosciences (iCRAG), University College Dublin, Belfield, Ireland (pablo.rodriguez-salgado@icrag-centre.org)*
[2]*Fault Analysis Group, School of Earth Sciences, University College Dublin, Belfield, Ireland*
[3]*Marine and Petroleum Geology Research Group, University College Dublin, Belfield, Ireland*

The Celtic Sea basins, on the continental shelf between Ireland and northwest France, consist of a set of elongate ENE – WSW trending basins that extend from St George's Channel Basin in the east to the Fastnet Basin in the west. The basins, containing a Triassic to Neogene sedimentary succession, evolved through a complex geological history that includes multiple Mesozoic rift stages and later Cenozoic inversion.

Cenozoic tectonic inversion was characterized by N-S oriented moderate contractional strains that led to broad regional uplift accompanied by the growth of a series of inversion structures widely distributed through the Celtic Sea basins. Over the last 50 years these structures have been the main target for hydrocarbon exploration as they provide structural closure for the main producing gas fields in offshore Ireland: Kinsale, Ballycotton and Seven Heads. Despite the importance of the inversion structures to the petroleum systems, their formation mechanisms are not yet well understood. This is partially due to historically poor seismic data quality which is locally compromised by the presence of thick Upper Cretaceous chalk subcropping at the seafloor. As a consequence, the deepest areas of the inversion structures are often poorly imaged resulting in uncertainty about whether mapped anticlines formed as fault propagation, fault bend or buttress folds.

The present work, based on structural mapping of several 2D regional and 3D seismic surveys, provides examples of different styles of inversion structures. The mapped inversion structures typically consist of 3-way and 4-way dip-closed anticlines and their structural style ranges between two end-member types. The first type is preferentially located within, and aligned parallel to, the basin axis in areas of thick Mesozoic cover. These structures are characterized by low relief, long wavelength asymmetrical anticlines bounded by Cretaceous and Jurassic normal faults that acted as rigid buttresses. The second type is preferentially located on the basin margins and is characterized by short wavelength anticlines associated with reverse reactivation of pre-existing basin bounding extensional faults and newly-formed reverse faults and folds. The related anticlines are elongate in map view, spatially linked to basin-bounding structures. The interpretation of these structures, especially in poorly imaged areas, is supported by three-dimensional geometrical analysis and structural restoration to provide a better understanding of the mode of formation of the range of structures observed.

The influence of tectonics on Shirband cave formation: Damqan, Northern Iran

H. Roohafza[1], R. Ramesani[1] & A. Taheri[1]
[1]geology department, Faculty of science, Shahrood University, Shahrood, Iran (Hamid.roohafza6@gmail.com)

The Shirband Cave is developed inside 221 m thick column of Permian limestone (massive, thick-bedded limestone intercalated with thin marl and mudstone beds called Ruteh series) in north of Damqan city, northern Iran. The Shirband cave with 700 m length is the longest and most extensive cave in north of Damqan. Karstification is related to folding and faulting during the mid-Miocene collision between central Iran and Eurasia. The cave can be interpreted to have been formed due to compression of the area in the carbonate rocks of the Shirband area.

Detailed structural geological mapping of fissure orientations within Shirband cave and fissure of the outside Shirband cave was accomplished and presented as rose diagrams. Regional geological structures were compared with statistical evaluation of structural geological elements obtained from field mapping. There is a good correlation between surface and underground fissure orientations and cave passage orientations with regionally important fault zones, including the north Damqan Fault system (E-W direction) and Shirband Fault (NE-SW direction). The most frequent cave passages orientation, in a nearly E-W direction, is associated with nearly N-S compression and nearly E-W extension from late Pliocene to mid-Pleistocene. A second tectonic stage from late Pleistocene to the present, with the tectonic stress field mainly of NNE-SSW compression and WNW-ESE compression, is in accordance with the most frequent fissure orientations in Shirband area with a direction of N50–60°W (23.5%). Final results show tectonic has important role in karstification and creation of Shirband cave.

Phase mixing and the spatial distribution of grain-boundary pores in a crustal fault zone: Insights from New Zealand's Alpine Fault

K.M. Sauer[1], F. Renard[2,3], V.G. Toy[1] & the DFDP-2 Science Team[4]
[1]*Department of Geology, University of Otago, Dunedin, New Zealand (Katrina.sauer@otago.ac.nz)*
[2]*ISTerre, Université Grenoble Alpes, Grenoble, France*
[3]*Department of Geosciences, University of Oslo, Oslo, Norway*
[4]*International Continental Scientific Drilling Program, Potsdam, Germany*

Large-scale continental faults represent zones of inherent weakness and focussed deformation in the crust. Heterogeneities in fault zone rocks, such as grain-boundary pores, fine-grained secondary phases, and fluid inclusions can provide nucleation points for deformation instabilities, which are required for strain localisation. However, these heterogeneities are not uniformly distributed at any scale within fault zones. Therefore, a systematic characterisation of the nature and distribution of fault rock heterogeneities will improve our understanding of the mechanisms of strain localisation and fault zone dynamics.

The Alpine Fault is the main Pacific-Australian plate-boundary structure on the South Island of New Zealand, with rapidly exhumed hangingwall mylonite and cataclasite sequences that are equivalent to the fault rocks currently deforming at depth. We have sampled across the ductile strain gradient of the Alpine Fault zone to examine how microstructures and material heterogeneities evolve with increasing strain. Synchrotron micro-computed x-ray tomography (Sμ-CT), electron microprobe analyses (EPMA), and scanning electron microscopy (SEM) imaging reveal that at lower strains, pure quartz domains are common and grain-boundary pores are concentrated on monophase quartz boundaries, while with increasing strain phase mixing is more prominent and pores are progressively found on boundaries between different phases. Electron backscatter diffraction (EBSD) is used to evaluate the evolution of fabric anisotropy, such as crystallographic preferred orientations (CPO) across the strain gradient. Using both the J-index and M-index to quantify quartz CPO strength, we find a decrease in the CPO intensity with increasing strain in polyphase rocks. We infer this is due to a switch in the dominant deformation mechanism associated with increased phase mixing. Additionally, we will compare surficial outcrop samples with samples collected from up to 893 metres drilled depth from the 2014 Deep Fault Drilling Project – phase 2 (DFDP-2, Whataroa River) to to investigate the possibility that grain-boundary dilation due to removal of confining pressure facilitates development of near-surface porosity. Here we explore the relationship between phase mixing, microstructural evolution, and the spatial distribution of material heterogeneities with increasing strain, and the overall affect this has on strain localisation in the Alpine Fault.

Evidence for paleo-seismic cycles in carbonated peridotite: microstructural analysis of carbonated-coated grains in fault damage zones (Voltri Massif, Ligurian Alps)

M. Scarsi[1], L. Crispini[1], P. S. Garofalo[2] & G. Capponi[1]

[1]*Dipartimento di Scienze della Terra, dell'Ambiente e della Vita (DISTAV), University of Genoa, Italy*
[2]*Dipartimento di Scienze Biologiche, Geologiche e Ambientali (BiGeA), University of Bologna, Italy*

In this work we examine thrust faults, developed inside the ultramafic rocks (peridotite and serpentinite) of the Voltri Massif (Ligurian Alps, Italy), and accompanied by unusual carbonate-coated grains fault rocks. In the footwall of the studied faults, the damage zones (up to 10 m thick) are characterized by different types of fault rocks, syntectonic hydrothermal alteration of the host peridotite, carbonate and chalcedony+quartz vein networks; in the hangigwall, the damage zones are narrower (about 4 meters) and display intense fracturing. Deformation was accompanied by fluid infiltration, that caused an almost complete replacement of the host peridotite, with a mineralogy characterised mainly by dolomite, magnesite and minor ankerite. Furthermore, in the fault core it occurs a ca. 70 cm thick level of fault rocks, made up of carbonated-coated grains, with very fine grained carbonate matrix and limited by discrete main slip surfaces, with grooves and slickenlines. Carbonated-coated grains are from mm to cm in size, mainly spherical and made up by several concentric layers, showing alternate radially and laminated texture. Within the fault core, secondary slip surfaces are accompained by intense grain size reduction (microbreccia), with evidence of rotation of the carbonated-coated grains. The microbreccia clasts are recycled by different subsequent episodes of carbonate coatings. The top of the carbonatic fault core, is cut by shear veins made up by nanocrystalline chalcedony, surrounded by amorphous silica matrix; micro-textures in the nanocrystalline chalcedony indicate recrystallization after amorphous silica gel.

The metasomatic alteration of ultramafite in carbonate rocks played a major role in the nucleation and propagations of deformations. Mineralogical, and structural variations in the damage zone accompanied by the replacement of serpentine by crystalline carbonate rocks, caused important variations in rheological characteristics of the rocks, and evidently influenced the permeability and strenght of the deformed rocks. For what concerns the level of carbonate-coated grains within the fault core, we relate its development to cycles of seismic events; during the fluid pressure build up stage, the radial coarse texture developed, whereas during the fluid circulation stage, the grains developed their laminated texture. We suggest that the deposition of amorphous or colloform silica is related to the boiling of fluid, in response to seismic activity and the related rising in the pressure of fluid, with consequent fault opening. The quick opening of fractures or fast fault slip can trigger a drop in the fluid pressure, causing the liquid phase to istantly vaporize, with precipitation of silica gel. Furthermore, the occurrence of multiple concentric layers in the carbonated-coated grains, their variability in size, the evidence of rotation along the secondary slip surfaces and the occurrence of reworked microbreccia suggest a fault-valve behaviour, together with the seismic pumping of hydrothermal fluids. We conclude that the analyzed thrust faults were linked to paleo-seismic cycle events with interseismic and seismic periods.

Modelling viscoelastic shear zones at large strains and rotations

C. E. Schrank[1,2], A. Karrech[3], D. A. Boutelier[4] & K. Regenauer-Lieb[5]
[1]*School of Earth, Environmental and Biological Sciences, Queensland University of Technology, Brisbane, Australia (christoph.schrank@qut.edu.au)*
[2]*School of Earth and Environment, The University of Western Australia, Crawley, Australia*
[3]*School of Civil, Environmental and Mining Engineering, The University of Western Australia, Crawley, Australia*
[4]*School of Environmental and Life Sciences, University of Newcastle, Callaghan, NSW, Australia*
[5]*School of Petroleum Engineering, University of New South Wales, Sydney, Australia*

We critically examine the most common rheological model for viscoelasticity, the Maxwell model, in the context of large strains and rotations, the hallmark of shear zones in the lithosphere. When elasticity is considered in the deformation of a solid to large non-coaxial strain, particular attention must be paid to formulating the time increment of the elastic stress tensor appropriately. If a rigid-body rotation occurs, this so-called “stress rate” must vanish. Otherwise, one would obtain an unphysical change of the state of stress experienced by the rotating volume element under consideration. This objectivity requirement can be satisfied by using a frame-indifferent co-rotational stress rate. Here, we present a comparative study of homogeneous isothermal simple shear of a viscoelastic shear zone investigating three different Maxwell models: the classic small-strain model without co-rotational terms, the model with the Jaumann stress rate, which accounts for rigid rotations only, and a new model using a logarithmic co-rotational stress rate and the Hencky strain tensor. We map out the validity and usefulness of all three models over the parameter space relevant to lithospheric deformation.

We find that all models yield essentially identical results at Weissenberg numbers $W \leq 0.1$. However, at Weissenberg numbers in the interval $]0.1;10]$, significant differences occur. The small-strain model incurs a systematic overestimation of shear stresses because it ignores elastic rotations. Hence, it also entails large errors in the energy budget. The Jaumann model violates the first law of thermodynamics. It exhibits erroneous stress oscillations at $W \geq 0.1$, which lead to artificial dissipation. Therefore, it should not be used for modeling large non-coaxial deformations in geomaterials. The new logarithmic large-strain model solves these problems and provides an energetically consistent approach to modeling viscoelastic shear zones at large strains and rotations.

Transient cnoidal waves: a new model for fault-damage zones

C. E. Schrank[1,2], M. Veveakis[3,4], T. Poulet[3,4] & K. Regenauer-Lieb[3]
[1]*School of Earth, Environmental and Biological Sciences, Queensland University of Technology, Brisbane, Australia (christoph.schrank@qut.edu.au)*
[2]*School of Earth and Environment, The University of Western Australia, Crawley, Australia*
[3]*School of Petroleum Engineering, University of New South Wales, Sydney, Australia*
[4]*CSIRO Mineral Resources, North Ryde, Australia*

Fault-damage zones constitute a wide halo of deformation bands around the principal-slip zone of faults and make up the largest portion of their volumetric footprint. They attract significant research interest because [a] they provide important information on the history of the host fault and the conditions during fault growth/slip, and [b] they affect the mechanical and transport properties of the damaged rock volume. Fault-damage zones typically display a characteristic pattern of deformation bands: band density decreases non-linearly with increasing distance to the fault core. Here, we propose a new model for the formation of fault-damage zones based on transient cnoidal waves.

It has been postulated recently that solids with internal mass transfer processes governed by a Fickian-type gradient law can exhibit localised volumetric instabilities under certain loading conditions. Rocks belong to this class of solids. Common geological examples of such internal mass transfer include Darcy flow, partial melting, grain crushing, or dehydration reactions. According to the cnoidal-wave hypothesis, such solids form strictly periodic instabilities at steady state under two conditions: [1] the interconnected strong phase of the specimen relaxes a pressure load about ten times faster than the weak phase, and [2] the volumetric inelastic rheology of the solid skeleton is non-linear, i.e., the stress exponent $n > 1$. When a fault slips, one can envisage that a sudden decaying pressure load is generated. Moreover, the associated deformation bands generally show inelastic volumetric deformation. Therefore, we hypothesise that fault-damage zones are the physical expression of transient cnoidal waves. In other words, the deformation bands of the fault-damage zone nucleate as volumetric inelastic instabilities in the wake of a transient viscoplastic p-wave. Their subsequent growth and interaction is then controlled by the slower viscoplastic s-wave.

Here, we first introduce some general properties of numeric solutions to the transient cnoidal wave. Then, we proceed to test our hypothesis by examining a natural fault-damage zone in porous siliciclastic rocks and fitting the spatial distribution of deformation bands within it with the transient solution. Our model reproduces the geometry of the examined damage zone very well. Moreover, the associated microstructures and independent measurements of the relevant rock transport and mechanical properties are consistent with the proposed model. Some surprisingly simple scaling laws relating damage-zone geometry to overpressure and material properties are presented. Hence, cnoidal waves have the potential for developing new tools for the deciphering of fault-slip evolution and seismic history and the inversion of material properties.

Fault core microstructures and resulting implications for faulting mechanisms of the Alpine Fault, New Zealand

B. Schuck[1], A. M. Schleicher[2], C. Janssen[1], V. G. Toy[3], & G. Dresen[1, 4]
[1]*Section 4.2: Geomechanics and Rheology, Helmholtz-Zentrum Potsdam, GFZ, Potsdam, Germany (bernhard.schuck@gfz-potsdam.de)*
[2]*Section 3.1: Inorganic and Isotope Geochemistry, Helmholtz-Zentrum Potsdam, GFZ, Potsdam, Germany*
[3]*Department of Geology, University of Otago, Dunedin, New Zealand*
[4]*Institut für Erd- und Umweltwissenschaften, Universität Potsdam, Potsdam, Germany*

The currently locked transpressive Alpine Fault is the main structure forming the Australian and the Pacific Plate boundary within New Zealand's South Island, and exposes rocks from 35 km depth with a long-term exhumation rate of 6 – 9 mm y^{-1}. The hanging wall is composed of the Alpine Schist, transposed to mylonite within 1 km of the fault. Fractured ultramylonites and cataclasites comprise the fault's damage zone within 50 m of the fault core. The fault core is characterized by a 2 to 30 cm thick package of cataclasites and fault gouge (Toy et al., 2015). In the outcrops sampled for this study, Quaternary sediments form the footwall. In this contribution, we present microstructural, mineralogical and geochemical analyses obtained from a transect across a principal slip zone (PSZ) of the Alpine Fault exposed at the Waikukupa Slip location. The PSZ forms a thin (<5 cm) and continuous band, which can be easily distinguished from the hanging- and the footwall units. Detailed investigation of the fault gouge however, reveals a complex structure that consists of several, clearly distinguishable layers ranging in size from <1 to 2 cm. The main mineral components in the transect determined by X-ray diffraction analysis are quartz, plagioclase, calcite, chlorite, illite and mica. The mineral components do not change from the hanging-wall cataclasites to the footwall Quaternary sediments, but the amount of the individual mineral phases varies significantly. Microstructural observations conducted by high-resolution scanning and transmission electron microscopy reveal a pronounced decrease in grain size from the hanging-wall towards the PSZ. Within the PSZ, distinct domains characterized by different prevailing microstructures are identified suggesting a contribution of different deformation mechanisms including grain scale fracturing, twinning, pressure solution and sealing. The upper part of the PSZ is dominated by large (up to 1.5 cm) reworked mylonitic clasts, pulverized rigid particles (down to around 100 nm) such as quartz, chemical alteration of feldspars with newly formed phyllosilicates (e. g. illite) and local concentration of calcite veins. The lower part of the PSZ is dominated by µm-sized particles and potentially reworked gouge clasts (up to 0.5 cm). Several vein generations are identified by cross-cutting relationships. The veins form a dense and anastomosing network in the basal portion of the gouge and consist of very fine-grained calcite crystals. The principal slip zone currently acts as an impermeable hydraulic seal (Menzies et al., 2016). However, our investigations imply that the PSZ served as a conduit for large quantities of Ca-rich fluids circulating within the fault gouge. Fluid flow pulses resulting in formation of several vein generations represent significant mass transfer and episodes of dilatant fracturing and healing within the PSZ.

Menzies, C.D., Teagle, D., Niedermann, S., et al. (2016): The fluid budget of a continental plate boundary fault: Quantification from the Alpine Fault New Zealand. – Earth and Planetary Science Letters 445: pp. 125 –135.
Toy, V.G., Boulton, C., Sutherland, R., et al. (2015): Fault rock lithologies and architecture of the central Alpine Fault, New Zealand, revealed by DFDP-1 drilling. – Lithosphere 7: pp. 155 – 173.

The deformation record of the HP-LT metamorphic lowermost tectonic units of the Cretan nappe pile in the Talea Ori

L. Seybold[1] & C.A. Trepmann[1]
[1]*Department of Earth and Environmental Sciences, Ludwig-Maximilians University, Munich, Germany, (claudia.trepmann@lmu.de)*

The lowermost tectonic units of the Cretan nappe pile are exposed in the Talea Ori mountains at the central northern coast of Crete, Greece. There, high-pressure low-temperature metamorphic rocks of the Bali and Rogdia formation occur to the north of the overturned lowermost carbonatic formations of the Talea Ori unit. The structural position of these units has been discussed controversially. Here we present a new structural mapping and a meso- and microstructural characterization of these rocks.

The Bali formation is characterized by a conspicuous black quartz conglomerate, black metasandstones, black slates and black metachert. The siliciclastic components in the conglomerate and sandstones partly stem from local sources, i.e. rocks that crop out in the Bali formation (metachert, slate, metasandstone) as well as rocks that crop out in the Rogdia formation (albite-gneiss, metavolcanics) but many pebbles stem from a source that is not exposed in the Talea Ori (black vein quartz). The rocks of the Bali formation merge gradually into interlayered phyllites, quartzites, albite-gneisses and chloritoid-schists of the Rogdia formation. In both formations, shear zones are abundant that are characterized by a prevalent slaty cleavage, extensional shear bands, a locally developed crenulation cleavage, kink bands and abundant quartz veins that are associated to the ductile deformation of the rocks. The vein quartz microstructures are locally showing micro-shear zones, short-wave-length undulatory extinction and localized recrystallization, suggesting high-stress crystal plastic deformation at temperatures of about 300-350°C.

Our field data support the interpretation that the carbonate-dominated formations of the Talea Ori unit form a large-scale anticline with overturned limb dipping to the north and fold axis plunging to the east. The Bali formation occurs likewise to the north of the overturned carbonatic formations of the Talea Ori unit and within the center of the anticline. The contact to the carbonatic formations of the Talea Ori unit is mostly characterized by steeply dipping normal faults and extensional shear bands with the northern block being down faulted but also concordant contacts are found. Fold axes are typically oriented WE and NS and foliations in the whole working area of the Talea Ori are unanimously dipping to the north and north east, with systematic variations consistent to the large-scale anticline structure.

These observations imply that the Bali and Rogdia formations are at least structurally occurring below the carbonate-dominated formations of the Talea Ori unit. Furthermore, we suggest that the Rogdia formation is representing the base of the Bali formation, given the lithologically gradual contact to the Bali formation, the fact that no major fault plane is visible in the field and the observation that one source of clastic components of the Bali metasediments is provided by the Rogdia formation. This finding has important implications, as the base of the Talea Ori unit is constituted of the lowermost units of the Cretan nappe pile and its basement has been unknown so far. The units structurally below the carbonate-dominated Talea Ori formations provide information on the original substratum and the conditions of detachment from it. Further geochronological data are needed to constraint the age relations of the formations and their paleogeographic significance.

The long path to steady state: Transient microstructures in the crust and upper mantle

P. Skemer[1], A. Cross[1], & Y. Boneh[1]
[1]*Department of Earth and Planetary Sciences, Washington University in St. Louis, St. Louis, USA*
pskemer@wustl.edu

Deformation microstructures provide evidence for specific microphysical processes and represent an important link between rock deformation experiments, field-based geological studies, and geophysical observations and theory. However, microstructural evolution is complex, reflecting the numerous feedbacks between deformation and recovery processes. Many geophysical interpretations assume that microstructures in nature are near steady-state. For example, the interpretation of seismic anisotropy in terms of mantle flow patterns is generally predicated on the assumption that the crystallographic preferred orientation (CPO) of olivine rapidly orients itself to reflect the kinematics of flow. However, several recent studies have shown that microstructural evolution, including CPO, grain-size, and phase mixing, may occur slowly over long increments of strain history. These observations, amongst others, suggest that there are long transient intervals between changes in the deformation conditions, kinematics, or mechanisms, during which microstructure and rheology continuously evolve. Hence, care must be taken when constructing geophysical models or inversions that depend in some way on microstructure. This presentation will include recent results from large strain, high pressure and temperature rock deformation experiments that constrain the conditions required to achieve microstructural and rheological steady state.

Fault zone architecture and deformation mechanisms of a normal fault in poorly lithified sediments, Miri (Malaysia)

S. Sosio de Rosa[1], Z. Shipton[1], R. Lunn[1], Y. Kremer[1] & T. Murray[2]
[1]Civil and Environmental Engineering, University of Strathclyde, Glasgow, UK (silvia.sosio-de-rosa@strath.ac.uk)
[2]FaultSeal Pty Ltd, Sydney, AU

Normal faults studied in Miri offer unprecedented 3D along-strike and sub-vertical exposure due to the clearing of an area of land of 1 km^2. Such an extensive along-strike exposure is very rare, but permits analysis of detailed along-strike variation in fault properties, and the impact this can have on hydraulic properties. The hydraulic behaviour of faults at depth plays an important role in the exploration and production of hydrocarbons, as well as in several other subsurface engineering applications. Faults can act as conduits, barriers and combined conduit-barrier systems to fluid flow, and their overall bulk hydraulic behaviour is strongly determined by the internal fault zone architecture.

The object of this study is a set of normal faults that cut poorly consolidated deltaic sandstone-shale sediments of the Baram Delta. The aim is to investigate the highly variable nature of 1) the architecture of the fault and 2) the properties of the deformation elements. In the study area the succession is dominated by sand beds, with some interbedded clay-rich beds 0.2-2 m thick. The outcrop contains a major fault trending ENE-WSW and dipping south. It is not possible to correlate any bed from the footwall to the hanging wall because the main fault displaces the entire exposed stratigraphy, therefore only the minimum offset is constrained by the thickness of the hanging wall (>20 m). The large fault is associated with a conjugate set of normal faults with the same trend dipping NNW and SSE at 45-70°.

The damage zone of the major fault is characterised by deformation bands, zones of shear and folding. The damage zone also contains fractures that postdate the faulting. The fault core is composed of dark grey, foliated clay. The foliation is marked by white sandstone lenses embedded in the matrix and elongated sub-parallel to the fault core edges. Key observations are related to the along-strike thickness (1 cm - 80 cm) and clay content (<5% - 90%) variability of the fault core. Six areas that could represent cross-fault pathways have been identified over the 85 m of fault exposure. Three of these are due to the thinning of the clay-rich fault core to less than 2 cm, while in the other three areas the clay gouge is interrupted, resulting in sand-on-sand juxtaposition. The fault core thickness variation is influenced by stratigraphic changes (bed composition and thickness) and by secondary shears (riedel shears).

Microstructural analysis of the samples collected in Miri show particulate flow as the dominant deformation mechanism, combined with minor cataclasis, pressure-solution and growth of authigenic clays. Both the secondary shear zones and the fault core are dominated by compositional banding driven by grain rotation and rearrangement, while there is no evidence of mixing at the grain scale.

The fault core thickness doesn't track linearly with throw, but it relates to the host rock composition. The average core thickness, 17 cm, would poorly represent the true thickness and the related hydraulic properties of the fault as these are mostly influenced by the six areas of thin clay gouge and sand-on-sand juxtaposition.

Deformation-resembling microstructure created by fluid-mediated dissolution-precipitation reactions

L. Spruzeniece[1], S. Piazolo[1,2] & H.E. Maynard-Casely[3]
[1]*Department of Earth and Planetary Sciences, Macquarie University, Sydney, Australia*
[2]*now at: School of Earth and Environment, University of Leeds, Leeds, UK*
[3]*Bragg Institute, Australian Nuclear Science and Technology Organisation, Lucas Heights, Australia*

Deformation microstructures are widely used for reconstructing tectono-metamorphic events recorded in rocks. In crustal settings deformation is often accompanied and/or succeeded by fluid infiltration and dissolution-precipitation reactions. However, the microstructural consequences of dissolution-precipitation in minerals have not been investigated experimentally. Here we conducted experiments where KBr crystals were reacted with a saturated KCl-H_2O fluid. The results show that reaction products, formed in the absence of deformation, inherit the general crystallographic orientation from their parents, but also display a development of new microstructures that are typical in deformed minerals, such as apparent bending of crystal lattices and new subgrain domains, separated by low-, and in some cases, high angle boundaries. Our work suggests that fluid-mediated dissolution-precipitation reactions can lead to a development of potentially misleading microstructures (Spruzeniece et al. in press). We propose the following set of criteria, which may help in distinguishing such microstructures from the ones that are created by crystal-plastic deformation:

(1) highly irregular and discontinuous subgrain- and grain boundaries;
(2) no correlation between the main crystal lattice orientations and grain boundary orientation;
(3) low angle boundaries and grain boundaries that are dominantly perpendicular to the reaction front;
(4) wide range of rotation axes orientations even within the same (sub-)grain boundary segment;
(5) irregularly shaped and “patchy” subgrains;
(6) differing rotation axes distribution and slip system solutions in corresponding parents and reaction products, even when microstructures seem visually similar;
(7) elevated MAD values at larger angles on a subgrain scale.

Although none of these features on its own can be a definite proof that the microstructure is generated by fluid-mediated dissolution-precipitation reactions, in their combination these features are distinct from crystal plastic deformation-generated microstructures.

Reference:
L. Spruzeniece, S. Piazolo, and H. E. Maynard-Casely (2017) Deformation-resembling microstructure created by fluid-1 mediated dissolution-precipitation reactions, *Nature Communications 8,* DOI: 10.1038/ncomms14032

Rheological effects of retrograde hydrous mineral assemblages; Insights from the Kuckaus Mylonite Zone, Namibia

C. Stenvall[1], Å. Fagereng[1], J. Diener[2] & C. Harris[2]
[1]*School of Earth and Ocean Sciences, Cardiff University, Cardiff, UK (stenvallca@cardiff.ac.uk)*
[2]*Department of Geological Sciences, University of Cape Town, Cape Town, South Africa*

Shear zones active during retrograde metamorphism, in fluid-present conditions, may experience growth of hydrous lower grade mineral assemblages. What effects do these minerals have on the strength, and rheological evolution of the shear zone? To address this question we present observations from the Kuckaus Mylonite Zone (KMZ), Namibia, a mid-crustal strike-slip shear zone which deformed granitoid gneisses and migmatites at amphibolite- to greenschist-facies conditions (2.7-4.2 kbar, 450-480°C), 40 Ma after granulite facies peak metamorphism (5.5 kbar, 825°C,1065-1045 Ma).

Detailed mapping of the KMZ shows irregularly spaced, anastomosing, thin (10s of cm) ultramylonites, traceable for at least 5 km along strike, within wider mylonite/protomylonite zones localised in previously migmatised host rocks. Transects across these bands reveal a fairly consistent mineralogy of approximately 60% feldspars, 25% quartz, 10% mica and 5% opaques and trace minerals. The protomylonite shows incipient alignment of phyllosilicates, forming interconnected weak layers in places. The K-feldspars range in size and are mostly highly fractured, although in strain shadows synkinematic recrystallization of K-feldspar is apparent. These small grains, together with other newly-formed metasomatic minerals, are smeared out into long tails that extend from the K-feldspar porphyroclasts. In the mylonites the percentage of plagioclase and trace minerals increases slightly. Here, the K-feldspar porphyroclasts have decreased in size and number, and the remaining mineralogy has formed a well-mixed matrix with a fairly uniform fine grain size (<50µm). The phyllosilicates in the mylonites are weakly interconnected. This interconnectivity is, however, not present in the ultramylonite, where all constituent minerals of the rock form a fine grained (<20µm) homogeneous mixture with a porosity of 5-8%. In the ultramylonites, plagioclase makes up half of the feldspar content, and there are no more K-feldspar porphyroclasts. The pores and minerals all display a shape-preferred orientation parallel to foliation.

The syn-mylonitic quartz vein $\delta^{18}O$ values (-1.2‰ to +11.6‰) indicate at least some involvement of meteoric fluids, and thus a permeable connection to the Earth's surface. As the host rock is nearly fluid absent, a local metamorphic fluid source is unlikely, and such a fluid would also generate higher $\delta^{18}O$ values. Isocon transects, assuming immobility of aluminium, give both positive and negative mass changes of <10% across the high strain zones. With the decrease in alignment and interconnectivity of phyllosilicates from mylonite to ultramylonite, and increased abundance of newly-crystallised fine grained phases, we suggest a switch to have occurred in the dominant weakening mechanism, from the alignment of phyllosilicates to activation of diffusional processes, assisted by pinning and phase mixing. Sustained weakening and strain localisation by these mechanisms would then have ensued, with the porosity in the ultramylonite retaining permeability for fluid flow. This switch in weakening mechanism also implies rheological changes. In the wall rock the strength lay in the load bearing framework consisting of strong K-feldspar. The development of interconnected networks of weak phyllosilicates then reduced the strength in the protomylonite and mylonite. In the presence of fluids, the fine grained ultramylonite, deforming by diffusive deformation mechanisms, constituted the weakest state. Therefore we conclude that retrograde shear zones, in fluid-present conditions, are strain softening.

Metasomatism, brecciation and slip dynamics in ultramafic-quartzofeldspathic shear zones: The Livingstone Fault, New Zealand

M.S. Tarling[1], S.A.F. Smith[1] & J.M. Scott[1]
[1]Department of Geology, University of Otago, 360 Leith Street, 9016 Dunedin, New Zealand (tarma723@student.otago.ac.nz)

The slab-mantle wedge interface in subduction zones is an area of important dehydration, hydration and metasomatic reactions that are thought to play a significant role in subduction dynamics. High fluid pressures in the fore-arc crust and mantle have been invoked as one possible explanation for deep slow slip and tectonic tremor. However, opportunities to study the geology of this portion of subduction zones are limited, and the specific mechanisms that might explain behaviour such as slow slip and tremor remain largely unknown.

The >1000 km long Livingstone Fault in New Zealand juxtaposes mantle peridotite and serpentinite against quartzofeldspathic schists and metavolcanics, providing a suitable analogue for the shallow slab-mantle wedge interface. Temperature constraints from metamorphic assemblages and metasomatic reactions suggest that faulting occurred at c. 300-350 ˚C. The fault is characterized by a zone of foliated serpentinite mélange tens to several hundreds of meters wide with well-defined scaly fabric, entraining ≲ 25-m long pods of massive serpentinite, rodingite and schist. Metasomatic reactions between serpentinite and schist at the fault and pod margins resulted in the sequential formation of talc and tremolite. Modelling indicates that such reactions could produce up to 25 vol.% hydrous fluids. Widespread networks of tremolite ‘crackle’ breccias cutting across the foliation, some of crack-seal type, suggest that fluid overpressures were repeatedly obtained within the foliated serpentine melange. Interacting with the crackle breccias are discrete cataclastic slip surfaces that occur along the margins of entrained pods within the melange. Significantly, slip surfaces that extend in to the foliated serpentinite show evidence (from sub-micron Raman mapping) for highly localized (<200 μm) serpentinite dehydration reactions, forming nanocrystalline olivine and a talc-like intermediate phase. Our observations point towards a mixed fault zone rheology dominated by long-term, pressure-solution-mediated creep within the serpentinite mélange. This was punctuated by repeated and energetic brecciation events triggered by high fluid pressures derived from metasomatic reaction, as well as localized shear failure possibly at seismic velocities.

Sub-micron Raman Spectroscopy analysis of pressure-solution microstructures in scaly serpentinite: the Livingstone Fault, New Zealand

M.S. Tarling[1], J.S. Rooney[2], S.A.F. Smith[1] & J.M. Scott[1] & K.C. Gordon[2]
[1]Department of Geology , University of Otago, 360 Leith Street, 9016 Dunedin, New Zealand (tarma723@student.otago.ac.nz)
[2]Department of Chemistry, University of Otago, Union Place West, 9016 Dunedin, New Zealand

In many geodynamic settings (e.g. subduction zones, mid-ocean ridges, oceanic transform faults, continental strike-slip faults) pressure-solution-mediated creep in serpentinite has been invoked as an important deformation mechanism. However, characterising the microstructures of serpentinite-bearing fault rocks is particularly challenging: conventional analytical techniques such as optical microscopy, quantitative XRD and SEM–EDS often fail to correctly identify the serpentine varieties (antigorite, chrysotile, lizardite and polygonal/polyhedral serpentine), and lack sufficient resolution to elucidate the often complex intergrowths and replacement textures that occur at the sub-micron scale. Transmission electron microscopy (TEM) has been used successfully, but complex sample preparation and very small sample sizes (1-10's microns) in TEM analysis means that microstructural context is difficult to maintain.

We present new methods of sub-micron Raman Spectroscopy mapping that unambiguously distinguish the main serpentine minerals within their microstructural context. The high spatial resolution (~360 nm), large-area coverage (100's of µm to ~mm scale) and ability to map directly on polished thin sections allows us to examine the key features of scaly serpentinites (e.g. dissolution seams, mineral growth in pressure shadows, distribution of serpentine varieties) and relate these features to the geometric development of anastomosing schistosity. Examples presented here inform our understanding of the spatial and temporal evolution of pressure-solution creep in serpentinite.

Mountain belts formed after rift basins

A. Teixell[1]
[1]*Dept. de Geologia, Universitat Autònoma de Barcelona, 08193 Bellaterra, Spain (antonio.teixell@uab.cat)*

A review of the characteristics of mountain belts derived from the inversion of rift basins is presented on the basis of lessons from the well-documented examples of the Pyrenees, the Atlas Mountains and the Eastern Cordillera (EC) of the Colombian Andes. These examples encompass former rifts formed by break-up of continental interiors or in back-arc settings. The pre-existing extensional structure influencing the orogenic development includes not only normal faults but also diapirs and salt walls in the common case of the occurrence of pre- or early syn-rift salt. A significant fraction of the observed folding structure may have been produced previous to the orogenic contraction by extensional salt tectonics. Thin and thick-skinned contractional deformation styles coexist depending on the role of fault inversion or the activation of efficient decollement levels. In the case of the Atlas and the EC, less shortened than the Pyrenees, sedimentary and thermochronogic data provide information to resolve the progression of compressional deformation within the rift basin infill. Early orogenic shortening localized in the rift interior, preferentially in weak salt structures when present. This shortening led to hardening and subsequent propagation of the deformation to the rift basin margins, accommodated by large-displacement fault inversion. Major crustal thickening was then acquired, which is recorded by rock uplift and changes in river geomorphological signature. A transient topography is preserved in the form of low-relief axial plateaus with old longitudinal river tracts flanked by steep belts with strongly incised transverse river valleys.

The case of the Pyrenees illustrates a more mature inverted rift with massive thrust stacking from the rift shoulders and a two-sided topographic wedge profile, with strong basement exhumation. Good deep-seismic coverage (reflection, wide-angle, receiver functions) encourages section balancing attempts at the crustal scale, providing a case for apparent differential shortening at different levels of the crust. These differences can be explained in terms of the precursor rift lithospheric architecture. The first stages of rift closure involved subduction of a central exhumed mantle tract and the shortening and pop-up expulsion of the sedimentary lid above. Crustal (basement) shortening does not account for the total magnitude of convergence, which is more closely approximated by detailed sections in the sedimentary cover where preserved, as in the west-central Pyrenees. In addition, seismic images of the lower crust and Moho (offset by thrust faults) imply even lower shortening at this level, which seems to be due to lower crustal removal during pre-orogenic hyperextension. Even in cases like the Atlas where the precursor rift was presumably entirely continental and two separate margins cannot be defined, a recent wide-angle seismic survey indicates as well an offset Moho discontinuity with a root of underthrust lower crust, although wide-angle data cannot resolve the amount of offset and shortening at that level.

In addition to crustal thickening, dynamic topography in inverted intracontinental rifts may be enhanced by the impingement of mantle thermal plumes in plate interiors, as is the case of the Atlas Mountains in the NW African plate. Relatively limited amounts of orogenic shortening and small lithospheric roots make in such cases unlikely the processes of delamination or slab detachment that are often invoked to account for high topography coupled with thin lithosphere in plate-boundary collisional belts.

Anisotropy of elasticity and its role in plastic deformation of minerals

N. Timms[1], D. Healy[2], & M. Pearce[3]
[1]*Department of Applied Geology, Curtin University, Perth, Australia (n.timms@curtin.edu.au)*
[2]*School of Geosciences, University of Aberdeen, Aberdeen, UK*
[3]*CSIRO Mineral Resources, Perth, Australia*

Minerals respond elastically before brittle or ductile yield, and elastic behavior influences the nature of inelastic strain in many materials. Yet, there are very few studies that quantify these relationships in rock-forming minerals. All minerals exhibit directional variations (anisotropy) of elasticity that is governed by their intrinsic lattice structure, the same crystal structure that governs crystal-plastic deformation. Different aspects of elastic behavior, i.e. relationships among different elastic stresses and strains, are commonly represented by Young's modulus (*E*), shear modulus (*G*), and Poisson's ratio (*v*), all of which can be highly anisotropic in minerals of all crystal systems. This anisotropy of elasticity is well described mathematically by 4th rank tensors of stiffness or compliance, however visualisation of these tensors is challenging. In this study, we investigate the relationships between elastic and plastic deformation responses of rock forming minerals, enabled by new calculations and visualisations of elastic anisotropy via open source toolbox of MATLAB scripts – AnisoVis. By way of a case study, we investigate the common accessory mineral zircon ($ZrSiO_4$), principally due to its importance in geosciences as a geochronometer, but also because it is known to deform in tectonic and shock conditions, and it can accumulate radiation damage that alters its intrinsic properties. The deformation of zircon by various mechanisms, including brittle fracture, dislocation creep, twinning, and transformation to a high-pressure polymorph (reidite), is preceded by elastic behaviour. Importantly, these deformation mechanisms of zircon can facilitate the resetting of zircon's radiometric clock by variable degrees. This study presents new visualisations of the anisotropy of elastic properties of zircon as a function of radiation damage and pressure, and investigates the links between elastic properties and deformation microstructures in zircon (Timms et al., 2017). Zircon is highly anisotropic in *E, G* and *v* elasticity. Anisotropy of *E*, *G*, and *v* decreases by radiation damage and increases with pressure from 0 to 24 GPa, with a peak in elastic stiffness at ~8 GPa. A switch in dislocation line energy factor K could indicate that (001)<100> dislocations are energetically more favourable than {100}<010> above ~17 GPa. Shock twinning of zircon occurs via plane of invariant shear K_1 = {112} and shear direction η_1 = <111>, which corresponds to the lowest values of $G_{<111>}$ (~98 GPa) and *v* (≈ 0) in zircon. Minima in $G_{<111>}$ at ~4 and ~16 GPa could indicate favourable pressures for twinning. Reduction of *E* and *G* associated with radiation damage inhibits the development of reidite lamellae during shock metamorphism because sufficient pressures to permit phase transformation cannot be supported, which is consistent with observations from naturally-shocked zircon grains.

By providing the ability to readily calculate and visualise directional variations elastic properties, and given that elasticity data are available for most minerals, we open up new possibilities to develop our understanding of the deformation of minerals and rocks.

References:
Timms, N.E., Healy, D., Erickson, T.M., Nemchin, A.A., Pearce, M.A., Cavosie, A.J., 2017. Role of elastic anisotropy in the development of deformation microstructures in zircon. In: Moser, D., Corfu, F., Reddy, S., Darling, J., Tait, K. (Eds.), AGU Monograph: Microstructural Geochronology; Lattice to Atom-Scale Records of Planetary Evolution. AGU Wiley (in press).

Re-interpretation of the INDEPTH deep seismic profiles (Himalaya)

T. Torvela[1], D. Grujic[2], J. Moreau[3] & G. Hetényi[4]
[1]*School of Earth and Environment, University of Leeds, UK (t.m.torvela@leeds.ac.uk)*
[2]*Department of Earth Sciences, Dalhousie University, Halifax, Canada*
[3]*Independent Researcher, Durness, UK*
[4]*Institute of Earth Sciences, University of Lausanne, Switzerland*

The project INDEPTH (INternational DEep Profiling of Tibet and the Himalaya) was an interdisciplinary programme led by the Cornell University. Its first two stages in 1992-1995 imaged the deep crust of the Himalaya and southern Tibet, using seismic reflection. The interpretations and models published by the INDEPTH working group have been fundamental for understanding the overall structure of the mountain belt. The INDEPTH data remain the only deep crustal seismic reflection images from the area, a situation that is unlikely to change in the foreseeable future.

Crustal seismic data, including INDEPTH, are conventionally interpreted by connecting strong amplitudes of distinct reflections. The connected strong reflections are interpreted as geological boundaries that may or may not be structural in nature. At the same time, many structural boundaries within the crust lack the acoustic impedance contrast to produce sufficient reflectivity. As a consequence, relying on interpretation of strong reflections only allows for partial interpretation of the data. The interpretation can be enhanced by including the distributed reflection patterns throughout the seismic image in the interpretation. These patterns can be analysed and emphasised with seismic attributes. The development of seismic interpretation software has made it possible to easily combine the pattern interpretation method with pattern enhancement, and to map the interpreted pattern distributions in 3D. We use the method of pattern interpretation to gain more detailed information from INDEPTH data, and to produce a new structural interpretation of the Himalaya and southern Tibet.

The new interpretation shows several enhancements to the previous large-scale interpretations. For example, the Kangmar Dome metamorphic “core complex” is associated with a hanging-wall fold above a thrust sheet. Furthermore, there are no indications that the much-debated South Tibetan Detachment. is the same extensional structure at Wagye La (just south of the Kangmar Dome) as at Zherger La (at the southern margin of the Tethyan Himalaya). These and other details of the new interpretations may challenge some aspects of the present tectonic models for Himalaya.

Style and distribution of deformation in partially molten continental crust

T. Torvela[1], A. L. Lee[1] & S. Coyle[1]
[1]*School of Earth and Environment, University of Leeds, UK (t.m.torvela@leeds.ac.uk)*

The syntectonic presence of granitic melt is widely believed to weaken the continental crust: already very small melt fractions have been modelled to induce a drastic strength drop and localize deformation. This is exemplified by e.g. the “channel flow” model by which ductile middle crust can extrude from beneath orogenic plateaux such as Tibet due to melt-enhanced weakening processes. However, very little is known about many key parameters that govern the rheology of the partially molten crust and, consequently, how it accumulates deformation in space and time. What is the longevity of the partial melts? How are they distributed? How much remains *in situ*, and how much is transported elsewhere? How does this transport happen and how fast? What other factors apart from melts control the crustal rheology and strain distribution? Without sufficiently reliable answers to these questions, the channel flow model, and more generally the behaviour of the partially molten crust during orogenesis, remain highly controversial.

The effect of syn-orogenic partial melts on deformation can be studied at outcrops of the exhumed parts of many orogens, both modern and ancient. Many studies address the deformation patterns in migmatites, the once-partially molten rocks typically found in middle and lower crust of orogens, while others look into detailed effect of e.g. shearing to melt distribution and transport. Few studies to date attempt to span all observation scales to address the potential linkages between migmatitic microstructures, outcrop patterns, and crustal-scale deformation patterns. This multi-scale approach may help to better understand how deformation is distributed in partially molten rocks.

We have studied two migmatitic regions: the Late-Svecofennian Granite-Migmatite belt of southern Finland, and the Western Gneiss Region, central Norway. Our microstructural, outcrop, and regional investigations show that deformation of a migmatitic continental crust is widely distributed and controlled chiefly by folded domains separated by steep shear zones. This appears to be true at a variety of scales. On the other hand, crustal-scale steep shear zones seem to be commonly very long-lived. Their inception predates the partial melting, but, equally, they continue to accumulate strain long after the partial melting and the associated deformation within the orogenic core has ceased. This suggests that pre-existing crustal architecture may play a more important role in localizing crustal-scale deformation than partial melting.

Sandstones along thrusts: their origins and implications

Y. Totake[1,2], R.W.H. Butler[1], C.E. Bond[1], D. Iacopini[1] & A. Aziz[3]
[1]Department of Geology and Petroleum Geology, University of Aberdeen, Aberdeen, UK (yukitsugu.totake@abdn.ac.uk)
[2]Technical Resources Unit, INPEX CORPORATION, Tokyo, Japan
[3]Resource Exploration Department, PETRONAS, Kuala Lumpur, Malaysia

Architectures of faults, or fault zones, are seldom simple – unlike single lines frequently drawn on seismic or geological sections. Fault zones mostly comprise many structural components and form complex structures that influence fluid flow within the fault zones and surrounding area. There is a high demand to characterise the complex architecture of fault zones to predict fault hydraulic properties, e.g. in exploration of hydrocarbon. Fault characterisation is, however, commonly challenging and requires a multi-disciplinary observations. In this contribution, we present a case study for better understanding a thrust zone developed through deep-water sequences, utilising seismic data, well information and field examples.

We report a thrust zone penetrated by a hydrocarbon exploration well in the slope of the NW Borneo margin, Malaysia, a region with a Neogene deep-water sandstone-shale sequence deformed into a fold-thrust belt. The presence of the thrust was known prior to the drilling based on good-quality 3D seismic data. The thrust fault was interpreted along a distinctive seismic reflector, showing positive acoustic impedance, which separates pre-growth horizons. Post-well evaluation reveals this seismically imaged thrust is correlated to an interval which is composed of a top-most shale unit, cut by calcite veins, and underlying two massive sandstones separated by shales; the upper and the lower sandstone is 28 m and 26 m in thickness, respectively. The positive-impedance reflector of the thrust zone is attributed to these sandstones. The reflector lies between pre-growth sandy horizons along the thrust zone, up-dip extent of the reflector enlarges with the thrust displacement. Based on these observations, the sandstones are interpreted as fault slices entrained along the thrust zone. Pore pressure profiles predicted from wireline logs show that the sandstones form a pressure baffle today, but it may once have acted as a fluid conduit, as indicated by abundant calcareous cements in the sandstones and calcite veins in shales.

The detailed architecture of the thrust zone in the subsurface is beyond seismic resolution, so we use field examples from the Western Champsaur Basin, SE France, as an analogue for the likely complexity in fault architecture along the thrust. This is part of the fore-deep Alpine basin, filled by Oligocene turbidites which have been deformed into fold-thrust arrays. The thrust zones, decorated by sandstone horses, are well observable. These sandstone slices are commonly cut by discrete thrust segments, postdating the folds in hangingwalls and footwalls. Some thrusts terminate in shaly units. These observations imply that a thrust zone in a well-layered sequence is formed through kinematic process controlled by the mechanical interaction between competent and incompetent units. We suggest that discrete, non-collinear thrust segments are developed around hard sandstone units, with separations at weak shaly units, during or after folding. With increasing strain, these thrust segments may become linked across shale layers. This model applies well to the subsurface example from the offshore Malaysia. These processes, increase the chance for sandy layers isolated in shaly units to evolve into fault slices. This could increase permeability across the thrust zone with enhanced sand-sand juxtaposition, and hence may influence the formation of hydrocarbon accumulations or mineral deposits. It is therefore important to consider the impact of local stratigraphy on fault zone evolution and final complexity, especially in multi-layered settings.

Striation and slickenline development on quartz fault surfaces at crustal conditions: origin and effect on friction

V. Toy[1], A. Niemeijer[2], F. Renard [3], L. Morales[4,5] & R. Wirth[5]
[1]*Department of Geology, University of Otago, Dunedin, New Zealand (virginia.toy@otago.ac.nz)*
[2]*Utrecht University, The Netherlands*
[3]*Department of Geosciences, PGP, University of Oslo, Norway, and ISTerre, University Grenoble Alpes, Grenoble, France*
[4]*ScopeM, ETH Zürich, Switzerland*
[5]*GeoForschungsZentrum Potsdam, Germany*

Fragments of optically flat silica discs embedded in synthetic gouge were deformed to examine the relationship between the development of striations and slickenlines, and deformation mechanisms, conditions, and fault rheology. Experiments were performed under hydrothermal conditions in a rotary shear apparatus at 100 or 450°C, to shear strains of $2.02<\gamma<8.25$. Slip hardening and softening prevail at low and high temperatures, respectively. In recovered samples, disc fragment surfaces are decorated by fine gouge, sometimes arranged in trails, pits, and scratch marks. Prominent grooves – inferred slickenlines – with constant orientation, wavelength <10μm and amplitude <0.7μm are only observed on disc fragments deformed at 450°C. Some parts of the grooves below the original disc fragment surface contain scattered rounded beads of silica ~200nm diameter. Conversely, close examination of pits in 100°C experiments reveals they contain angular particles <2μm diameter. 200nm diameter crystalline quartz can precipitate at 450°C in only 250 seconds, well within the timeframe of the experiments but precipitation at 100°C would take at least 8 years. No systematic dislocation arrays were observed in the quartz disc fragments, but microfractures are sporadically present. This indicates that at both temperatures brittle failure generated microfractures and micro-comminution occurred where gouge particles impacted disc fragment surfaces. These observations suggest formation of silica beads by precipitation from amorphous silica facilitates slip weakening, smoothing of the fault surface parallel to the slip vector, development of undulations perpendicular to the slip vector by a pressure solution creep mechanism, weakening, and maintenance of a constant slip direction. Extrapolation of the experimental conditions to nature suggests that, for major earthquakes of long duration this process would only be important at temperatures in excess of 450°C – ie. below the seismogenic zone where creep mechanisms typically dominate. However, for slower-than-seismic slip rates we expect it to be effective at lower greenschist facies conditions.

Recrystallization of quartz after low-temperature plasticity – the record of stress relaxation in different tectonic regimes

C.A. Trepmann[1], C. Hsu[1] & F. Hentschel[1]
[1]*Department of Earth and Environmental Sciences, Ludwig-Maximilians University, Munich, Germany, (claudia.trepmann@lmu.de)*

The quartz microfabrics from two shear zones in the Alps, the Silvretta basal thrust and the Defereggen-Antholz-Vals (DAV) shear zone, as well as experimental vein-quartz deformation, record that stress-loading and stress-relaxation rates play an essential role for the localization and accumulation of strain. We consider two stages for the development of localized high-strain zones: (1) stress-loading, where deformation at transient high stresses results not necessarily in a high amount of strain on sample scale, but in localized highly damaged zones enabling grain-size reduction during (2) stress-relaxation, where a high amount of strain can be accumulated, dependent on the rate of stress relaxation.

The quartz microfabrics from the two shear zones in the Alps are analyzed by polarized light and electron microscopy. The microfabrics from both shear zones record a switch from low-temperature plasticity at transient high stress to recrystallization at relaxing stresses at greenschist facies conditions. The development of new grains is dominantly by subgrain rotation and subsequent strain-induced grain-boundary migration in areas of localized high strain originally formed during initial low-temperature plasticity. The findings suggest that new grains develop at almost random crystallographic orientations at fast rates of stress relaxation (i.e. at low stress), as indicated by recrystallized quartz zones in the Silvretta fault rocks. In contrast, at slow rates of stress relaxation, new grains develop at moderately high stresses with crystallographic preferred orientation characterized by high Schmid factor for basal <a> glide, as indicated by vein quartz samples from the DAV shear zone. Both recorded histories with transient peak stresses and different rates of stress relaxation are interpreted to be related to seismic activity of the fault systems. The difference in stress relaxation rates is suggested to be correlated with the tectonic regime of thrusting for the Silvretta fault rocks and strike-slip faulting for the DAV shear zone. This study demonstrates that characteristic microfabrics provide important information about the deformation history of natural shear zones developed in different tectonic regimes.

New insights to late-Variscan geodynamic evolution of the south-western Moldanubian Zone (Bohemian Massif)

K. Verner[1,2], O. Pour[1,2], F. Tomek[3], L. Megerssa[2,4], D. Buriánek[1] & J. Žák[3]
[1]*Czech Geological Survey, Klárov 3, Prague, Czech Republic (krystof.verner@geology.cz)*
[2]*Institute of Petrology and Structural Geology, Charles University, Albertov 6, Prague, Czech Republic*
[3]*Institute of Geology and Paleontology, Charles University, Albertov 6, Prague, Czech Republic*
[4]*Geological Survey of Ethiopia, CMC Road, P.O.Box 2302, Addis Ababa, Ethiopia*

We bring new insights to Variscan tectonometamorphic evolution in the Šumava Region (southwestern Moldanubian Zone, Bohemian Massif). This area is built by high-grade paragneisses to migmatites revealing two superimposed tectonometamorphic events during Variscan orogenic processes. The first event was associated with later stages of continental collision and rapid exhumation in the Central Moldnubian Zone (~350–340 Ma), the second one with late-Variscan high-temperature, and low-pressure overprint with increasing intensity southward to the Bavarian part of the Moldanubian Zone (~ 330–320 Ma). The results of K-Ar dating indicate the cooling ages below ca 350 °C in Central Moldanubian Zone at 340–332 Ma and at 322–305 Ma in the Bavarian Moldanubian Zone. Three distinct generations of successive metamorphic fabrics were identified in this region. Relatively oldest ~W(NNW) or ~E(ESE) steeply dipping foliation was heterogeneously reworked into flat-lying compositional banding with well-developed ~N to ~NNE plunging stretching lineation. The latest overprint increasing southward is represented by formation of steeply to moderately ~NE to N dipping metamorphic foliation, often associated with ~W(NW) or ~E(SE) moderately to gently plunging lineation. These later metamorphic fabrics reveal a neutral to oblate shape of AMS ellipsoid (shape parameter T) with relatively lower values of degree of anisotropy (P in range 1.045 to 1.11). Magnetic foliations dip moderately to the NNE to NE, exhibit slightly prolate to oblate shape of AMS ellipsoid, and the associated degree of anisotropy (P) range from 1.10 to 1.15. Magnetic foliations in localized mylonite Pfahl and Danube shear zones dip steeply to the ~NNE bearing with subhorizontal ~WNW to ~ESE magnetic lineations. These mylonites show prolate to slightly oblate shape of AMS ellipsoid with stronger fabric intensity (P=1.1–1.21), which indicates the localization of deformation during final stages of regional deformation, possibly caused by similar strain field. In addition, the result of thermodynamic P-T modelling of late-Variscan overprint indicates a larger extent of retrograde reactions in the migmatites at around pressure 4–6.5 Kbar and temperature 650 to 800 °C with systematically increasing degree of metamorphism towards the south. This multidisciplinary approach allows to develop an overall model of geodynamic and tectonothermal evolution including extensive granite magmatism during post-collisional late-Variscan event in the southwestern Moldanubian Zone.

The role of fluids in the brittle-ductile transition at oceanic transform faults

J.M. Warren[1] & C. Teyssier[2]
[1]*Department of Geological Sciences, University of Delaware, Newark, DE, USA (warrenj@udel.edu)*
[2]*Department of Earth Sciences, University of Minnesota, Minneapolis, MN, USA*

Oceanic transform faults are a major category of plate boundaries, yet the mechanisms accommodating slip across the plate interface are poorly understood. The formation of hydrous phases, such as serpentine and talc, may account for the aseismic accommodation of a large proportion of the shallow strike-slip motion. Fluid circulation is assumed to end at the transition from brittle failure to ductile flow, which previous estimates placed at a depth corresponding to the 600°C isotherm. However, recent seismic observations indicate that microseismicity can extend to greater depths. This deep seismicity may indicate seawater circulation into the brittle-ductile transition on transform faults.

To assess the role of fluids in deformation at the base of the seismogenic zone, we examined peridotite mylonites from active transform faults (St. Paul, Shaka, Molloy Deep) and exhumed mantle shear zones (New Caledonia). These samples contain evidence for hydration over a wide range of temperatures, from >800°C down to 500°C. Evidence for mylonite hydration includes fluid inclusion planes in porphyroclasts that terminate at the boundary with the fine-grained matrix. This morphology suggests that micro-cracking and transient fluid circulation occur prior to dynamic recrystallization, which neoblast mineral thermometry indicates was >550°C. Hydration is also indicated by the occurrence of up to 20% amphibole in the mylonites, in the form of either tremolite (~400-700°C) or pargasite (>800°C). The occurrence of a crystallographic preferred orientation in the amphibole suggests that amphibole formed prior to or coincident with ductile deformation. Alternatively, if amphibole formed by topotactic growth, phase relations require that amphibole formed at temperatures >400°C. In either case, the abundance of amphibole and the porphyroclast fluid inclusion planes require deep circulation of seawater.

Oceanic mylonites also contain evidence for later, lower temperature fluid flow, recorded by cross-cutting serpentinite veins and fractures. As serpentine is only stable at <400°C, this provides a lower temperature limit for ductile deformation. At the localities studied, two sets of conjugate serpentinite veins occur, one utilizing the subvertical foliation plane and another at an angle of 30-50°. The shear sense is not consistent and the foliation parallel planes can record dextral or sinistral shearing, suggesting a maximum horizontal compression direction nearly normal to the shear zone. A third set of subvertical fractures, subparallel to the maximum horizontal compression, occurs at a high angle to the mylonitic foliation and may represent the fluid feeding system. Positive feedback between slip on serpentinized zones and pervasive fluid flow may make the transform zone extremely weak.

Overall, the peridotite mylonites preserve evidence for fluid circulation deep into transform faults, with hydration occurring over a wide temperature range. If cracking and fluid circulation promote the grain size reduction that leads to mylonite formation, the depth to the brittle-ductile transition may evolve over time, with mylonite formation resulting in a shallowing of the transition depth. This implies that hydration controls fault rheology at all depths, driving the occurrence of seismic versus aseismic behaviour.

Anisotropy in seismic velocity and magnetic susceptibility in antigorite-bearing serpentinite mylonites

T. Watanabe[1], K. Kawasaki[1] & K. Michibayashi[2]
[1]*Department of Earth Sciences, University of Toyama, Toyama, Japan (twatnabe@sci.u-toyama.ac.jp)*
[2]*Institute of Geosciences, Shizuoka University, Shizuoka, Japan*

Petrofabrics, elastic wave velocities and magnetic susceptibility were studied in three antigorite-bearing serpentinite mylonite samples, which were collected from the Happo ultramafic complex in the Hida Marginal Tectonic Belt, central Japan. Mylonite samples show well-developed foliation (XY-plane) and lineation (X). The foliation is made by the compositional layering, while the lineation by a mineral elongation direction. The antigorite content was 37, 61 and 80 vol.% in samples HPS-M, HKB-D and HKB-B, respectively. Antigorite CPO data show distinct concentration of b- and c-axes. The b-axes of antigorite are aligned subparallel to the lineation (X), and the c-axes perpendicular to the foliation plane. The a-axes are weakly aligned subparallel to the Y-direction. Olivine CPO data show weak concentration of axes. In samples HPS-M and HKB-B, the c-axe of olivine are aligned subparallel to the lineation and the a-axes subperpendicular to the foliation plane. On the other hand, HKB-D shows a weak concentration of a-axes parallel to the Y-direction.

Compressional- and shear-wave velocities were measured by the pulse transmission technique at ambient temperature and confining pressures of up to 180 MPa. All samples show strong anisotropy in velocity. Compressional-wave velocity is fastest in the direction parallel to the lineation, and slowest in the direction perpendicular to the foliation. The shear wave oscillating parallel to the foliation has higher velocity than that oscillating perpendicular to the foliation. Comparison between measured and calculated velocities shows that the velocity anisotropy is dominated by the CPO of antigorite.

Magnetic susceptibility was measured with Kappabridge. The mean bulk susceptibility of HKB-B (Atg: 80 vol.%) is 4.97×10^{-3}. The degree of anisotropy, which is defined by the ratio of the maximum principal susceptibility to the minimum, is 3.7, and the magnetic fabric is planar. The ratio of the intermediate principal value to the minimum is 2.2, and that of the maximum to the intermediate is 1.7. The direction of the maximum principal susceptibility is parallel to the lineation, and that of the minimum principal susceptibility perpendicular to the foliation. The anisotropy in magnetic susceptibility must be caused by the spatial distribution of magnetite grains, which reflects the history of deformation. The origin of magnetic fabric will be discussed.

Controls on fracture intensity and orientation on a plunging carbonate anticline; Sawtooth Range, Montana

H. Watkins[1], C. E. Bond[1], A. J. Cawood[1], M. Cooper[2] & M. Warren[3]
[1]*School, University, City, Country (h.watkins@abdn.ac.uk)*
[2]*Sherwood Geoconsulting Inc., Calgary, Canada*
[3]*Jenner GeoConsulting, Calgary, Canada*

The Swift reservoir anticline exposes bedding surfaces of the Upper Carboniferous Madison Formation (Castle Reef Dolomite). Outcrops reveal an asymmetric anticline with a clear north westward plunge. The anticline is located on the northeastern margin of the Sawtooth Range in Montana. The range is part of the Cordilleran Orogenic belt, and is seen as a partial equivalent to the Canadian Front Ranges further north. Outcrops from the forelimb, hinge and backlimb of the structure all contain abundant macro-scale fractures in micritic to grain supported lithologies. Fracture data from field transects is digitised from outcrop photographs, and fracture intensities are estimated using a circular scanline method. Digitised fracture traces are used to determine fracture orientation distributions at each sampling site. High resolution bedding data, collected in the field is used to construct a series of cross sections, from which a 3D model of the fold is built.

The digital 3D surface of the folded top Madison Formation is analysed to determine variations in fold curvature. We compare fracture intensity data with results from the 3D surface geometry analysis to determine how intensity varies with structural position and fold geometry. We also compare fracture intensity with lithological observations to identify any lithological control on fracture formation and variation. Results of the fracture intensity analysis are compared to determine whether structural factors, such as structural position and fold curvature, have a greater influence on fracture occurrence than lithological variation. Fracture orientation data is tied to the 3D model to analyse how fracture orientation varies across the structure, and how minor variations in surface geometry might influence the formation of different fracture sets.

Forelimb damage styles in carbonate fold-thrust structures; French Sub-Alpine Chains

H. Watkins[1], R. W. H. Butler[1] & C. E. Bond[1]
[1]School of Geosciences, University of Aberdeen, UK
(h.watkins@abdn.ac.uk)

We present an outcrop analogue study of macro-scale deformation styles in a carbonate forelimb of a fold-thrust structure. Fractures are a commonly studied deformation style due to their impact on fractured reservoir quality. However a huge range of deformation styles can be found in fold forelimbs that are less well studied, and yet can be present in equal abundance. We use field examples from the frontal fold structure of the Vercors fold-thrust belt in the French Sub-Alpine Chains to assess deformation styles. The structure formed due to WNW-directed compression associated with the Alpine orogeny. It is the most westwardly positioned major fold structure thought to be associated with Alpine compression. Strike-parallel transects through the fold forelimb of Urgonian Limestone are used to illustrate the range of damage styles that can occur and their potential influence on reservoir quality. Transects expose calcite-filled veins, open fractures, stylolites, cemented breccias, uncemented breccias and faults.

The range of damage styles appears to relate to lithological variation; stronger rocks lacking significant mud content behave in a brittle manner, exhibiting high intensity deformation. Weaker rocks that contain mud exhibit much lower intensity deformation. The presence of mud in the limestone also appears to inhibit pressure solution meaning muddier rocks lack any secondary calcite precipitation, and therefore voids remain open. Had this fold forelimb example been in the subsurface, the reservoir quality would vary significantly over very short distances due to the alternating presence and absence of secondary calcite precipitation, meaning reservoir quality would be unpredictable. Fractures that are infilled with calcite or breccias with a calcite cement would have low secondary porosity and permeability, whereas rocks lacking secondary calcite precipitation would have much higher secondary porosity and permeability. Despite the fact that almost all outcrops studied have relatively high damage intensity, they are all cut by late-stage faults, indicating that following forelimb deformation the rocks have retained enough bulk strength to behave in a cohesive manner.

Grain shapes and geometric weakening during diffusion creep

J. Wheeler[1]
[1]*Dept. Earth, Ocean and Ecological Sciences, Liverpool University, Liverpool L69 3GP, U.K.*

It is well known that pressure solution (or the “dry” equivalent, diffusion creep) give rise to flow laws with grain size dependence. Localisation is thus described as resulting from grain size reduction. Here I show that there is an additional and marked dependence of strength on grain *shape,* using analytic and numerical models based on the same assumptions that are normally used for quantifying diffusion creep (e.g. negligible shear stress along grain boundaries). Mechanical anisotropy depends on grain shape, and for a model tessellation of a single grain shape, there exists a zero strength direction. In more complicated microstructures even a slight grain elongation parallel to the shear plane gives rise to a marked strength reduction. One digitized natural microstructure known to have been formed during diffusion creep gives an anisotropy of 16; other models predict factors of 100 or more. Numerical experiments show that shear bands sometimes develop but even if deformation is fairly uniform on a scale of (for example) 100 grains, drastic strength decrease may occur. This is a new type of geometric weakening which may influence localisation behavior throughout the Earth, from fault rocks to orogens through to the lower mantle.

References:
Wheeler, J., *Anisotropic rheology during grain boundary diffusion creep and its relation to grain rotation, grain boundary sliding and superplasticity.* Philosophical Magazine, 2010. **90**: p. 2841-2864.

A 400,000-year Record of Earthquake Recurrence for an Intraplate Normal Fault: Inferences on the Role of Fluids in Determining Earthquake Periodicity

R. Williams[1], L. Goodwin[1], W. Sharp[2] & P. Mozley[3]
[1]*Department of Geoscience, University of Wisconsin-Madison, Madison WI, USA*
[2]*Berkeley Geochronology Center, Berkeley CA, USA*
[3]*Department of Earth and Environmental Sciences, New Mexico Tech, Socorro NM, USA*

We present the results of U-Th geochronology of calcite veins in the Loma Blanca normal fault zone (Rio Grande rift, New Mexico) that constrain earthquake recurrence intervals over the past ~550 ka, thereby providing the longest paleoseismic record ever documented. U-Th analysis of these calcite veins allows us to delineate 13 distinct earthquake events. These results demonstrate that for a period of over 400 ka the Loma Blanca fault produced earthquakes with a mean recurrence interval of 40 ± 7 ka. The coefficient of variation for these events is 0.43, indicating strongly periodic seismicity consistent with the time-dependent model of earthquake recurrence. However, this time-dependent series is punctuated by an episode of clustered seismicity at ~430 ka Recurrence intervals within the earthquake cluster were as low as 5-11 ka. Breccia veins formed during this episode exhibit carbon isotope signatures consistent with having formed through pronounced degassing of a CO_2 charged brine during post-failure, fault-localized fluid migration. The ~40 ka periodicity of the long-term earthquake record of the Loma Blanca fault is similar in magnitude to recurrence intervals documented through paleoseismic studies of other normal faults in the Rio Grande rift and Basin and Range Province. We propose that it represents a background rate of failure in intraplate extension. The short-term, clustered seismicity that occurred on the fault records an interruption of the stress renewal process, likely by elevated CO_2 pore-fluid pressure in deeper structural levels of the fault. The relationship between recurrence interval and inferred fluid degassing suggests that pore fluid pressure along the fault may have been driven by variations in CO_2 content, thereby fundamentally affecting earthquake frequency, consistent with “fault-valve” behavior.

Insights into strain rate cycling and localisation of strain on a grain-scale during high temperature creep

C.J.L. Wilson[1], M. Peternell[2] & D.M. Hammes[2]
[1]School of Earth, Atmosphere and Environment, Monash University, Australia (chris.Wilson@monash.edu)
[2]Institute of Geosciences, University of Mainz, 55128 Mainz, Germany

Strain rate histories and strain magnitude are two crucial factors governing the evolution of dynamic recrystallized grain size and crystallographic preferred orientation (CPO) in rocks and ice masses. To understand the effect of strain localisation and cyclic variations in strain rate or non-steady state deformation we have conducted 2D, co-axial plane strain experiments in polycrystalline ice with time-lapse observations from a fabric analyser. The changes in crystal structure, fabric and strain path involving polycrystalline ice in a dynamic deformation regime, can transition from compression to extension and is controlled by the distribution of hard vs soft grains. Accompanying this there may be the evolution of shear domains, though a process of continuous re-equilibration of microstructure and CPO development associated with constant and oscillating strain rate cycles. These can be correlated with *c*-axis small circle distributions, diagnostic of dynamic recrystallization involving new grain nucleation and grain boundary migration (GBM) as observed in the high temperature deformation of ice and quartz. Inhomogeneous stress distribution can lead to grain size reduction for relatively slower strain rates and GBM for relatively faster rates within a long-interval cycling event, a behaviour that contradicts the classical view for dynamic recrystallization processes. Where there is a rapid short-term cycling of strain rate, GBM is hampered and nucleation dominates and is accompanied by a marked reduction of grain size and no new CPO development. During such short-term cycling, GBM and crystallographic change is impeded not by impurities, but through an inability of newly nucleated grains to grow.

Glaciers of salt or deformed gypsum rich caprock? A new perspective on the episodic halokinesis in the eastern Fars province, Iran.

P. Závada[1], J. Bruthans[2], S. Adine[3] & M. Zare[3]
[1]*Institute of Geophysics ASCR, Boční II 1a/1401, Prague, Czech (zavada@ig.cas.cz)*
[2]*Faculty of Science, Charles University in Prague, Albertov 6, 128 43 Praha 2, Czech Republic*
[3]*Institute of Geophysics, University of Tehran, Iran*
[4]*Department of Earth Sciences, Shiraz University, Shiraz, Iran*

Numerous salt plugs consisting of Infra-Cambrian and Cambrian rock salt deposits surface at more than 150 sites throughout the Zagros Mountains. It is known that almost all structures in the Fars region were active before the development of the Zagros fold and thrust belt (ZFTB) and that many of these diapirs emerged on the surface before the recent folding. The morphological classification of the surfaced diapirs shows a zonality across the ZFTB marked by active domes forming islands in the Persian Gulf, mountain glaciers (namakiers), retreating fountains or namakiers and wasting chimneys in the inland, middle part of the ZFTB. The waning activity of the diapirs towards the central part of the ZFTB is explained by attenuation of the mother salt layer or by cutting-off their feeding channels by the propagating thrusts of the ZFTB.

We suggest that the simple morphological categorization of the salt diapirs outlined above may lead to erroneous reconstructions of the halokinetic history in the region. This is because many of the diapirs in the Fars province do not show only salt on the surface, but also thick capping deposits of gypsum and Hormuz debris rich sediments. These sediments frequently form the residuum left behind the dissolution of the salt stocks by fluids circulating close to the surface and may be compared to the classical gypsum rich caprock deposits of the Louann salt diapirs in Texas (USA).

We explored two diapirs in the Laristan (Fars), the Kharmostaj and Siah-Taq, located 20 km SE of the Lar city in Iran. These two diapirs are frequently presented as classical examples of glaciers of salt (namakiers) or resurgent domes feeding a glacier that breach the Zagros anticlines. However, instead of salt, the transverse valleys cut into the indurated flat and low-lying parts of these diapiric structures show fragmented clasts of Hormuz deposits in strongly plastically deformed gypsum matrix. The foliations of these gypsum rich breccias or mylonites are subvertical and strike parallel with the outer rims of the diapirs. Another profile along another valleys cut into these plateaus below the resurgent domes revealed large folded stringers of Hormuz dolomites that are again underlain by the strongly plastically deformed breccias and gypsum mylonites. The lateral parts of the diapirs flanked by large alluvial fans revealed that the salt shows up only at the bottom of the thick solid caprock. In contrast to the vertical fabrics of the plastically deformed gypsum in the caprock, this salt shows flat layering, sheath folds and lense-like slivers imbricated with the deposits similar to those found in the overlying caprock, all showing directions of transport perpendicular to the long axis of the diapirs in the map. In summary, the structural reconstruction suggests that these two diapirs may have originally represented two large downbuilt diapirs with a thick caprock. The north-south shortening during the ZFTB development then deformed the capping sequence to form the vertical fabrics of the gypsum mylonites and gypsum supported breccias in the caprock. This late folding also squeezed out some of the salt that breached locally through the caprock upwards or sideways, from under the capping lid.

Porous melt flow in high pressure felsic crust driving weakening and exhumation dynamics of subducted continents

P. Závada[1,2], M. Racek[3], P. Hasalová[2], P. Jeřábek[3], K. Schulmann[2,4], A. Roberts[5], R.F. Weinberg[5] & P. Štípská[2,4]

[1]*Institute of Geophysics ASCR, Boční II 1a/1401, Prague 4, 14131, Czech Republic (zavada@ig.cas.cz)*

[2]*Centre for Lithospheric Research, Czech Geological Survey, Klárov 3, Prague 1, 11821, Czech Republic*

[3]*Institute of Petrology and Structural Geology, Faculty of Science, Charles University, 128 43, Prague, Albertov 6, Czech Republic*

[4]*Institut de Physique du Globe de Strasbourg; UMR 7516, University of Strasbourg/EOST, CNRS ; 1 rue Blessig, F-67084 Strasbourg CEDEX, France*

[5]*School of Earth, Atmosphere and the Environment, Monash University, Clayton, Vic 3800, Australia*

A section of anatectic felsic rocks from a high-pressure (~730-800°C, 13-17 kbar) continental crust from the Variscan orogeny (Bohemian Massif) preserves unique evidence for coupled melt flow and deformation during continental subduction. The profile reveals parallel layers of grey migmatitic granofelses interlayered with anatectic banded orthogneisses, mylonites, and felsic granulites that alternate within a single deformation fabric related to the prograde metamorphism. The major question asked here is: what is the physical process responsible for the formation of the dark grey, leucosome-bearing granofelses that form an equigranular fine grained mosaic of K-feldspar, plagioclase, quartz and muscovite?

Abundant melt patches in the form of leucosomes in the granofelses or melt accumulations in the surrounding orthogneisses suggest that their origin is somehow related to either in-situ anatexis or melts that percolated through the rocks and originated in external sources. Several lines of evidence suggest that the granofelses represent high strain zones and traces of localized porous melt flow that infiltrated the host banded orthogneisses and crystallized granitic melt in their interstices: i) gradational contacts, where the compositional layering of the orthogneisses merges with the dark gray, homogeneous granofels, ii) slightly depleted composition of the granofelses in incompatible elements in contrast to the orthogneisses, iii) grain size decrease and weakening of crystallographic preferred orientation of major phases in the granofelses in comparison with surrounding orthogneisses suggesting granular flow by melt assisted grain boundary diffusion creep mechanisms, and iv) P-T equilibria modeling showing that the melts were not generated in-situ.

We propose that the melt was transported at the grain scale upward through the subducting continental crust along the deformation induced layering. During this grain-scale porous melt flow, percolating melt infiltrated the framework of host layered mineral aggregates of the orthogneisses, resorbed them and precipitated new grains from the melt in their interstices to form homogeneous granofelses with granoblastic texture. This model outlines a new paradigm for melt transport and weakening of rocks in high-pressure felsic crust. We consider the pervasively flowing melt as an agent that decreases the strength of the layered sequence to layer-parallel shortening and promotes decoupling and exhumation of the entire multilayer by detachment folding, thrusting and backflow along the newly developing fold axial planar cleavage.

3-D seismic interpretation and structural analysis in the exploration of geothermal energy in Munich, Germany

J. Ziesch[1], D. Tanner[1], S. Hanstein[2], H. Buness[1], C.M. Krawczyk[3,4] & R. Thomas[1]
[1]*Leibniz Institute for Applied Geophysics, Hannover, Germany (Jennifer.Ziesch@liag-hannover.de)*
[2]*DMT GmbH & Co.KG - Geo Engineering & Exploration, Essen, Germany*
[3]*GFZ German Research Centre for Geosciences, Potsdam, Germany*
[4]*Technical University of Berlin, Berlin, Germany*

In the context of geothermal exploration the detailed analysis of the tectonic setting in the underground plays an essential role. As a part of the research project GeoParaMoL*, we explore the hydrothermal Malm carbonate reservoir (at a depth of ~3 km) as a source of deep geothermal energy and the overburden of Tertiary Molasse sediments within the Bavarian Molasse Basin. We interpreted six stratigraphic horizons and all major fault zones within a 3-D seismic cube (170 km^2) that was acquired during the winter of 2015/2016 in Munich (Germany). We use a 3-D retro-deformation workflow to predict potential fluid pathways within the reservoir and overburden below the seismic scale.

The stratigraphic horizons; Top Aquitanian, Top Chattian, Top Oligocene (Bausteinschichten), Top Eocene (Lithothamnien limestone), Top and Base Upper Jurassic (Malm), together with the detailed interpretation of the faults in the study area are used to construct a 3-D geological model. The study area is characterised by synthetic normal faults that strike parallel to the alpine front. Most major faults were active from Upper Jurassic up to the Miocene. The Munich Fault, which belongs to the Markt-Schwabener Lineament, has a maximum vertical offset of 350 metres in the central part, and contrary to a previous interpretation based on 2-D seismic, this fault dies out in the eastern part of the area.

The south-eastern part of the study area is dominated by a very complex fault system. Three faults that were previously detected in a smaller 3-D seismic survey at Unterhaching, to the south of the study area, with strike directions of 25°, 45° and 70° (Lüschen et al. 2014), were followed in to the new 3-D seismic survey interpretation. Particularly noticeable are relay ramps and horst/graben structures. The fault with a strike of 25° ends in three large sinkholes with a maximum vertical offset of 60 metres. We interpret this structure as fault-tip horsetail structure, which caused a large amount of sub-seismic deformation. Consequently, this area could be characterised by increased fluid flow.

This detailed understanding of the structural development and regional tectonics of the study area will guide the subsequent determination of potential fluid pathways in the new 3-D subsurface model of urban Munich.

This project is funded by the Federal Ministry for Economic Affairs and Energy (BMWi).

References:
Lüschen, E., Wolfgramm, M., Fritzer, T., Dussel, M., Thomas, R. & Schulz, R. (2014): 3D seismic survey explores geothermal targets for reservoir characterization at Unterhaching, Munich, Germany, Geothermics, 50, 167-179.

* https://www.liag-hannover.de/en/fsp/ge/geoparamol.html


IUGS
TecTask
TSG
Tectonic Studies Group
1 4 9 5
UNIVERSITY
OF ABERDEEN